

The deleterious role of neutrophil extracellular traps (NETs) in pneumococcal pneumonia and therapeutic treatment with adrenomedullin

Inaugural-Dissertation to
obtain the academic degree

Doctor rerum naturalium (Dr. rer. nat.)

submitted to the Department of Biology, Chemistry, Pharmacy

Freie Universität Berlin

by

Luiz Gustavo Teixeira Alves

2020

Work developed between January 2015 and July 2019

at the

Division of Pulmonary Inflammation

Charité – Universitätsmedizin Berlin

Germany

1st Reviewer: Prof. Dr. Martin Witzernath

2nd Reviewer: Prof. Dr. Rupert Mutzel

Date of defense: 19.06.2020

Table of contents

Statement of authorship.....	IV
Acknowledgments	V
Abstract	VI
Zusammenfassung.....	VII
Index of figures	IX
1. Introduction	1
1.1. Community-acquired pneumonia.....	1
1.2. <i>Streptococcus pneumoniae</i>	2
1.3. The immune system	4
1.3.1. The innate immune system	4
1.3.2. The adaptive immune system.....	5
1.4. Mechanism of pneumococcus recognition and clearance.....	6
1.5. Neutrophil granulocytes	8
1.5.1. Phagocytosis.....	11
1.5.2. Degranulation and cytokine release	11
1.5.3. NETosis.....	12
1.6. Mechanism of NET formation	14
1.7. NETs and pneumonia	16
1.8. NET formation and related complications	18
1.9. Therapies targeting NET formation	21
1.10. Adrenomedullin.....	22
2. Aim.....	24
3. Material and Methods.....	25
3.1. Mouse experiments and ethical approval.....	25
3.2. <i>In vivo</i> murine model of pneumococcal pneumonia	25
3.3. Permeability quantification	28

3.4.	Cytokine and chemokine quantification.....	29
3.5.	Histology.....	29
3.6.	Flow cytometry	29
3.7.	Murine bone marrow cell isolation	33
3.8.	Cell selection using magnetic beads	33
3.9.	Human neutrophil isolation.....	34
3.10.	Immunohistochemistry.....	35
3.11.	RNA expression of adrenomedullin receptors	36
3.12.	Western Blot.....	37
3.13.	ROS quantification.....	39
3.14.	NET measurement.....	39
3.15.	Statistical Analysis	41
4.	Results	42
4.1.	<i>Streptococcus pneumoniae</i> induces NET formation <i>in vivo</i>	42
4.2.	DNase improves lung barrier function in pneumococcal pneumonia	44
4.2.1.	DNase reduces NETs and lung permeability <i>in vivo</i>	44
4.2.2.	DNase does not affect animal clinical symptoms and bacterial burden.....	45
4.2.3.	DNase does not affect cellular recruitment and cytokine levels in the lungs and systemically.....	46
4.3.	PAD4 inhibition reduces NETs in the lungs and improves the clinical condition of infected mice.....	49
4.3.1.	PAD4 inhibition efficiently reduces NETs in the lungs.....	49
4.3.2.	GSK484 leads to increased bacteremia in mice.....	50
4.3.3.	GSK484 affects inflammation and neutrophil recruitment to the lung.....	51
4.4.	PSA protects against pneumonia related lung injury	55
4.4.1.	PSA reduces pulmonary NETs during pneumonia	55
4.4.2.	PSA affects bacterial burden in different compartments	56

4.4.3.	PSA reduces neutrophil recruitment and levels of pro-inflammatory cytokines in the lungs	58
4.5.	Reduced NET production upon adrenomedullin treatment is associated with lower pulmonary permeability in pneumonia.....	62
4.6.	Adrenomedullin affects NET formation in murine neutrophils <i>in vitro</i>	63
4.7.	Adrenomedullin treatment affects NET formation in human neutrophils	65
4.8.	Adrenomedullin receptors are expressed in murine and in human neutrophils	67
4.9.	Adrenomedullin reduces NET formation via CRLR-RAMP receptor complex ligation and cAMP production	69
4.10.	Adrenomedullin affects NET production via ROS inhibition.....	71
4.11.	ERK phosphorylation is diminished after adrenomedullin treatment.....	73
5.	Discussion.....	75
5.1.	NETs are produced in the lungs upon pneumococcal infection.....	75
5.2.	Hindering NET formation is beneficial in pneumococcal pneumonia.....	77
5.3.	Adrenomedullin affects NETosis via ERK phosphorylation and NOX inhibition....	83
5.4.	Targeting NETs is efficient against pneumococcal pneumonia.....	86
6.	Bibliography	88
7.	Abbreviations.....	107

Statement of authorship

I hereby certify that this doctor thesis has been composed by myself, and describes my own work, unless otherwise acknowledged in the text. All references have been quoted and all sources of information have been specifically acknowledged. It has not been accepted in any previous application for a degree.

Signature: _____ Date: _____

Acknowledgments

I would like to thank Prof. Dr. Martin Witzernath for giving me the opportunity to join his lab, supporting me financially and allowing me to develop my PhD work during the last years. The guidance and support he provided were essential for the development of my project, for my carrier in research and for my personal growth. His working group was fundamental in providing a pleasant working atmosphere that led to improvements of this thesis. I also need to thank Dr. Holger Müller-Redetzky, my supervisor, for the fruitful discussions during the whole project development and by enlightening my work with the clinical view of the subject. Also, for providing me the opportunity to grow independently and critical, supporting my ideas to finish this project.

I would like to thank all my working group that have supported me during this entire PhD with their knowledge and through many constructive discussions. Also, for their happiness and support that helped me to survive the past difficult winters lived far away from home. In special, I would like to thank my colleagues Dr. Sandra Wienhold, Dr. Eleftheria Letsiou, Dr. Jasmin Lienau, Dr. Matthias Felten, Dr. Birgitt Gutbier, Dr. Chaterine Chaput, Dr. Ling Yao, Ulrike Behrendt, Denise Bartel, Dr. Cengiz Gökeri, Dr. Sarah Berger, Kevin Braun and the whole working group for their support.

I would like to thank the ZIBI Graduate School for the opportunity of participating in discussions, seminars, courses and many important international conferences, which has allowed me to grow and develop my carrier. By exchanging ideas with students from different areas and providing me interesting discussion during the retreats, ZIBI gave me the opportunity to show and defend my project, preparing myself for the future.

I really need to thank Anja and the coffeehouse Container for providing me the “strength” necessary for these last 5 years, with an average of 20 coffees a month.

I would like to thank in special all my friends and family that have always supported and motivated me and my carrier and somehow contributed in helping me to achieve my goals.

Finally, but importantly, I would like to thank Prof. Dr. Rupert Mutzel for the internal supervision, for reading and grading this thesis.

Abstract

Introduction: Community-acquired pneumonia (CAP) promotes dysregulation of the innate immune system and disruption of the endo-epithelial barrier function, leading to acute lung injury and edema formation. It represents a significant health burden worldwide with high mortality rates despite adequate antibiotic treatment. *Streptococcus pneumoniae* (*S.pn.*) is the predominant pathogen causing CAP. Upon *S.pn.* infection, neutrophils infiltrate and accumulate in the lungs, aiming at bacterial clearance. Neutrophil extracellular traps (NETs) are produced by the infiltrating neutrophils and may contribute to an enhanced inflammation of the tissue. This study investigates if NETs are also released after infection with *S.pn.* and if these structures contribute to the pneumonia-related tissue damage. It was previously demonstrated that the hormone-peptide adrenomedullin (ADM) protects mice against *S.pn.*-induced lung epithelial barrier disruption, pulmonary edema formation and extra-pulmonary organ damage. Here, it is further proposed that ADM protects against barrier failure by affecting the process of NET formation. **Methods:** A murine model for severe pneumococcal pneumonia was assessed to clarify the role of NETs in the disease. For this purpose, we evaluated different strategies aiming at NET degradation or inhibition of the process of NETosis, with DNase or PAD4 inhibition, respectively. Moreover, we targeted histones, the main cytotoxic component of NETs, with polysialic acid. The underlying mechanistic of ADM interference in NET formation were evaluated *in vitro*. **Results:** Neutrophils accumulate in the lungs and release NETs after infection with *S.pn.* NET degradation with DNase attenuated *S.pn.*-induced lung permeability. Targeting NETs and NETs-related components could reduce the inflammation in the lungs and was beneficial in improving the animal clinical outcome. ADM treatment led to a significant reduction in NET release, suggesting a direct effect of ADM on this process. *In vitro*, ADM suppressed NET production from activated neutrophils through a mechanism that involves receptor ligation, cAMP production, inhibition of ERK phosphorylation and ROS reduction. **Conclusions:** The results indicate that NETs have a deleterious role in the pathology of pneumococcal pneumonia and its inhibition may be beneficial for the disease outcome. ADM was shown to have beneficial properties apart from the stabilization of the endo-epithelial barrier, also by inhibiting NET production.

Zusammenfassung

Einführung: Die ambulant erworbene Pneumonie (engl. community-acquired pneumonia, CAP) führt zu einer Dysregulation des angeborenen Immunsystems und zu einer Störung der endo-epithelialen Barrierefunktion. Dies kann eine akute Lungenverletzung und Ödembildung zur Folge haben. Die Behandlung der CAP stellt weltweit eine erhebliche Herausforderung dar und es besteht trotz adäquater Antibiotikabehandlung eine hohe Sterblichkeitsrate. Der häufigste Erreger der CAP ist *Streptococcus pneumoniae* (*S.pn.*). Bei einer Infektion mit *S.pn.* sammeln sich Neutrophile in der Lunge an, so dass es zu einer verstärkten Entzündung des Gewebes kommt. In dieser Studie wurde untersucht, ob nach einer Infektion mit *S.pn.* auch Neutrophile Extrazelluläre Traps (NETs) freigesetzt werden und ob diese Strukturen zur Schädigung des Gewebes beitragen. Im Mausmodell konnte bereits gezeigt werden, dass das Hormon-Peptid Adrenomedullin (ADM) vor *S.pn.*-induzierten Störungen der Lungenepithelschranke und extra-pulmonalen Organschäden schützt. Hier wird vorgeschlagen, dass ADM vor Störungen der Barriere schützt, indem es den Prozess der NETs-Bildung beeinflusst. **Methoden:** In einem Mausmodell für schwere Pneumokokken-Pneumonie wurde untersucht, welche Rolle NETs bei der Pneumonie-Erkrankung einnehmen. In verschiedene *in vivo*-Ansätzen wurde dabei die NETs-Degradation (durch DNase) und die Verringerung der NETosis (durch PAD4-Hemmung) untersucht. In einem weiteren Ansatz wurden Histone - die zytotoxische Hauptkomponente der NETs - mit Polysialicssäure gezielt behandelt. Mögliche Mechanismen der ADM-Interferenz bei der NETs-Bildung wurden *in vitro* untersucht. **Ergebnisse:** Neutrophile reichern sich in der Lunge an und setzen NETs nach einer Infektion mit *S.pn.* frei. Der NETs-Abbau mit DNase hat die *S.pn.*-induzierte Lungenpermeabilität abgeschwächt. Die gezielte Steuerung von NETs und NETs-bezogenen Komponenten konnte die Entzündung in der Lunge reduzieren und eine Verbesserung des klinischen Parameters der Versuchstiere bewirken. Die Behandlung mit ADM führte zu einer signifikanten Verringerung der NETs-Freisetzung, was auf eine direkte Wirkung von ADM auf diesen Prozess hindeutet. *In vitro* unterdrückte ADM die NETs-Produktion von aktivierten Neutrophilen durch einen Mechanismus, der die Rezeptor-Bindung, die cAMP-Produktion, die Hemmung der ERK-Phosphorylierung und die ROS-Reduktion umfasst. **Schlussfolgerungen:** Die Ergebnisse weisen darauf hin, dass NETs eine schädliche Rolle in der Pathologie der Pneumokokken-Pneumonie spielen und ihre Hemmung sich vorteilhaft auf den Krankheitsverlauf auswirken könnte. Es hat sich zudem gezeigt, dass ADM neben der Stabilisierung der endo-epithelialen Barriere auch durch Hemmung der NETs-Produktion einen positiven Einfluss hat.

Eu quero dizer, agora, o oposto do que eu disse antes, também vou lhe desdizer aquilo tudo que eu lhe disse antes. Eu prefiro ser essa metamorfose ambulante, do que ter aquela velha opinião formada sobre tudo (Raul Seixas).

Index of figures

Figure 1: Structure of the Gram-positive bacterium <i>Streptococcus pneumoniae</i>	4
Figure 2: Neutrophil effector functions for pathogen clearance	10
Figure 3: NET formation and bacteria entrapment	12
Figure 4: Mechanisms of NET formation	16
Figure 5: Neutrophils in the pathogenesis of acute respiratory distress syndrome	18
Figure 6: Gating strategy for murine BALF cell populations	31
Figure 7: Gating strategy for murine blood cell populations	32
Figure 8: Magnetic positive selection of murine bone marrow-derived neutrophils	34
Figure 9: Isolation of blood-derived human neutrophils.....	35
Figure 10: NETs are generated and accumulates in the lungs after <i>S.pneumoniae</i> infection .	43
Figure 11.1: DNase reduces NETs and lung permeability.....	45
Figure 11.2: DNase treatment does not affect clinical symptoms and bacteria burden in pneumococcal pneumonia.....	46
Figure 11.3: DNase treatment does not affect neutrophil recruitment and cellular activation.....	47
Figure 11.4: DNase treatment does not affect cytokine production.....	48
Figure 12.1: PAD4 inhibition reduces NETs after pneumococcal pneumonia.....	50
Figure 12.2: PAD4 inhibition leads to increased bacteremia in mice.....	51
Figure 12.3: GSK484 influences neutrophil recruitment into the lungs	52
Figure 12.4: GSK484 influences cytokine production in the lungs and systemically	54
Figure 13.1: PSA reduces NETs and barrier dysfunction of the lungs after pneumococcal pneumonia.....	56
Figure 13.2: PSA delays disease symptoms and affects bacterial burden.....	57
Figure 13.3: PSA influences the cellular recruitment into the lungs	59
Figure 13.4: PSA influences the inflammatory status of the lungs and systemically	60

Figure 13.5: PSA affects neutrophil infiltration into the alveolar space.....	61
Figure 14: Adrenomedullin reduces NETs in mice infected with <i>S.pneumoniae</i>	62
Figure 15: Adrenomedullin affects NET formation in murine neutrophils <i>in vitro</i>	64
Figure 16: Adrenomedullin affects NET formation also in human neutrophils	66
Figure 17: The adrenomedullin receptors, CRLR and RAMP, are expressed in murine and human neutrophils	68
Figure 18: Adrenomedullin affects NET formation via receptor activation and subsequent cAMP production	70
Figure 19: ROS production is reduced after treatment of neutrophils with adrenomedullin..	72
Figure 20: Adrenomedullin inhibits ERK phosphorylation in human neutrophils	74
Figure 21: Possible mechanistic pathway of adrenomedullin interference in NET formation	86

1. Introduction

1.1. Community-acquired pneumonia

Pneumonia is the inflammation of the lower respiratory tract, mainly caused by microbial infections. Pneumonia is very complex, once it can be triggered by different organisms, causing many distinct manifestations and sequelae. The most common organisms causing pneumonia are bacteria, viruses and fungi (Mackenzie, 2016). Community-acquired pneumonia (CAP) refers to the acquisition of the disease with no relation to the healthcare system. It opposes to hospital-acquired pneumonia (HAP), where contact to the pathogen is facilitated by the hospital facilities. In the USA, pneumonia was the eighth leading cause of death in 2004 (Niederman, 2009) and in Germany 14% of the overall in-hospital mortality in the same year was due to CAP, according to a study from the German Competence Network for CAP (CAPNETZ). CAP accounts for an estimated 3.5 million deaths worldwide. Its overall incidence rises dramatically with age, with rates ranging from 18.2/1000 person per year in people with 65–69 years, up to 52.3/1000 person per year in those aged over 85 years. Smoking, chronic obstructive pulmonary disease, alcohol abuse, liver disease (hepatitis and/or cirrhosis), congestive heart failure, diabetes mellitus or HIV infection may facilitate predisposition to the disease. Altogether, the costs involved in the healthcare system carries a high economic burden (Drijkoningen and Rohde, 2014). Symptoms of pneumonia are the acute onset of cough, fatigue, shortness of breath and dyspnea with documented or subjective fever, chills, sweats, purulent sputum, and pleuritic chest pain. Chest radiography revealing pathogenesis or necrotizing tissue, stain of sputum and microscopic analysis of the sample may help in the characterization of the disease. In a large European review, *Streptococcus pneumoniae* (*S.pn.* or pneumococcus) was found to be the most frequently isolated pathogen in CAP, occurring in around 35% of the identified cases (Drijkoningen & Rohde, 2014; Black et al., 2010). Among patients with pneumococcal pneumonia, up to 25% have detectable bacteremia in analysis of sputum and blood samples (Janoff and Musher, 2014; Lewis and Surewaard, 2018; Weiser et al., 2018). Pneumonia is frequently associated with sepsis and septic shock and is a frequent cause of the acute respiratory distress syndrome (ARDS). ARDS is characterized by excessive vascular endothelial and alveolar epithelial cell damage, leading to the disruption of the blood-alveolar barrier and pulmonary edema formation. This results in severe impaired gas exchange (Matthay et al., 2012; Grailer et al., 2014). With the aim of improving gas exchange capacities of the patients with acute respiratory failure, mechanical ventilation (MV) is a highly recommended

intervention. However, this non-physiological stretching of the lung tissue can lead to tissue damage and promote further inflammation. With an uncontrolled hyper-inflammation, increased permeability and lung injury, ventilator-induced lung injury (VILI) develops, where mortality rates can rise to 55% of the inflicted patients. Neutrophils are strongly implicated in this inflammatory process and in the pathogenesis of VILI (Yildiz et al., 2015; Grommes and Soehnlein, 2011).

1.2. *Streptococcus pneumoniae*

S.pn. is a Gram-positive, extracellular opportunistic pathogen that grows as lancet-shaped diplococci in short chains and colonizes the mucosal surfaces of the human upper respiratory tract (Yahiaoui et al., 2016). They can cause a wide range of infections apart from CAP, including otitis media, sepsis and meningitis. *S.pn.* remains a major cause of respiratory and invasive diseases, contributing significantly to high mortality rates in the elderly and young children. This sums up more than one million deaths worldwide annually, more than AIDS, malaria and measles combined (Janoff et al., 2014; O'Brien et al., 2009; Ampofo and Byington, 2018). In CAP, the early intervention with effective antimicrobial agents provides a substantial survival advantage in severe pneumonia patients. Historically, pneumococci are susceptible to different antibiotics, as penicillin, cephalosporins, macrolides (including erythromycin), clindamycin, rifampin, vancomycin and trimethoprim sulfamethoxazole. The use of pneumococcal conjugate vaccines (PCVs) against pneumococcal polysaccharide from specific serotypes has significantly reduced manifestation of the disease after its introduction around the year 2000. The currently available 23-valent vaccine (PPSV23) is composed of purified capsular polysaccharide antigens of 23 serotypes, offering some protection against 59 to 68% of the invasive pneumococcus (Ampofo and Byington, 2018). However, transformation and horizontal gene transfer may occur in *S.pn.*, with incorporation of exogenous DNA from many sources, as different pneumococcus serotypes, extracellular matrix of pneumococcal biofilms and closely related streptococci, ensuring a high rate of variation in their genome. This facilitates the spread of antibiotic-resistant pathogens and evasion of vaccine-induced immunity. The continued high burden of the disease and rising rates of resistance to penicillin and other antibiotics have renewed interest in alternative mechanisms of prevention. Clinical evidences have shown that combinatory therapies against pneumonia can be more efficient than monotherapies (Dockrell et al., 2012; Weiser et al., 2018).

Morphologically, the pneumococcus genome is disposed in a covalently closed circular DNA structure with approximate 2 to 2.1 million base-pairs. It can comprise up to 10% of variations

between strains and contain conjugative transposons, which mediate antibiotic resistance (Poll and Opal, 2009). *S.pn.* has a cell wall structure composed of several layers of peptidoglycan intercalated with teichoic acid molecules. Different proteins are present on the pneumococcal cell surface, including pneumococcal surface proteins A and C (PspA, PspC), surface adhesin (choline-binding protein) A (CbpA), CbpC, the surface adhesin and manganese-transporter pneumococcal surface antigen (Psa) A and proteins involved in DNA acquisition. Additionally, nearly every clinical isolate of *S.pn.* contains an external negatively charged polysaccharide capsule. Antigenic differences in their capsule are used to distinguish the 92 serotypes of pneumococci identified so far (Janoff et al., 2014). The capsule is crucial during colonization, invasion and dissemination from the respiratory tract, being considered the most important virulence factor of pneumococcus in experimental and clinical studies. It prevents phagocytic clearance by blocking immunoglobulin (Ig), complement deposition on the bacteria cell surface and mechanical clearance by mucous secretion (Poll and Opal, 2009). *S.pn.* has many other potent virulence factors, as lipoteichoic acid (LTA), the PspA and PspC, autolysin (LytA) and cytolysins. Pneumolysin (PLY) is a cholesterol-dependent pore-forming toxin, conserved in all pneumococcal isolates. It is released during pathogen autolysis as a soluble monomer that oligomerizes on host cell membranes, forming pores. It is cytotoxic in lower concentrations, altering many cellular functions and lytic to mammalian cells in higher amounts (Figure 1). PLY is generally evaluated for its contribution to inflammation, influencing initiation of ARDS and being required for bacterial dissemination from the lungs (Lewis and Surewaard, 2018). It has many other pathological effects as the ability to inhibit ciliary function from epithelial cells, activate cluster of differentiation (CD)4⁺ T-cells, impair respiratory burst of phagocytic cells, induce production of pro-inflammatory chemokines and cytokines, as tumor necrosis factor (TNF) alpha, interleukin (IL)-1, IL-6 and IL-18, and activate the classical complement pathway (Weiser et al., 2018; Moorthy et al., 2013; Poll et al., 2009; Lewis and Surewaard, 2018; Hirst et al., 2004; Grailer et al., 2014; Kerr, 2002).

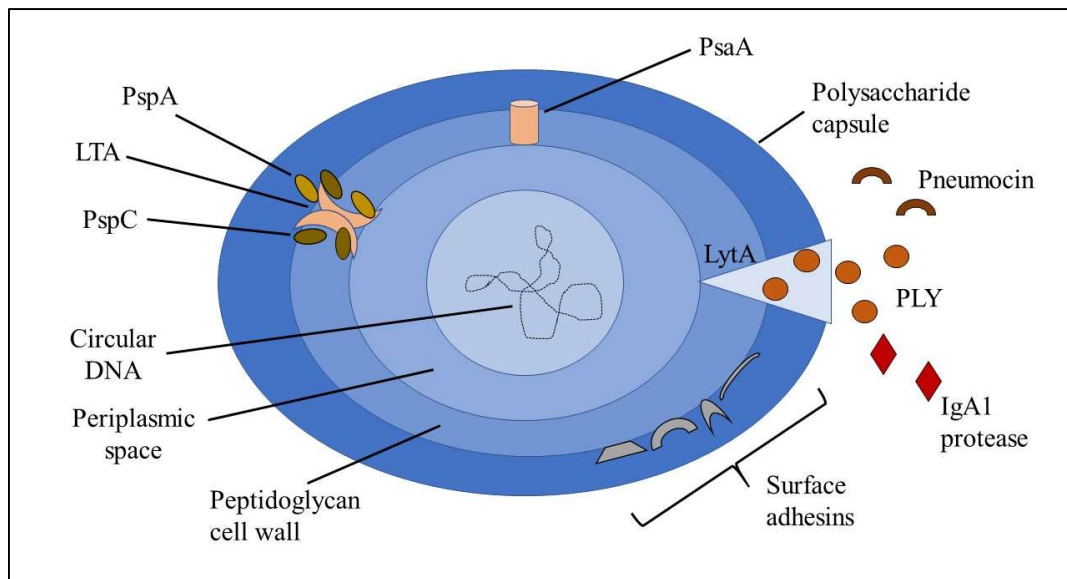


Figure 1: Structure of the Gram-positive bacterium *Streptococcus pneumoniae*. Scheme of the cellular structure of pneumococcus and its virulence factors. PspA/C (pneumococcal surface protein A/C); LTA (lipoteichoic acid); PsaA (pneumococcal surface antigen A); Ply (pneumolysin); LytA (autolysin) (adapted from Poll & Opal, 2009).

1.3. The immune system

The response to invasion of infectious agents or factors that disturb the homeostasis of the organism is coordinated by a network of cells, tissues and organs belonging to the innate and the adaptive immune system. Both systems aim to protect against diseases and have the ability to distinguish between self and non-self. The innate immunity is composed of many cell types, as phagocytic and epithelial cells and distinct products that regulate cell activity, as the complement system and cytokines. The adaptive immune system consists mainly of lymphocytes and their products, including antibodies, which provide the humoral immunity. The cells from both innate and adaptive immune system circulate via blood and lymphatic system, actively identifying pathogens. Both are complementary to each other and through coordinated interactions between their specialized cells, they initiate distinct effector programs against the different pathogens (Parkin and Cohen, 2001).

1.3.1. The Innate Immune System

The innate immune system provides the first line of defense against invading pathogens and has an important role in establishing a strong adaptive immune response. Mucosa and epithelial surfaces represent a first physical barrier against invading organisms. The contact provided by these surfaces to the pathogens enhances the possibility of antigen recognition by immune cells

and the proper immune response against them (Medzhitov and Janeway, 1997). Danger signals released by the host after tissue injury or infection activate a contingent of cells that aim to control the invasive agent. These molecules influence a series of inflammatory responses and the recruitment of myeloid phagocytic cells, as neutrophils, macrophages and dendritic cells (DCs), and innate lymphoid cells, including the natural killer (NK) cells. These cells are directed towards the infectious site and promptly fight pathogens. Antigen-presenting cells (APCs), as macrophages and DCs, engulf the pathogens and present their digested structures at the surface together with major histocompatibility complex (MHC)-Class II receptors. This will further activate cells from the adaptive immune system, enhancing the immune response to the infection. Neutrophils play an important role in this first line of defense, recruiting and activating APCs and modulating other cell responses (Nathan, 2006). This inflammatory signaling can persist beyond the acute phase of inflammation, modulating cells from the adaptive immune system, as B and T-cells (Pietrosimone, 2015).

1.3.2. The Adaptive Immune System

The adaptive immune system, present in vertebrates, is a sophisticated strategy in the control of infectious organisms that escape the first barrier of defense provided by the innate immunity. Somatic hypermutation and recombination of receptor domains are typical features of those cells, resulting in the generation of a broad range of receptors, which recognize a large repertoire of antigens. A unique capacity of this immune system is the ability to develop memory, leading to faster and enhanced responses upon subsequent infections. Lymphocytes, as B- and T-cells, form the adaptive immune system and have both effector and memory functions. B-cells have a large role in the humoral immune response, secreting high amounts of antibodies that circulate in blood and lymph, neutralizing specific pathogens and activating the complement system and other immune responses. T-cells play a central role in cell-mediated immunity and comprise many different cell subtypes, including CD8⁺ cytotoxic T-cells, CD4⁺ helper T-cells (T_H) cells and CD4⁺ regulatory T-cells (T_{reg}), which are distinct in the immunological functions they provide. The T_H cell family includes many different cell subsets that are defined based on their distinct cytokine profile, which lead to specific and efficient types of immune responses. T_{H1} cells, characterized by production of interferon (IFN)- γ , drive to protection against intracellular pathogens. T_{H2} cells are defined by secretion of IL-4, IL-5 and IL-13, contributing to the control of extracellular parasite infections. T_{H17} cells produce the pro-inflammatory cytokine IL-17 in the surveillance of mucosal barriers. In mice, the T_{H17} response is necessary for an efficient response against pneumococcal infection (Ampofo and Byington, 2018; Wright et al., 2013).

1.4. Mechanism of pneumococcus recognition and clearance

The respiratory tract represents the interface between the organism and the external environment, providing the first line of contact to pathogens. The lung epithelium is therefore of great importance for the initial immune response, sensing bacteria, secreting antimicrobial peptides, initiating an inflammatory process and for the pathogen clearance (Bals and Hiemstra, 2004). The first obstacle that *S.pn.* encounters upon colonization of the nasopharynx is provided by mucus entrapment. The glycocalyx or pericellular matrix overlying the upper respiratory tract epithelium is composed of gel-like mucin glycoproteins and contains antimicrobial peptides and Igs. Although it provides a barrier to the underlying cell surface, the mucin can also help bacteria in the colonization of the infectious site, providing a favorable niche with nutrients (Weiser et al., 2018). For a successful colonization of the upper respiratory tract, *S.pn.* must overcome also a niche competition with other colonizing bacteria, including other serotypes of pneumococci. This is the first selective force encountered by the pathogen before disease development. Therefore, the host microbiome is of great importance for bacterial colonization. Upon contact with the pathogen, the respiratory epithelium starts immune responses, releasing cytokines, chemokines and antimicrobial peptides, such as lysozyme and defensins, contributing to the innate immunity against the pneumococcus (Bals and Hiemstra, 2004). Moreover, respiratory epithelial cells have the potential to continuously remove pathogens from the lower airways through their mucociliary activity. *S.pn.* can persist dormant for weeks or months without any manifestation or adverse sequelae. This dormant state can favor the maintenance of the pathogen and its spread within the population (Poll and Opal, 2009). Resident alveolar macrophages represent the first line of phagocytic defense in the lungs, eliminating the lower number of invading bacteria. After phagocytosis, macrophages undergo apoptosis, favoring the killing of the pathogens and keeping pneumococcal levels to a minimum (Dockrell et al., 2003). The contact of macrophages and epithelial cells with the pathogen activates the production of C-X-C chemokines and other factors, favoring the recruitment of neutrophils to the infectious site. With an increased number of bacteria arriving, neutrophils become the main phagocytic cells in the inflamed lungs, relegating the alveolar macrophages to the role of clearing the apoptotic neutrophils. Neutrophils can readily kill phagocytized pneumococci by releasing pathogenic serine proteases from their granules and reactive oxygen species (ROS). After bacteria invasion of the circulation, their elimination is highly dependent on opsonization by complement components. Therefore, many of the virulence factors of *S.pn.* target components of the complement system, aiming to minimize phagocytosis and clearance by the immune system (Ampofo and Byington, 2018; Weiser et al., 2018).

Recognition of the invading pathogens by the innate immune cells is mediated by pattern-recognition receptors (PRRs). They recognize evolutionary conserved motifs expressed by pathogens, referred as pathogen-associated molecular patterns (PAMPs). Staphylococci and pneumococci present several conserved motifs that are promptly recognized by cell surface and intracellular receptors on immune and epithelial cells. The PRRs contribute to the initiation of an effective innate immune response against the pathogen. PRRs also recognize endogenous molecules, like chromatin or cytosolic proteins, released by the damaged tissue upon infection, which are referred as the danger-associated molecular patterns (DAMPs). Release of DAMPs is observed not only after tissue injury, but through other active processes, like apoptosis and necroptosis (Iba et al., 2013; Kaczmarek et al., 2013). Other molecules may be released by the injured tissue after infection, including histones, the nuclear protein high mobility group box 1 (HMGB1) and shock proteins, known as alarmins. These molecules can activate the innate immune system and are potent mediators of inflammation (Rittirsch et al., 2008; Iba et al., 2014; Xu et al., 2009). Recognition by PRRs leads to cellular activation, enhanced phagocytosis, induction of local inflammation, as well as activation of the adaptive immune system (Artis et al., 2010). Once initiated, inflammation must be tightly regulated in order to rapidly restore tissue homeostasis, thereby avoiding excessive tissue damage and chronic inflammation (Maas et al., 2018). The PRRs comprise different receptor groups, including Toll-like receptors (TLRs), nucleotide-binding oligomerization domain (NOD)-like receptors (NLRs), RIG-I-like receptors (RLRs) and the manifold cytosolic DNA sensors (Koppe et al., 2012; Medzhitov and Janeway, 2000). In general, activated receptors initiate intracellular signal transduction cascades regulating a variety of genes involved in defense, enhancing phagocytosis, inducing cytokine production and enhancing inflammation. There are 10 members of TLRs known in humans and 12 in mice. They all possess a common extracellular recognition domain and an internal TLR/IL-1R domain that binds to the common TLR-adaptor protein myeloid-differentiation primary response protein 88 (MyD88). Mice deficient in MyD88 are very susceptible to pneumococcal pneumonia, probably in part for an impaired innate immune activation. TLR2 is an important pattern-recognition receptor for Gram-positive pathogens, recognizing peptidoglycan, lipoteichoic acid and bacterial lipopeptides. Bacteria lipoproteins are also recognized by other receptors, as TLR1 and TLR6. TLR3 is essential for recognition of double stranded RNA, common in viral infections, and TLR8, found in the endosomal compartment, recognizes single stranded RNA released by internalized viruses (Makni-Maalej et al., 2015). TLR4 is known for the recognition of lipopolysaccharide (LPS) of Gram-negative bacteria and PLY (Dessing et al., 2007; Koppe et al., 2012). Upon investigation of many

different types of TLR-deficient mice, TLR9 was shown to be the most essential for the immunity against pneumococcus infection. It detects bacterial-rich CpG DNA and seems to be essential for effective phagocytosis and killing of pneumococci by lung macrophages (Albiger et al., 2007). Among the NLR receptors, NLRP2 is important for recognition of a common fragment of peptidoglycan muramyl dipeptide from internalized bacteria. NLRP1, NLRP3 and NLRC4 can form inflammasome complexes, initiating an inflammatory process and regulating the innate immune response. Inflammasomes will further regulate activity of caspase-1, which processes the three major host-defense cytokines, namely IL-1 β , IL-18, and IL-33 in macrophages and DCs, necessary for defense against *S.pn.* (Opitz et al., 2004; Koppe et al., 2012). PLY also leads to activation of inflammasomes, as the NLRP3 inflammasome (Poll and Opal, 2009; Witzenrath et al., 2011; Dockrell et al., 2012).

1.5. Neutrophil Granulocytes

Neutrophils are the most abundant white blood cells found in the circulation. They correspond to approximately 60% of the leukocytes in human blood, whereas in mice they can reach 30%. Neutrophils have a lobulated nucleus with 3-5 segments, allowing its classification as polymorphonuclear cells (PMN). This possibly enables them to easily translocate across the gaps in the endothelial layer towards the infectious sites. They are also rich in granules containing antimicrobial molecules, which gives them the name neutrophil granulocytes. They originate from hematopoietic progenitor cells in the bone marrow (BM) and are constantly released in the circulation, where they patrol for pathogens. Neutrophils found in blood represent a heterogeneous population with distinct phenotypes and functions during the inflammatory process. They have a considerable short lifespan of some hours after release into the circulation, but are able to live for few days upon stimulation (Bekkering, 2013; Pillay et al., 2010). Inflammation or infection, as caused by *S.pn.*, leads to release of several chemoattractants by different cells of the infected tissue, stimulating neutrophils to leave circulation and translocate into the tissue in an attempt to eradicate the pathogen. The recruitment cascade into the tissue can be divided into four distinct stages: neutrophil rolling and/or tethering on endothelial cells, cell adhesion and crawling, transmigration and chemotactic migration. The first step requires circulating phagocytes to slow down their speed near the site of infection. Chemotactic signals mainly released by host cells, such as IL8, C-X-C chemokine ligand 1 (CXCL1 or GRO α), leukotriene B4 (LTB4) and complement component C5a, are sensed by circulating neutrophils, arresting them around the affected areas. Upon arresting in the inflamed area, neutrophils become partially activated by cytokines,

inflammatory mediators and interactions to other cell types, a crucial step for the migration process. Endothelial cells rapidly express P- and E-selectins, which are able to interact with the glycoprotein P-selectin glycoprotein ligand-1 (PSGL-1), CD44 and E-selectin ligand-1 on the neutrophil surface (Grommes and Soehnlein, 2011; Bekkering, 2013). The progression from rolling to complete arrest on the endothelial layer occurs via integrin-dependent interactions from leukocyte adhesion molecules, such as CD11a/CD18 (LFA-1) and CD11b/CD18 (Mac-1), to intercellular adhesion molecule 1 (ICAM-1) molecules on endothelial cells. This interaction activates intracellular pathways connected to the cellular cytoskeleton of the neutrophil (Grommes and Soehnlein, 2011). Once arrested on endothelial surface, neutrophils will flatten and shift towards the extravasation site. Transmigration into the tissue occurs through endothelial junctions and is facilitated by complex interactions between the receptors CD31 and Mac-1, together with junction adhesion molecules A–C, CD47 and CD44 (Phillipson et al., 2006). Alternative adhesion molecules may also be involved, as recruitment of neutrophils to the lungs and liver may not require selectins. Moreover, the vessels in the different organs show distinct cellular composition and structural differences, influencing neutrophil recruitment (Maas et al., 2018). Upon internalization across the endothelial barrier, neutrophils are guided towards the site of infection by chemotaxis and become more and more activated. Neutrophils are able to cross-talk to many other cell types, modulating inflammation and regulating immune responses (Costantini et al., 2010). In the alveolar space, neutrophil infiltration is controlled by several chemokines mainly produced by alveolar macrophages, such as the keratinocyte-derived chemokine (KC or CXCL1), the macrophage inflammatory protein-2 (MIP-2 or CXCL2) and the lipopolysaccharide-induced C-X-C chemokine (LIX or CXCL5) (Grommes and Soehnlein, 2011). In the site of infection, neutrophils are able to fight the invading pathogens by different effector mechanisms, as phagocytosis, degranulation, cytokine release and the recently described process of neutrophil extracellular trap (NET) formation, or NETosis (Figure 2).

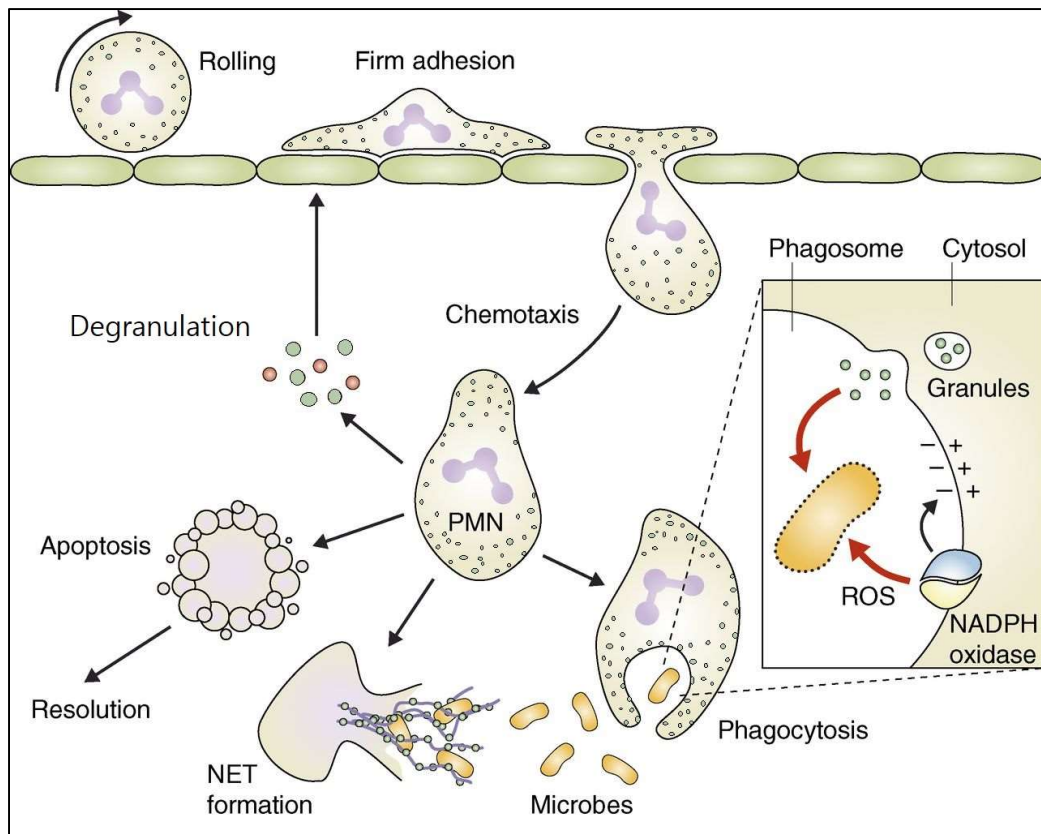


Figure 2: Neutrophil effector functions for pathogen clearance. The neutrophil granulocyte (PMN) infiltrates the site of infection via chemotaxis factors and acts through different mechanisms aiming at pathogen clearance. They are able to kill the invading microorganism with help from reactive oxygen species (ROS) via phagocytosis, release of highly cytotoxic molecules and cytokines via degranulation or produce NETs via NETosis. After activation, they might migrate out of the tissue, modulating other cell types or go into apoptosis and are cleared by macrophages (adapted from Mócsai, 2013).

Neutrophils may also undergo a process of reverse transmigration out of the inflammatory site, returning to blood vessels, where they communicate with distinct cell types and contribute to the propagation of the immune response (Bekkering, 2013). Absence of neutrophils or presence of non-functional cells, as seen in chronic granulomatous disease (CGD) and leukocyte adhesion deficiency are highly associated with severe bacterial infections, showing the great role of neutrophils for the immune response against bacteria. After their activation phase, they undergo apoptosis, via CD11b/CD18 signaling, production of ROS and activation of caspases, and are finally removed by macrophages. If not activated, they may enter a period of senescence, with increased expression of the homing chemokine CXCR4, directing them to the BM, where they become apoptotic and are phagocytosed by macrophages (Poll and Opal 2009; Maas et al., 2018).

1.5.1. Phagocytosis

The process of phagocytosis starts with recognition and binding of the neutrophil to the pathogen, followed by its ingestion and subsequent digestion. Complement and Ig present in serum may greatly enhance phagocytosis through coating of the extracellular surface of the pathogen by opsonization. During phagocytosis, neutrophils engulf and uptake microbes into specialized compartments called phagosomes. This process activates neutrophil internal signaling pathways that are responsible for the generation of ROS. The non-mitochondrial reduction of oxygen, known as respiratory burst, produces reactive forms of oxygen molecules that are less reduced than water. Fusion of ROS with phagosomes leads to the acidification of the medium, necessary for the inactivation and killing of the pathogen (Nathan, 2006). In addition to oxidant-dependent killing mechanisms, phagosomes undergo fusion with specific neutrophil granules containing potent proteases, originating phagolysosomes. In the phagolysosomes, ROS is responsible for the activation of important antimicrobial proteins, as bactericidal/permeability-increasing proteins (BPI), lysozyme, defensins, lactoferrin and serine proteases, as neutrophil elastase, proteinase 3 and cathepsin G. These positively-charged antimicrobial proteins can disrupt integrity of the bacterial membrane, killing the pathogen efficiently (Lewis and Surewaard, 2018; Brinkmann and Zychlinsky, 2007; Branzk and Papayannopoulos, 2013; Cortjens et al., 2017; Amulic et al., 2012).

1.5.2. Degranulation and cytokine release

Neutrophils that fail to encounter and phagocyte bacteria within a short period of time, release their granular arsenal in the extracellular space. Degranulation leads to release of many antimicrobial substances in the extracellular space, including ROS and many highly cytotoxic peptides and proteins. By actively releasing proteases and cytokines, neutrophils can further modulate the immune response extracellularly (Nathan, 2006). This process is tightly controlled by a receptor-mediated mechanism and the active release of granules occurs by fusion of the phagosomes to the plasma membrane, in a process denominated exocytosis. As neutrophils migrate along a gradient concentration of stimulus, they can progressively discard different sets of granules. The primary or azurophilic granules contain peroxidase-positive molecules that are extremely toxic to the pathogen. Among them, myeloperoxidase (MPO), neutrophil elastase (NE), cathepsin G, lysozyme and α -defensins have potent antimicrobial capacities. The secondary or specific granules and tertiary or gelatinase granules are enriched in peroxide-negative molecules. These granules have some proteins in common, as lactoferrin, lysozyme, and metalloproteases (MMP), including MMP8 and MMP25, lipopolysaccharide-binding BPI

and protease 3 (Nathan, 2006; Branzk and Papayannopoulos, 2013). The azurophilic granules released later during the process of degranulation, together with the different cytokines, are important for the coordination of the immune response and control of pathogens extracellularly. Release of azurophilic granules is also important for the process of NETosis (Nathan, 2006).

1.5.3. NETosis

The most recently described strategy of neutrophils to control pathogen infection is termed NETosis and was first described in 2004 by Brinkmann and colleagues. During NETosis, neutrophils actively expel their highly cytotoxic granular content attached to the decondensed chromatin structure, aiming at pathogen control outside the cellular membrane. NETs are large extracellular web-like decondensed chromatin structures that snare pathogens, exposing them to a high localized concentration of antimicrobial proteins, enhancing the killing of pathogens (Figure 3).

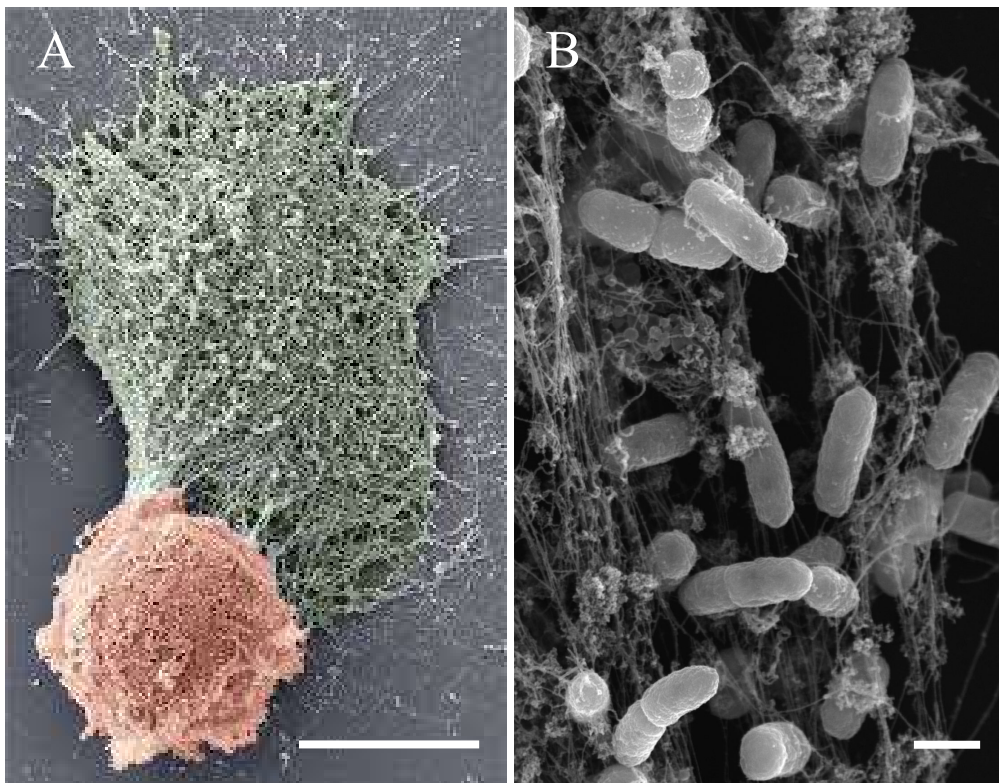


Figure 3: NET formation and bacteria entrapment. (A) Scanning electron micrograph shows the process of NET formation after neutrophil activation and the subsequent release of the nuclear cellular content together with the highly cytotoxic proteases; scale bar: 5µm (Wong & Wagner, 2018). (B) The magnified area of the NET structures facilitate the entrapment of microbes and their killing by the many cytotoxic components, as observed by electron microscopy after neutrophil culture with *S. aureus*; scale bar: 1µm (Brinkmann & Zychlinsky, 2012).

The process of NET formation is well established and has been described in many different species of vertebrates. NET-like structures were even found to be produced by specialized plant root cells, as a convergent evolutionary defense system (McDonald et al., 2012; Brinkmann and Zychlinsky, 2012; Röhm et al., 2014; Schönrich and Raftery, 2016; Abdallah et al., 2012). The released DNA originates mainly from the nucleus, however, NET formation from mitochondrial DNA has also been reported (Jorch and Kubes, 2017). DNA is known to have a strong bactericidal potential, due to its ability to sequester surface bound cations, leading to membrane rupture and lysis of the pathogen (Halverson et al., 2015). Apart from the DNA, chromatin is also composed of core-histones that are highly toxic to the pathogen. More than 30 proteins were already identified to be attached to the NET structures. Serine protease NE, MPO, calprotectin, MMP, cathelicidins and defensins are released by neutrophils during NETosis and enhance the antimicrobial property of NETs (Papayannopoulos, 2017; Ermert et al., 2009; Urban et al., 2009). NETs were shown to be involved in the killing of many pathogens, including bacteria, fungi, viruses and parasites and were linked to various autoimmune diseases. Neutrophils that undergo NETosis can occupy an area 10-15 times larger than the initial volume of the cell. This enhanced area may help NETs to prevent further pathogen dissemination by trapping them in their chromatin structure via charge interactions. NETs can also help to contain the dispersion of their own cytotoxic proteases and thus prevent additional tissue damage. NETosis differs from apoptosis and necroptosis, where chromatin slowly decondenses and is released in the cytoplasm without being degraded. Differently from apoptosis, it does not require caspases and no apoptotic bodies are formed. Moreover, necrostatin-1, a potent inhibitor of necroptosis, does not affect NET formation after stimulation with phorbol-12-myristate-13-acetate (PMA) (Brinkmann and Zychlinsky, 2007; Remijnsen et al., 2011). NETs are of great importance in the early post-infection period, as their degradation in a mouse model of polymicrobial sepsis led to increased bacterial spread and organ injury (Meng et al., 2012). One of the most significant experiments showing the importance of NETs for the immune defense was published by Bianchi et al. (2009) with CGD. CGD is a disease in which patients fail to produce ROS, and consequently NETs, due to a defect in the nicotinamide adenine dinucleotide phosphate (NADPH) oxidase (NOX) subunit. Patients are more susceptible to recurrent life-threatening infections, as with *Aspergillus nidulans*, a fungus causing pneumonia. NET production is necessary for pathogen clearance when the hyphae are too large to be eliminated by phagocytosis. Gene therapy in a CGD patient suffering incurable fungal infections was used to restore NOX function, contributing to the complete clearance of the fungus (Brinkmann et al., 2004; Kaplan and Radic, 2012; Brinkmann and Zychlinsky, 2012; Yousefi et al., 2008).

1.6. Mechanism of NET formation

Different molecules and pathogen antigens can activate neutrophils to produce NETs. This activation occurs through distinct mechanistic pathways after recognition via TLRs, Fc receptors, cytokine receptors or complement receptors. This may lead to the generation of NET structures with distinct composition of proteins. The classical molecular pathway leading to NETosis includes generation of ROS, nuclear decondensation involving the enzymatic activities of MPO and NE and chromatin extravasation of the cell. ROS generation seems to be an essential step for the process and is generated by the NOX complex found in phagosomes or in the cytoplasm. ROS is also generated by a NOX-independent pathway by mitochondrial oxidative phosphorylation complexes. However, these complexes are not abundant in neutrophils. NOX generates superoxide radical anions of O_2^- from oxygen molecules after the transfer of electrons across the membrane. This first superoxide is almost instantly converted into hydrogen peroxide (H_2O_2) by a superoxide dismutase. MPO released upon stimulation catalyzes the reaction between H_2O_2 and chloride, generating hypochlorous acid (HOCl). HOCl is highly microbicide and oxidize many substances, including nucleic acids, lipids and proteins, and is the key ROS involved in NET formation. MPO is further activated by ROS and leads to permeabilization of other granules and the dissociation of azurosome complex, which contains several proteases. MPO and ROS are required for NE release from azurosome. Released, NE binds to F-actin filaments and degrades the cytoskeleton. Afterwards, MPO triggers translocation of NE to the nucleus, facilitated by the absence of F-actin, where it binds to histones. NE proteolytic activity processes histones, favoring chromatin decondensation. NE translocation to the nucleus is necessary for NET formation, as NE-knock out murine cells did not present nuclear decondensation and NET formation (Metzler et al., 2014; Parker et al., 2012; Stoiber et al., 2015; Ermert et al., 2009; Björnsdottir et al., 2015; Martinod et al., 2016). Another process necessary for NET formation is the deamination or citrullination of histones through the protein arginine deiminase type 4 (PAD4). PAD4 is the only isoform of PAD that can be found in the nucleus. This nuclear enzyme citrullinates arginine residues on histones, converting positively charged amine groups to neutral ketones. After citrullination, histones lose affinity to DNA, allowing the packed chromatin to decondense (Papayannopoulos et al., 2010; Metzler et al., 2014; Wong and Wagner, 2018; Li et al., 2010). Branzk et al. (2014) showed that NET formation is probably dependent on pathogen size, as observed by the hyphae and yeast-state of fungi. This could be due to an intracellular machinery competition for access to the antimicrobial protease NE between NETosis and phagocytosis. Smaller microorganisms would be preferentially taken by phagocytosis, where NE would fuse to the phagosomes and avoid

nuclear translocation. Larger pathogens would not be phagocytized and NE would be directed to the nucleus, committing cells to NETosis (Papayannopoulos, 2017). However, other studies showed that NETs are also generated upon microbial infections, such as *Salmonella enterica*, *Shigella flexneri*, *S. aureus* and *Candida albicans* (Beiter, et al. 2006; Halverson et al., 2015; Moorthy et al., 2013; Papayannopoulos and Zychlinsky, 2009). PMA is one of the most used and better described pharmacological stimulator of NETosis. It can activate many different pathways in the cell, including protein kinase C (PKC). Many other stimuli are able to activate a signal transduction pathway via PKC, such as bacterial antigens, cytokines, LPS and chemoattractants. Activated, PKC triggers cytoplasmic calcium elevation and activate mitogen-activated protein kinase (MAPK) members of the canonical Raf-mitogen-activated protein kinase kinase (MEK)-extracellular signal-regulated kinases (ERK) pathway by phosphorylation and subsequently, NOX enzymes (Kaplan and Radic, 2012; Papayannopoulos, 2017; Gray et al., 2013). Neutrophils present 2 members of the MAPK family, the ERK1/2 and p38 MAPK, which are upstream of the superoxide formation. These molecules are necessary for NET formation, once their inhibition can affect ROS production and prevent NETosis (Hakkim et al., 2011; Keshari et al., 2013). Many authors have described production of NET-like structures by distinct cell types, such as eosinophils and mast cells, leading to a more general classification of the process as ETosis. In all cases, ET formation was shown to be dependent on ROS production, as observed in neutrophils (Brinkmann and Zychlinsky, 2012; Branzk and Papayannopoulos, 2013; Yousefi et al., 2008).

Neutrophils undergo several morphological changes during the process of NETosis. Upon stimulation, the cell flattens and strongly attaches to the ground. This was shown to be an important feature for proper cellular activation, as detached cells do not get the same level of stimulation and NET formation. Afterwards, neutrophils lose their typical nuclear lobes with chromatin decondensation. Later, all internal membranes disappear, allowing the nuclear and the cytoplasm content to mix, before membrane rupture and material release in the extracellular space (Nakazawa et al., 2017; Brinkmann et al., 2004; Fuchs et al., 2007). Intravital microscopy have shown that neutrophils can also release NETs without cell membrane rupture, in a process known as vital NETosis. Neutrophils exposure to *S. aureus* or *E. coli* together with platelets could lead to the release of their chromatin and granular contents rapidly, within minutes (Figure 4). As a result, an enucleated cytoplasm could freely crawl and further phagocytize pathogens (McDonald et al., 2012; Apel et al., 2018; Yipp et al., 2012; Yousefi et al., 2009).

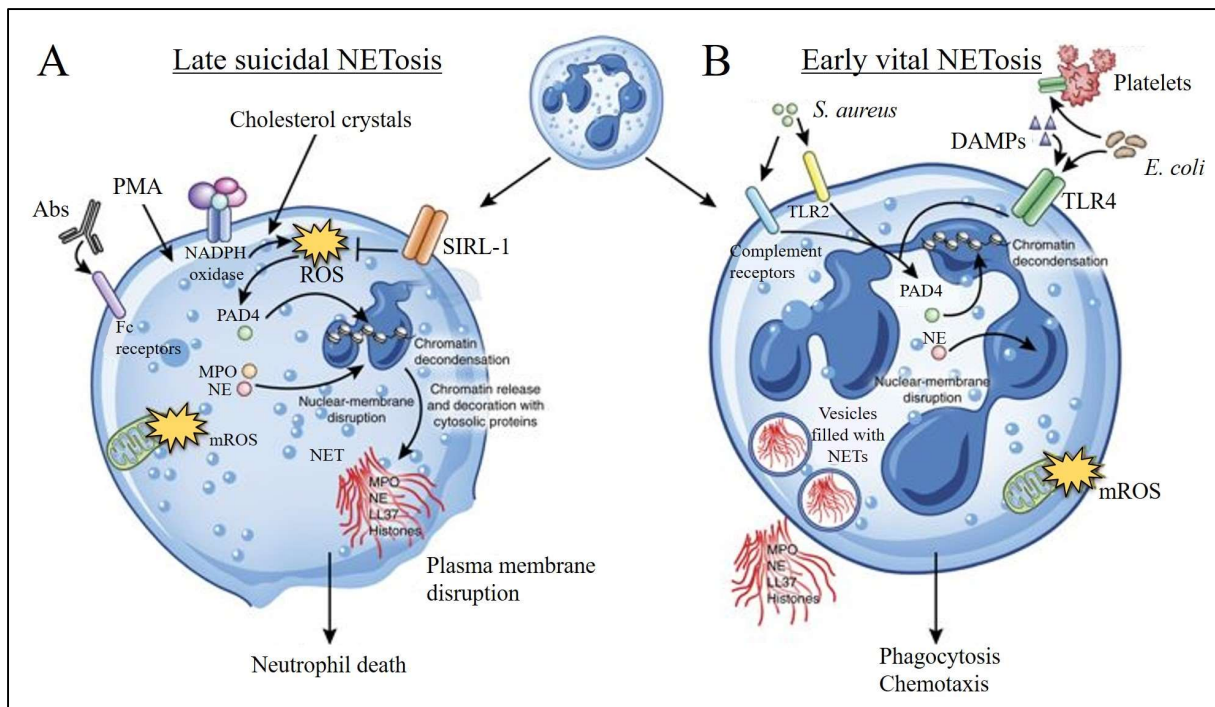


Figure 4: Mechanisms of NET formation. Neutrophils undergo NETosis through different mechanisms depending on the stimulus received. (A) The classical mechanism of suicidal NETosis is characterized by the final rupture of the cellular membrane with release of the nuclear content together with cytotoxic proteases. (B) The vital NETosis, observed in some specific cases, as stimulation by *S. aureus*, leads to release of vesicles containing NET structures without cell-membrane rupture. This allows the enucleated cell to further provide its basic functions, as phagocytosis (adapted from Jorch and Kubes, 2017). DAMPs (Danger Associated Molecular Patterns), TLR (Toll-like Receptors), Abs (Antibodies), PMA (Phorbol-12-Myristate-13-Acetate), MPO (Myeloperoxidase), NE (Neutrophil Elastase), PAD (Protein Arginine Deiminase), ROS (Reactive Oxygen Species), SIRT (Signal Inhibitory Receptor on Leukocytes).

1.7. NETs and pneumonia

Upon infection and inflammation of the lung, neutrophils are promptly recruited to the alveolar space and become the main effector cells responsible for bacteria clearance. Although these cells are professional phagocytes and efficient in bacterial clearance, their accumulation and exacerbated activation can lead to uncontrolled inflammation and tissue injury (Dockrell et al., 2012; Kantrow et al., 2009). The vascular endothelium extended around the alveoli is a cellular barrier that has a crucial role in maintaining the integrity of the vessels and controlling the exchange of small molecules between the vascular space and the alveoli. Increased endothelial permeability is a hallmark of almost every acute inflammatory disorder, resulting in extravasation of fluid, plasma molecules and inflammatory mediators into the tissue. This results in edema formation and subsequent organ dysfunction. Increased permeability is

specially critical in the context of the lungs, where edema may compromise gas-exchange functions, deteriorating the state of the disease (Temmesfeld-Wollbruck et al., 2007; Matthay et al., 2012). Together with the pro-inflammatory mediators released by activated neutrophils, it has been shown that NETs are highly cytotoxic to the tissue and directly damage lung epithelial and vascular endothelial cells. DNA and extracellular histones are important pro-inflammatory mediators, once they are recognized as DAMPs by the immune system, activating TLR-signaling cascades and the NLRP3 inflammasome (Gray, 2018; Grailer et al., 2014). NET production may also contribute to barrier dysfunction, playing some role in the complications of acute lung injury (ALI), ARDS and the associated extra-pulmonary organ damage (Cortjens et al., 2016; Narasaraju et al., 2011) (Figure 5). High levels of NETs in plasma from ARDS patients were greatly correlated with increased inflammation, organ damage and the worst outcome of the patient (Lefrancais et al., 2018). During the life-saving strategy of MV, NET formation was also associated with local alveolar inflammation and has been implicated in the pathogenesis of VILI (Mikacenic et al., 2018). Yildiz and colleagues (2015) showed that breakdown of NET structures in the lungs after MV could be protective, ameliorating gas exchange (Porto and Stein, 2016). *S.pn.* has many antigens that can trigger NET production in neutrophils. PLY was described to induce neutrophils to produce NETs in a rapid mechanism independent of ROS and TLR4 recognition (Nel et al., 2016). The surface protein α -enolase produced by *S.pn.* to facilitate bacterial invasion, is also involved in neutrophil activation, inducing NET formation (Mori et al., 2012; Hazeldine et al., 2014). Interestingly, *S.pn.*, like *S. aureus* and *P. aeruginosa*, have developed mechanisms to evade NETs and avoid their killing. Modifications of the bacterial cell surface is an important strategy used by the bacteria to avoid NETs. Their polysaccharide capsule is able to reduce binding of the bacteria to NETs and by this way avoid its toxicity (Beiter et al., 2006). Moreover, these pathogens secrete catalase, which can suppress the ability of neutrophils to produce NETs. Secretion of endonucleases, as EndA, is also a powerful strategy for NET evasion, with degradation of the extracellular DNA and further extravasation towards the circulation (Beiter et al., 2006; Halverson et al., 2015; Moorthy et al., 2013; Papayannopoulos and Zychlinsky, 2009).

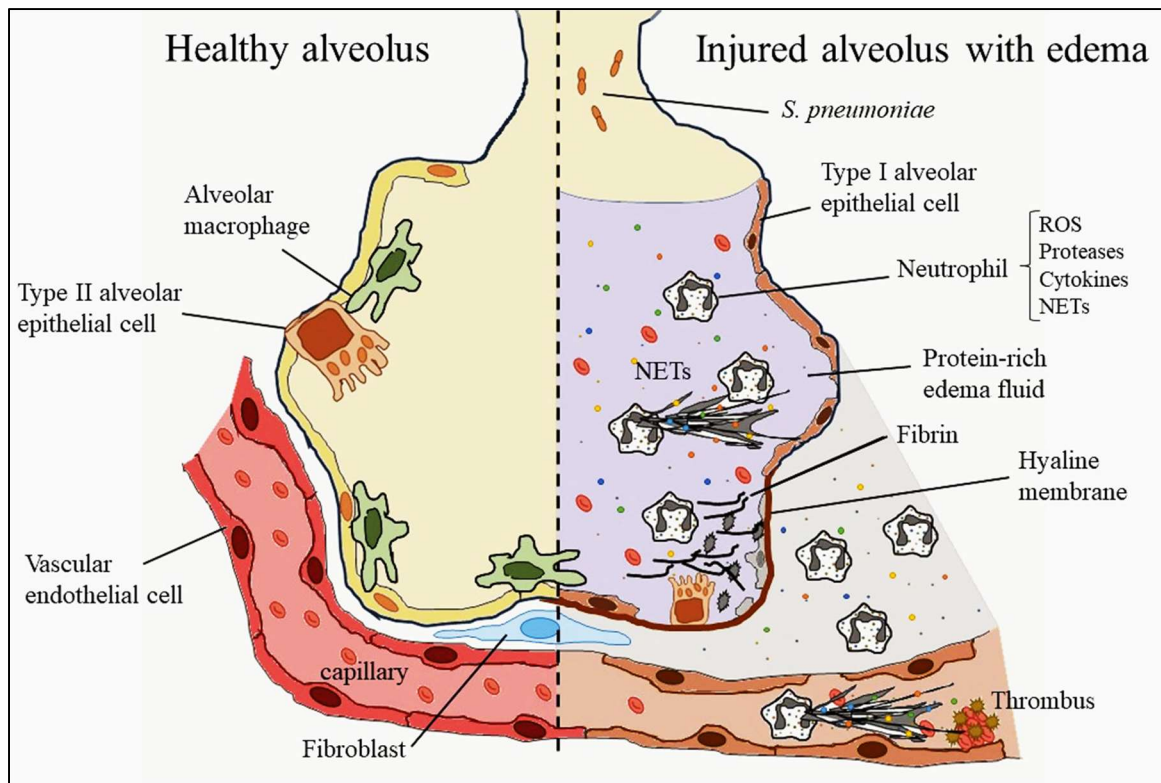


Figure 5: Neutrophils in the pathogenesis of acute respiratory distress syndrome (ARDS). Uncontrolled inflammation and generation of multiple pro-inflammatory molecules contribute to the injury of the alveolar-capillary barrier, leading to edema formation and the onset of ARDS (right side of the figure). Neutrophils are particularly involved in lung tissue damage through secretion of various inflammatory mediators which, together with NETs, are highly cytotoxic to lung epithelial and endothelial cells (adapted from Matthay & Zimmerman, 2005).

1.8. NET formation and related complications

NETs are described as the double-edged sword of the innate immunity because of their essential role in bacteria clearance and their many negative cytotoxic effects. Therefore, its production and accumulation must be tightly regulated in order to prevent tissue pathologies (Kaplan and Radic, 2012). It is believed that NETs persist for several days at the site where they were produced, before being dismantled by plasma secreted nucleases, as DNase I (Apel et al., 2018). Macrophages are also involved in this clearing process via phagocytosis of NET fragments (Papayannopoulos, 2017; Nakazawa et al., 2016). NET production can modulate immune cells to release great amounts of pro-inflammatory molecules and activate the complement system. In these cases, a hyper-inflammatory process initiates and elevated levels of cell-free DNA is found in the tissue. If this inflammatory disorder is not precisely regulated and removal of NET components fails, inflammatory or autoimmune diseases may originate (Gould et al., 2015).

NETs were linked to many inflammatory and autoimmune diseases, as sepsis, thrombosis, cystic fibrosis (CF), systemic lupus erythematosus (SLE), rheumatoid arthritis (RA), anti-neutrophil cytoplasmic antibody (ANCA)-associated vasculitis (AAV) and even influencing tumor metastasis initiation (Yuen et al., 2016; Gould et al., 2015; Menegazzo et al., 2018).

Sepsis and trauma. Sepsis is a life-threatening condition characterized by systemic inflammation and activation of coagulation pathways in response to microbial infection. Mortality rate can reach 50% in adults and 70% in children, being the most common cause of mortality in intensive care units. In trauma, increased levels of circulating DNA originated from tissue necrosis and cell death can be detected, which is capable of inducing systemic inflammation. DNA levels found in the vasculature are elevated in sepsis and trauma and originate partly from activated neutrophils (McDonald et al., 2012). NETs are produced in small vessels and sinusoidal capillaries in different tissues during sepsis, helping in the capture of bacteria, preventing its dissemination. However, these DNA structures can cause collateral damage if accumulated in the microcirculation during sepsis, being related to hepatic damage and organ failure (McDonald et al., 2012; Clark et al., 2007).

Thrombosis. Thrombosis is described as the activation, adhesion and aggregation of platelets in the microvasculature, leading to vascular occlusion. Thrombus formation is associated to infection and inflammation of the vasculature and it is enhanced by endothelial dysfunction. During sepsis, NETs are released in the vasculature and provide a scaffold facilitating thrombus formation and tissue damage. NETs are also essential in providing pro-thrombotic stimulus for platelet binding and aggregation. Targeting NETs with DNase or anti-histone antibodies was sufficient to disrupt platelet aggregates and were protective in disease development (De Meyer et al., 2012; Fuchs et al., 2010).

Cystic fibrosis. CF is a fatal hereditary disorder that occurs due to a mutation in the CF transmembrane conductance regulator (CFTR) anion channel. This channel promotes the transport from chloride ions across the epithelial layer of the airways, necessary for mucus production. CF patients have an uncontrolled production of abnormal thick mucus, which may obstruct the airways and provide colonization of bacteria. *P. aeruginosa* is the main bacterium infecting CF patients. Increased neutrophil infiltration to the lungs and release of NETs is seen, which may lead to an enhanced pulmonary inflammation and tissue dysfunction. Chronic inflammation contributes to the high morbidity and mortality rates (Akong-Moore et al., 2012).

Rheumatoid arthritis, SLE, vasculitis and gout. RA is a chronic systemic immune disease, characterized by synovial joint inflammation, bone destruction and presence of autoantibodies (Zhong et al., 2007). Neutrophils from RA-patients undergo spontaneous NET formation, enhancing DAMP release and inflammation (Apel et al., 2018; Chowdhury et al., 2014). Interestingly, autoantibodies are mainly directed against NET components, as dsDNA, histones, MPO, PR3 and NE. SLE is a multifactorial autoimmune disease affecting different organs. Pathogenesis combines dysregulated innate and adaptive immune responses with intolerance to self-antigens, aggravating articular inflammation. Normally, SLE patients have an impaired clearance of neutrophils by macrophages with an increased generation of NETs and nuclear free antigens (Apel et al., 2018; Spronk et al., 1996). Vasculitis and small-vessel vasculitis are chronic diseases that present inflammation of blood vessels, sometimes accompanied by necrotizing cell death. Presence of autoantibodies and inflammatory events are common to the disease. Around 90% of the autoantibodies are against proteins located in the cytoplasm of neutrophils as for SLE, therefore ANCA-associated vasculitis (Hakkim et al., 2010; Apel et al., 2018; Macanovic et al., 1996). Gout is the inflammation caused by precipitation of uric acid in the form of needle-shape monosodium urate crystals. Inflammasome activation by such crystals leads to a rapid inflammatory process with increased neutrophil recruitment to the synovial fluid and synovium which leads to intense clinical symptoms during an acute gout attack. In gout, NET formation was observed after crystal stimulation, accumulated in bigger structures denominated aggregated NETs (Maueröder et al., 2015). A common feature among these autoimmune diseases is the generation of autoantibodies targeting typical molecules of neutrophils. NETs are therefore great targets for the treatment of these disorders. Inhibition of NETosis and neutralization of NET molecules are beneficial in reducing autoantibody formation (Kessenbrock et al., 2009; Wang et al., 2015; Kusunoki et al., 2016).

Cancer. Cancer patients normally do not die from their original primary cancer, but from metastases that arise in distant tissues. Disseminated cancer cells can remain dormant for long periods of time before awaking and originating metastatic cancer. Inflammation was shown to have an important role in activating cancer cells from dormancy, promoting metastasis initiation. Upon LPS and tobacco smoke-induced lung inflammation, NETs and inflammatory factors produced by neutrophils were important for awaking dormant cells to cause metastasis in mice. In a vicious cycle, NETs can also further induce cancer growth. Neutrophil depletion and NET inhibition or depletion with DNase were efficient in preventing metastasis initiation (Wong and Wagner, 2018; Parker et al., 2011).

1.9. Therapies targeting NET formation

The standard treatment used for many of the inflammatory and autoimmune diseases described above is the suppression of the immune responses with glucocorticoids and other activity modifying drugs. These strategies can also influence NET generation and thus reduce the formation of autoantigens. Targeting NETs directly by neutralization of proteases or histones and treatment with DNase are interesting strategies to reduce autoantigen generation and local inflammation (Apel et al., 2018; Saffarzadeh and Preissner, 2013). The use of DNase, which aims the breakdown of the DNA backbone structure, is the most commonly used strategy and has high therapeutic potential in ameliorating inflammation (Zeerleder et al., 2014; Gould et al., 2015). Treatment with DNase or anti-histone antibodies was efficient in reducing lung injury and ameliorating lung oxygenation in ALI and ARDS (Sayah et al., 2015; Caudrillier et al., 2012). Inhibiting the process of NETosis with PAD4 inhibitors that prevent chromatin decondensation is also a widely used strategy. This approach is particularly interesting, because basic functions of neutrophils, as phagocytosis and degranulation, remain unaffected. Many inhibitors have been described for the inhibition of PAD activity, as the pan-PAD inhibitor Cl-amidine and the PAD4-specific inhibitor GSK484. They were shown to inhibit efficiently histone citrullination and NET formation in human and in murine models of LPS-induced endotoxemia, cancer-associated kidney injury and arthritis, leading to reduction of NET-mediated inflammation, tissue dysfunction and lethality (Kusunoki et al., 2016; Lewis et al., 2015; Chaput and Zychlinsky, 2009; Abrams et al., 2013; Liang et al., 2018; Cedervall et al., 2017). Histones released together with NETs also have great pro-inflammatory capacities. They were shown to be highly cytotoxic to endothelial and epithelial cells due to their cationic properties, compromising cell membrane integrity (Narasaraju et al., 2011; Saffarzadeh et al., 2012; Cortjens et al., 2016). Histones are frequently used as potential biomarkers for disease progression and are interesting targets for therapeutic treatment (Saffarzadeh et al., 2012; Xu et al., 2009; Monestier et al., 1993). Treatment of sepsis and other inflammatory diseases with the aim of neutralizing histones proved to be highly effective in reducing tissue injury. The activated protein C (APC) is a plasma serine protease that can act in diverse processes, inhibiting coagulation and apoptosis. APC degrades extracellular histones released with NETs, being effective in attenuating inflammation in thrombosis and sepsis. However, due to its many distinct properties, APC may also increase risk of internal bleeding (Wen et al., 2013; Xu et al., 2009). Polysialic acid (PSA) is a homopolymer of 2.8-linked sialic acids found in innumerable organisms, expressed in different cell types and exhibiting a wide diversity in structure and functions. It was firstly described in *E. coli* as a sialic acid, the colominic acid, which is also

found in humans. It is normally linked to mammalian glycoproteins present on cell surface of neurons, immune cells and in hematopoietic progenitor cells. PSA is normally attached to the protein scaffold neural cell adhesion molecule (NCAM), typically found in NK and NKT cells, which undergoes posttranslational modifications upon contact with PSA. Only 4 protein were described to bind this molecule, showing its highly selective scaffold choices (Drake 2008). Upon binding, it can alter many distinct cellular functions, such as cell adhesion, migration and cytokine response. *In vitro* and in a mice model of acute lung inflammation after LPS stimulation, PSA was efficient in neutralizing histone cytotoxicity, minimizing organ damage and reducing mortality (Saffarzadeh et al., 2012; Ulm et al., 2013).

1.10. Adrenomedullin

Adrenomedullin (ADM) is a biologically active endogenous peptide discovered in pheochromocytoma, a neuroendocrine tumor of the medulla of adrenal glands, that can activate second messengers, as the adenosine 3',5'-cyclic monophosphate (cAMP). ADM and its receptors were found to be expressed by different cell types of the immune system, as macrophages, monocytes and T-cells, but also in cells from heart, lung, kidney, adipose tissue and the vascular endothelium. It acts as a circulating hormone, inducing many biological processes in a paracrine or autocrine way (Idrovo et al. 2015). ADM consists of 52 amino acid, belonging to the calcitonin gene-related peptide (CGRP) superfamily due to sequence similarities to CGRP. It is recognized simultaneously by two types of receptors, the calcitonin receptor-like receptor (CRLR) and a receptor activity-modifying protein (RAMP). The different peptides from the CGRP family are recognized by different RAMP receptors, associated to a common CRLR protein. ADM is specifically recognized by CRLR together with RAMP2, but similarities between the RAMP receptors have shown a degenerated response by non-specific receptors, as with RAMP1 (Kuwasako et al., 2012). After peptide binding, the CRLR-RAMP complex activates a G-protein coupled receptor, further activating different regulatory pathways in the cell. It is known that calcium ion concentration and cAMP levels are increased upon ADM/CGRP binding, showing a connection from G-proteins to adenylyl cyclase. Since its discovery by Kitamura et al. (1993), many pharmacological studies have been done showing its highly pleiotropic actions, with distinct roles in modulating biological functions in various cell types, tissues or organs. Studies in angiogenesis also showed the importance of ADM for the normal embryonic development, due to an impaired vascular development in its absence (Kato and Kitamura, 2015). However, *in vivo* studies have faced a problem with its bioavailability, where it is rapidly degraded within minutes by proteolytic enzymes. Peptide

modifications made in the attempt to increase the half-life of this molecule achieved a 7 to 8-fold increase in its viability (Kubo et al., 2014; Gonzalez-Rey et al., 2006). Many bench-to-bedside pharmacological studies have shown enhanced levels of ADM in plasma during severe inflammation. Therefore, ADM is thought to have a potent immunomodulatory role, attenuating the inflammatory response and restoring homeostasis (Gonzalez-Rey et al., 2006; Pleguezuelos et al., 2004). Multiple mechanisms could be responsible for this protective role, including suppression of the signal transduction Akt pathway and the oxidative stress and inhibition of apoptosis in some cell types (Hamid et al., 2010; Kato and Kitamura, 2015). ADM promotes vascular protection in acute inflammation and infections by preventing inter-endothelial cell gap formation and inducing vasodilation, resulting in stabilization of the endothelial barrier, with a decrease in vascular leakage and edema formation, and reducing organ dysfunction (Temmesfeld-Wollbruck et al., 2007; Hippenstiel et al., 2002; Kato and Kitamura, 2015). Murine studies in ARDS/ALI, sepsis, systemic inflammatory response syndrome and inflammatory bowel disease showed that ADM has an important role as an anti-inflammatory peptide, affecting secretion of pro-inflammatory mediators in the tissue, reducing infiltration of inflammatory cells and protecting lung, liver and gut (Gonzalez-Rey et al., 2006; Müller-Redetzky et al., 2014; Muller et al., 2010; Agorreta et al., 2005; Dackor and Caron, 2007).

2. Aim

DAMPs are known to have strong pro-inflammatory properties, being highly cytotoxic to the host. In pneumonia, DAMPs are also produced after infection of the respiratory tract by the infiltrating neutrophils in the form of NETs. NETs are of great importance for the organism because of their role in pathogen clearance. However, their many cytotoxic components can lead to further inflammation and increased tissue damage. Controlling the amount of NETs released in the tissue after infection could have a major impact in reducing pulmonary inflammation and lung injury. This study aimed to investigate whether NETs are produced by activated neutrophils in pneumococcal pneumonia and to understand the role of NETs in the pathogenesis of pneumonia and the related lung tissue injury. Therefore, NETs were targeted with different potential therapeutic substances to reduce their cytotoxicity, thus minimizing lung injury and extra pulmonary organ damage. Müller-Redetzky et al. (2014) showed in a combined murine model of pneumococcal pneumonia and VILI that ADM was able to improve lung functions by decreasing vascular permeability and protecting mice against tissue injury. ADM is an interesting multifunctional peptide with an important role as anti-inflammatory mediator and able to restore tissue homeostasis. In this model, no decrease in bacterial burden, neutrophil infiltration and the production of important pro-inflammatory cytokines was seen after treatment with ADM. Treatment with ADM led to a substantial decrease in the amount of NETs accumulating in the lungs. Therefore, we wondered if this peptide could also affect neutrophil effector functions, and thus aimed to analyze whether ADM could lead to a reduction in the generation of NETs, being protective in lung tissue inflammation after pneumococcal infection.

3. Material and Methods

3.1. Mice and ethical approval

Animals used in this study were obtained from Charles River (Charles River Laboratories, Sulzfeld - Germany and Écully - France) and Janvier Labs (Le Genest -Saint-Isle - France). Conditions for housing and handling of the animals were approved by the German Office for Health and Social Affairs in Berlin (LAGeSo), aiming to minimize animal stress. Mice were kept under specific pathogen-free conditions at the internal animal facility at Charité - Universitätsmedizin Berlin (Berlin - Germany) prior to experiment, with a 12/12 hours (h) light/dark cycle, with temperature around 23°C and humidity close to 40%. The animals used were all wild type (WT) C57BL/6J, 9-10 weeks old female mice, weighting between 19-22g.

3.2. *In vivo* murine model of pneumococcal pneumonia

a) Treatment strategies

The *in vivo* model of pneumococcal pneumonia was used with the aim to study the development of the acute inflammation of the lungs caused by bacterial infection and the subsequent sequela with lung injury, bacteremia and extra-pulmonary tissue damage. To understand the deleterious role of NETs in the pathogenesis of pneumonia, including their main components DNA and histones, three different treatment strategies were applied, aiming at inhibition of NET formation, its degradation or neutralization of its cytotoxic components. In a first set of the experiments, mice were treated with 5mg/kg bodyweight DNase I (AppliChem, Germany) aiming at the disintegration of the DNA structure and thereby decreasing its cytotoxicity to the host. Secondly, NETosis was blocked by inhibition of histone H3 citrullination with 20mg/kg bodyweight of the PAD4-inhibitor GSK484 (Cayman Chemical Company, USA). This not only prevented the DNA cytotoxicity, but also the release of NET-associated, potentially toxic, proteins, not affecting further neutrophilic effector functions. As a last strategy, also targeting the chromatin, the histone neutralizing molecule PSA (Sigma-Aldrich Chemie GmbH, Germany) was applied at 100mg/kg bodyweight. All treatments were performed with an intra-peritoneal (i.p.) injection of the substance, immediately before infection of the animals and every 12h after infection until 12h prior to final mouse preparation. Control mice received the same volume of the substance diluent, 0.9% NaCl (B. Braun, Germany). Treatment with the hormone-peptide ADM was performed in the combined model of pneumococcal pneumonia and MV, as previously described by Müller-Redetzky et al. (2014). Briefly, 24h after infection

with *S.pn.*, mice were prepared for ventilation and intubated in the MiniVent machine (Hugo-Sachs-Electronics, Germany). Mice were ventilated for 6h with a tidal volume of 12mL/kg bodyweight with a respiratory rate of 120 breaths/minute and a positive end-expiratory pressure of 2cm H₂O for VILI generation and had a continuous infusion of 0.05mg/kg/h ADM (Phoenix pharmaceuticals, Germany) through a catheter fixed to the carotid artery.

b) Bacteria culture

The bacteria strain used for infection of the mice was the Gram-positive bacterium *Streptococcus pneumoniae* serotype 3, strain PN36. The day before infection, a small amount of bacteria was collected from frozen medium (20% glycerol (Merck, Germany) in Todd Hewitt Broth (BD, Germany) medium supplemented with 0.5% yeast extract (THY medium)), plated on Columbia agar plates with 5% sheep blood (BD, Germany) and allowed to grow for 8-10h at 37°C with 5% CO₂. Viable colonies were transferred to THY medium added to 10% fetal calf serum (FCS; Gibco, USA) until an optical density (OD) of 0.03-0.04 at 600nm. Bacteria were grown to mid-log phase at 37°C in water bath for around 2h until an optimal OD of 0.3-0.4, which corresponds to an amount of 0.3-0.4 x 10⁹ colony-forming units (CFU) per mL. Total bacteria number was calculated, solution was centrifuged with 3100rpm without breaks at room temperature (RT) and pellet resuspended in phosphate-buffered saline (PBS; Gibco, USA) for a concentration of 1 x 10⁹ CFU/mL. Serial dilution of 1:10 with PBS was made until 5 x 10¹ CFU/mL. Lower concentrations of this serial dilution were plated on blood agar plates for bacteria concentration control and the higher concentration used for infection of the mice.

c) Intranasal infection

Infected and mock-infected mice were divided into 8 groups with two distinct time-points, 24h and 48h, and animals received one of the specific treatments described above or the same volume of 0.9% NaCl solution, as control. Body weight and temperature of all mice were documented before infection and animals were monitored every 12h after infection until final preparation to characterize disease progression. Mice were anesthetized i.p. with 3mL/kg of a mixture of 100mg/mL ketamine (CP-pharma, Germany) and 20mg/mL xylazine (CP-pharma, Germany), diluted in 0.9% NaCl solution according to their weight. Under anesthesia and without reflexes, mice were hanged by their teeth on a line to reach a vertical position and allow exposure of their nostrils. To avoid eye dryness, a small portion of 3mg/g Thilo-tears gel (Alcon, USA) was applied in the ocular region of the animals. The bacteria solution was diluted 1:1 with Hyaluronidase (Sigma-Aldrich Chemie GmbH, USA) to facilitate bacterial colonization of the lungs and mice were infected intranasally with 20µL of bacteria. The mock-infected control group was inoculated with the same volume of PBS. Infection was performed

in two steps, to avoid blockage of the nasal cavity of the mouse. Altogether, mice were infected with 5×10^6 CFU *S.pn.* and placed back in cages heated with infrared light, for the waking phase after infection.

d) Animal preparation

One hour before sacrifice, a solution of 13.34mg/mL human serum albumin (HSA; Baxalta, USA) diluted in 0.9% NaCl was applied into the caudal vein for the posterior permeability quantification assay. After 1h resting time, animals were anesthetized with 80µg/g bodyweight ketamine and 25µg/g bodyweight xylazine for preparation. Under deep narcosis, animals were fixed on a working surface with needles and prepared for lung ventilation. Stomach area was opened parallel to body length until trachea region and skin were fixed with needles. The muscle tissue covering the trachea was carefully separated with forceps, avoiding collapse of the arteries and the trachea was released. To fix the ventilator tube, a surgical thread was passed around the trachea. Using fine dissection scissors, a small incision was made at the posterior part of the trachea, the ventilation tube was inserted into the trachea and fixed by the surgical knot. Ventilation was performed with a MiniVent machine (Hugo Sachs Elektronik, Germany) with 150µL stroke volume at 150 strokes per minute. To avoid blood coagulation, 5000 i.E./mL heparin (Rotexmedica, Germany) diluted 1:1 with NaCl were injected directly into the heart and after 1 minute, blood was collected from the *Vena cava caudalis* in a tube containing ethylenediaminetetraacetic acid (EDTA)-K (Sarstedt, Germany). Small blood aliquots were kept for bacteria counting and for flow cytometry with the fluorescence-activated cell sorting (FACS) analysis. For FACS analysis, erythrocyte lysis was performed prior to staining with red cell lysis buffer (containing 0.01M KHCO₃, 0.155M NH₄Cl and 0.1mM EDTA diluted in distilled water). The remaining blood was centrifuged at 4°C for 10 minutes with 4000 x g and the plasma collected was frozen for quantification of cytokines, NETs, lung permeability and extra-pulmonary organ damage parameters. After death of the animals, the diaphragm was cut to release lung and the thorax was opened through the sternum. The connective tissue was removed for the detachment of the lung. The ventilation tube was separated from the ventilator and a small syringe with PBS containing cOmplete Mini protease inhibitors (Roche Diagnostics GmbH, Germany) attached for the acquisition of the bronchoalveolar lavage fluid (BALF). Two lavages were performed with 800µL each and stored separately for independent analysis. A small aliquot from the first lavage was used for bacteria counting and FACS analysis and both tubes were centrifuged for 10 minutes at 4°C with 300 x g. Supernatant was frozen in liquid nitrogen for later analysis of the different parameters. For lung perfusion, inferior vena cava in the thorax region was cut and the heart was washed with PBS in the right ventricle until the

lung became whitish to avoid blood cell contamination of the sample. The left lung was isolated and immediately frozen for mRNA isolation. The right lung with the four lobes was prepared and kept in a solution of PBS and protease inhibitors, similarly to liver and spleen. These organs were cut into smaller pieces and homogenized through a 100µm filter for cell analysis and CFU counting. Tissue solution was centrifuged at 1100 x g for 10 minutes at 4°C and supernatant frozen for further analysis.

e) Bacteria quantification

The bacteria concentration after infection in blood, BALF, liver, spleen and lung were calculated by counting the CFU in Columbia blood agar plates after a serial dilution. Tissue homogenate or fluid was diluted 5 times 1:10 and plated with a known volume in the blood agar plates and incubated overnight (ON) at 37°C. Bacteria colonies were counted and the total concentration for each tissue calculated.

3.3. Permeability quantification

The permeability of the pulmonary vascular barrier was assessed by three distinct methodologies. The first assay quantifies the total amount of proteins present in the alveolar space, which increases upon breakdown of the alveolar/vascular barrier. The DCTM Protein Assay (Bio-Rad Laboratories Inc., USA) reagents were mixed with BALF samples or standards, according to the manufacturer's instructions and incubated for 15 minutes at RT. After reaction, the plate was analyzed at 750nm using a plate reader SpectraMax M2^e (Molecular Devices, USA). The second and third methodology are based on the continuous leakage of the HSA applied into the caudal vein 1h prior to mouse preparation or the mouse serum albumin (MSA) present in the alveolar space, according to the level of tissue damage. The specific mouse albumin and the human albumin enzyme-linked immunosorbent assay (ELISA) quantitation kit (BETHYL laboratories, USA) were used according to the manufacturer's instructions. Briefly, a 96-well ELISA plate was coated with a primary antibody against human or murine albumin diluted in 0.05M carbonate-bicarbonate buffer and left ON at 4°C. Plate was washed several times with PBS containing 0.05% Tween 20 (Sigma-Aldrich Chemie GmbH, USA), 0.14M NaCl and 50mM Tris (Carl ROTH GmbH, Germany). Blocking was performed with PBS containing 1% bovine serum albumin (BSA; Sigma-Aldrich Chemie GmbH, USA), 0.14M NaCl and 50mM Tris for 30 minutes. After additional washing steps, different dilutions of BALF, plasma samples and standards were added and incubated at RT on an orbital shaker for 1h. The plate was washed again and a secondary antibody coupled to horseradish-peroxidase (HRP) was added and incubated on a shaker for 1h at RT. After washing, the 3,3',5,5'-

tetramethylbenzidine (TMB) substrate solution 1x (eBioscience, USA) was added. After approximately 15 minutes at RT, the reaction was stopped with a solution of 2M H₂SO₄. The plate was read at 450nm wavelength using a plate reader and the ratio between HSA/MSA measured in BALF and plasma was calculated.

3.4. Cytokine and chemokine quantification

Quantification of cytokines from both BALF and plasma samples was performed with the ProcartaPLEX multiplex immunoassay (Invitrogen, USA). Six different cytokines and chemokines known to play an important role in inflammation were evaluated. Expression of IL-1 β , growth-regulated oncogene (GRO) α (known as CXCL1 in humans), IL-6, the MIP-1 α and MIP-2 (known as CCL3 and CXCL2 in humans, respectively) and TNF α were assessed by this assay. Samples and specific capture magnetic beads were added according to the manufacturer's instructions and analyzed using a Bio-Plex Array System (Bio-Rad Laboratories Inc., USA).

3.5. Histology

Mice infected with *S.pn.* or mock-infected control animals, treated with the different substances described previously were also prepared for histology. Lung, liver, kidney, thymus, heart, intestine and spleen were carefully isolated to avoid tissue damage, disposed in Rotilabo embedding cassettes (Carl ROTH GmbH, Germany) and immersed in 4% formalin (Labochem International, Germany) for later embedding in paraffin. Sections of the paraffin block were made and prepared for immunostaining. Typical NET-proteins were stained with a primary neutrophil elastase antibody (Abcam, United Kingdom) or citrullinated histone H3 (Abcam, United Kingdom) at 0.8 μ g/mL. A secondary antibody Alexa 488nm-conjugated goat anti-rabbit IgG (Molecular Probes, USA) was used at 1:4000 and the DNA marker 4',6'-diamidino-2-phenylindole (DAPI; Carl ROTH GmbH, Germany) was used at 0.5 μ g/mL. Characterization of disease progression and presence of NETs was performed in histological sections in the different organs.

3.6. Flow Cytometry

Flow cytometry was used to phenotypically characterize the cells obtained from the different compartments in the mouse model of pneumococcal pneumonia and isolated for the *in vitro* experiments. The *in vivo* cell populations and the isolated neutrophils from mice and human were labeled with the following monoclonal Abs: phycoerythrin (PE) anti-F4/80 (BM8) and

anti-CD18 (M18/2), PE-cyanine 7 (PE-Cy7) anti-CD11b (M1/70), Alexa Fluor 700 (A700) anti-MHC Class II (I-A/I-E) (M5/114-15-2) (purchased from eBioscience, USA), A700 anti-CD3 (17A2) (Invitrogen, USA), fluorescein isothiocyanate (FITC) anti-Ly-6G (1A8), Brilliant Violet 510 (BrV510) anti-Ly-6C (HK1.4) (purchased from BioLegend, USA), Alexa Fluor 647 anti-NOS2 (C-11) (Santa Cruz Biotechnology, USA), FITC anti CD3e (145-2C11), anti-CD19 (1D3), anti-NK1.1 (PK136), BrV510 anti-CD19 (1D3), Brilliant Violet 421 (BrV421) anti-Siglec-F (E50-2440), Pacific Blue V450 anti-Ly-6C (AL-21), anti-Ly-6G (1A8), peridinin chlorophyll protein (PerCP) anti-CD45 (30-F11), PerCP-Cyanine 5.5 anti-Ly-6G (1A8), anti-Siglec-F (E50-2440), APC anti-NK1.1 (NKR-P1B/NKR-P1C) (PK136), anti-CD11c (HL3) (purchased from BD Bioscience, Germany) and APC anti-CD62L (Mel14) (conjugated at the MPI for Infection Biology - Berlin). Quantification of cell number from the *in vivo* samples was performed by addition of counting beads (Invitrogen, USA). Intracellular staining of cytokine-inducible nitric oxide synthase (iNOS) was performed after fixation with 1% formalin (formaldehyde solution from paraformaldehyde - PFA; Sigma-Aldrich Chemie GmbH, USA) for 30 minutes at RT and permeabilization with 2% saponin (Sigma-Aldrich Chemie GmbH, USA) for 30 minutes at 4°C, and staining for 30 minutes. First, the cells were analyzed for size (FSC) and granularity (SSC) and doublets were excluded. For the mouse FACS analysis, the following strategy was used to identify cell populations in BALF (Figure 6) and blood (Figure 7): CD3, CD19 and NK1.1 were used as lineage markers; neutrophils identified as Ly-6G⁺CD11b⁺ cells; eosinophils as siglec-F⁺CD11b⁺Ly-6C^{-/low}F4/80⁺ SSC^{high}; DCs as CD11c⁺MHC-classII⁺F4/80⁻; inflammatory monocytes as Ly-6C^{high}CD11c⁻Ly-6G⁻CD11b⁺F4/80⁺; monocytes and macrophages as Ly-6C⁺CD11b⁺MHC-classII⁺F4/80⁺ and alveolar macrophages as siglec-F⁺CD11c⁺F4/80⁺ cells. For human neutrophils staining, BrV510 anti-CD11b (ICRF44), Alexa Fluor 488 anti-CD62-L (DREG-56), PE-Cy7 anti-CD16 (3G8) and Pacific Blue anti-CD66b (G10F5) (purchased from BioLegend, USA) were used. Viable cells were controlled using 7-AAD viability staining solution (eBioscience, USA). Surface staining of cells was performed at 4°C for 20 minutes. Stained cells were analyzed with a BD FACSCanto™ II employing FACSDiva Software (BD Biosciences, Germany). The data obtained was analyzed using the FlowJo software (Tree Star Inc., USA).

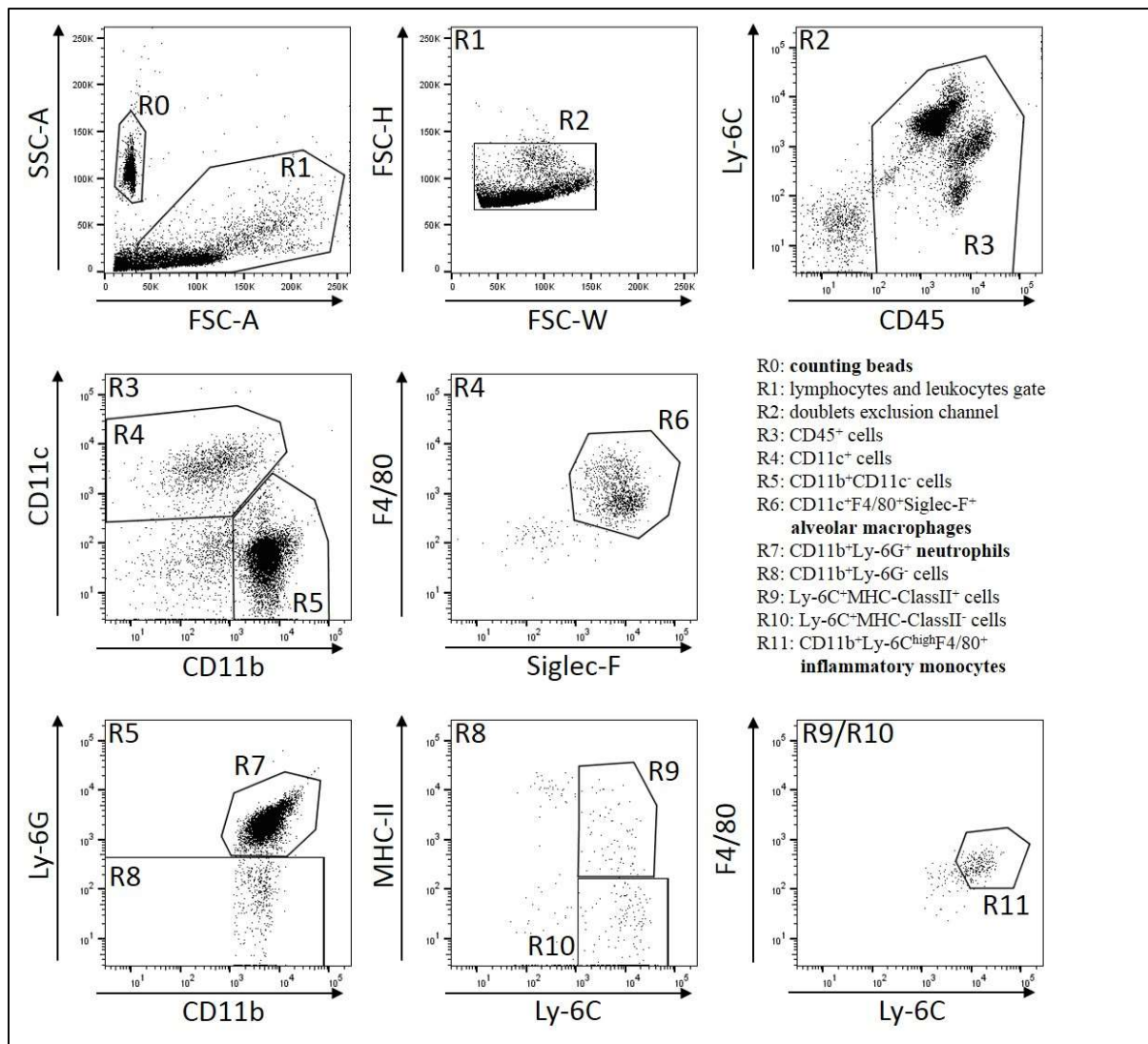


Figure 6: Gating strategy for murine BALF cell populations. Total BALF cells were analyzed by flow cytometry using a FACSCanto II and employing the FACSDiva software. Counting beads were used for cell quantification (R0) and the cell populations present in BALF were analyzed according to the expression of different surface markers, as well as according to their granularity (SSC) and size (FSC).

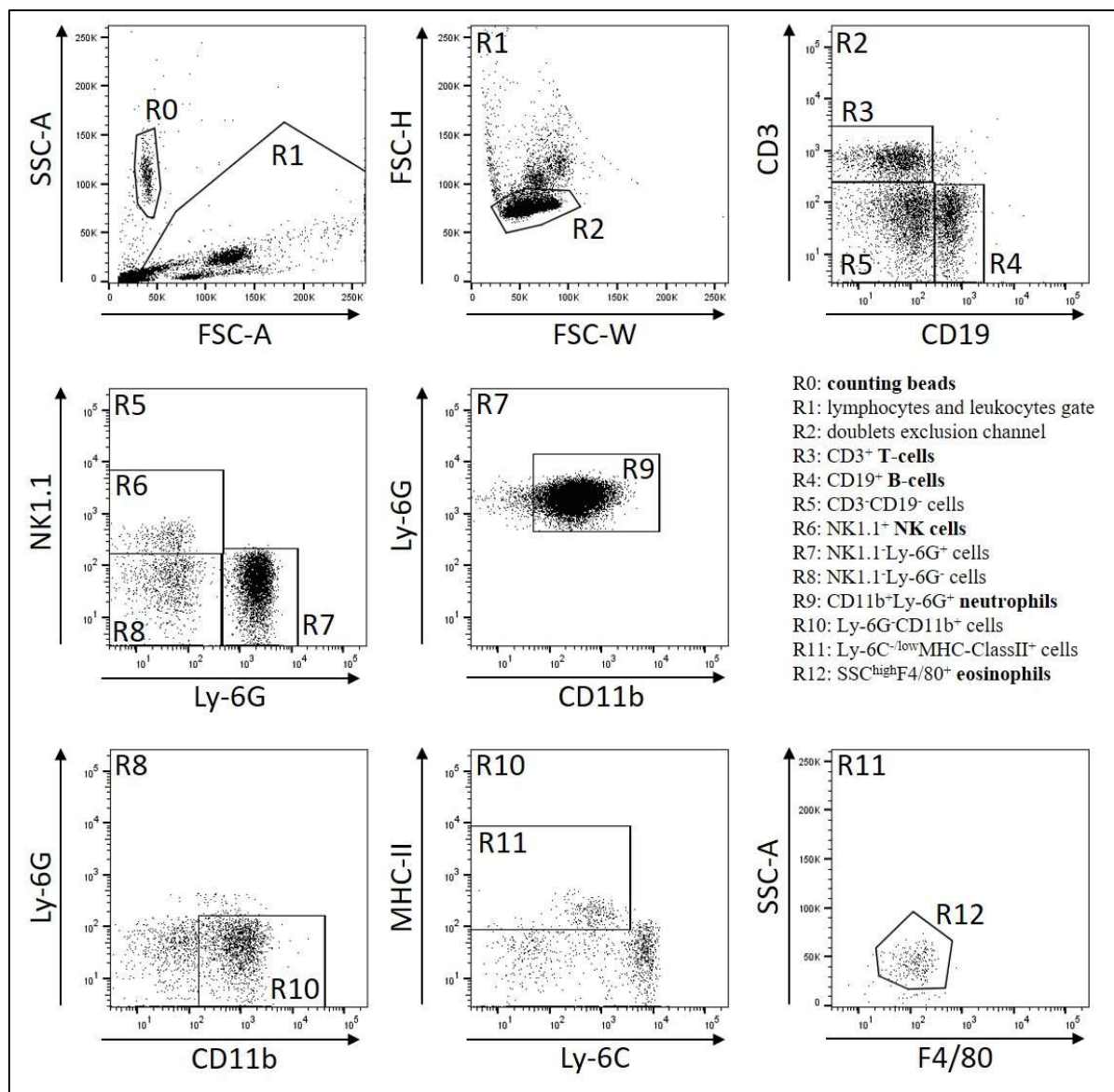


Figure 7: Gating strategy for murine blood cell populations. Blood cells after erythrocyte lysis were analyzed by flow cytometry using a FACSCanto II and employing the FACSDiva software. Counting beads were used for cell quantification (R0) and cell populations present in blood were analyzed according to the expression of different surface markers, as well as according to their granularity (SSC) and size (FSC).

3.7. Murine bone marrow cell isolation

For isolation of cells from the BM, hind legs of mice from independent projects were collected, aiming to reduce animal number. Briefly, both hind legs were cut out of the pelvis region avoiding damage to the femur. First, bands connecting fibula to the feet were cut and feet was separated. Cleaning tibia from musculature allowed its direct extraction through breaking of the knee region. The femur was cleaned from flesh and the head of the femur was separated from the pelvis bones. Both tibia and femur, isolated from the two hind legs, were briefly submersed in ethanol 70% and incubated in PBS added to 2% BSA for cell isolation. A small part of the extremities of the bones was cut and BM was flushed with 5mL PBS from one extremity into a 15mL Falcon tube. Flushed material was filtered with a 100µm sieve and cells were centrifuged with 300 x g at RT. The cell pellet was resuspended in red cell lyses buffer and equilibrated with PBS, added to 0.5% BSA after 3 minutes. Number of total BM-derived cells without erythrocytes were quantified for isolation with magnetic beads.

3.8. Cell selection using magnetic beads

In order to enrich the percentage of neutrophils among the total murine BM-derived cells for the *in vitro* experiments, a positive or negative selection was performed with specific antibodies coupled to magnetic microbeads. For the positive selection of neutrophils, anti-Ly-6G microbeads (Miltenyi, Germany) were used as specified by the company. This technique uses 50 nm magnets coupled to a highly specific antibody targeted against an epitope of the neutrophil (Ly-6G). Total BM cells were washed in a MACS separation column, which contains ferromagnetic spheres, and labeled cells were retained at the column by the magnetic field. Cells not expressing Ly-6G, were not attracted by the magnetic field and were flushed through the column and discarded. For the negative selection (depletion) the EasySep mouse neutrophil enrichment kit (Stem Cell Technologies, Canada) was used. This method has the advantage of not priming the neutrophils by Ly-6G binding. A cocktail of magnetic beads attached to different antibodies specific to all other cell types, but lacking typical neutrophil markers, was added to the total cell solution. The solution was incubated at a magnetic column for separation and the supernatant was collected. Due to the magnetic field, all cell types coupled to antibodies were separated, leaving an enriched solution of neutrophils. Neutrophil concentration was analyzed at a glass chamber within a confocal microscope and left at RT in PBS and 0.5% BSA for further analysis (Figure 8).

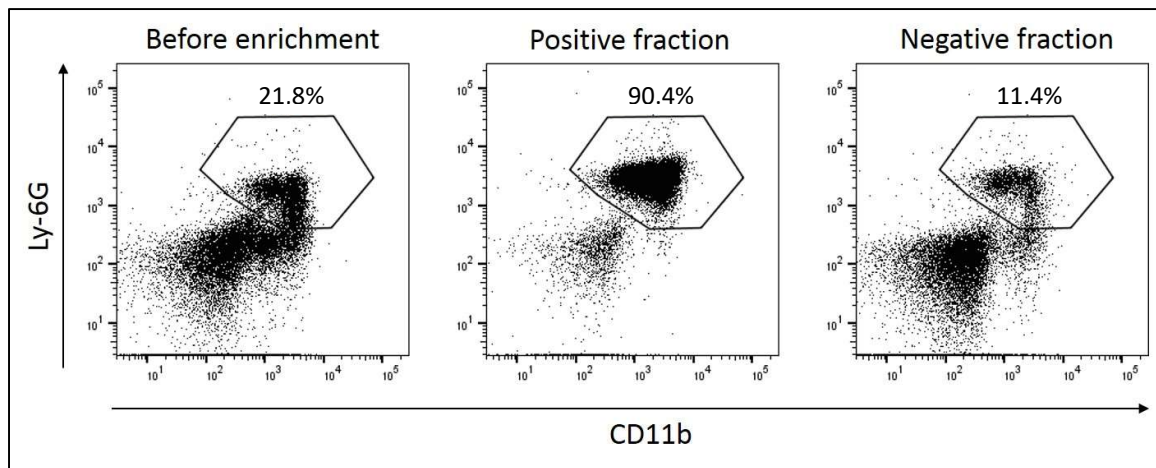


Figure 8: Magnetic positive selection of murine bone marrow (BM)-derived neutrophils. Magnetic microbeads were used to enrich the neutrophil population among total BM cells. At left, middle and right, respectively, a representative analysis shows the percentage of CD11b⁺Ly-6G⁺ neutrophils among CD45⁺ cells before enrichment, the positive fraction and the negative fraction after enrichment with Ly-6G microbeads. Granularity and size were gated with SSC and FSC for the lymphocytes and leucocytes gating, excluding doublets and viable cells were selected after 7-AAD staining. Enrichment obtained reached up to 90% neutrophil purity.

3.9. Human neutrophil isolation

Human blood was obtained from the Center for Medical Transfusion and Cell Therapy (ZTB) from Berlin (Charité - Universitätsmedizin Berlin - together with the German Red-Cross Blood Donor Service North-East - DRK Nord-Ost) after approval by the Ethics Committee of the Charité. Blood samples and reagents were kept at RT during the whole process of enrichment in order to avoid any prior stimulation of the cells by lower temperatures. Samples were centrifuged for 10 minutes at 300 x g and microparticles-enriched plasma was discarded. Samples were equilibrated with same amount of Hank's balanced salt solution (HBSS) lacking Ca²⁺/Mg²⁺ (-/-) (Gibco, USA). Dextran T500 (Carl ROTH GmbH, Germany) 3% diluted in HBSS -/- was mixed 1:1 to the sample and let for 20 minutes resting at RT for the separation of erythrocytes, as dextran promotes erythrocytes aggregation and sedimentation. Yellowish supernatant was collected and added over a 1.077g/mL Pancoll solution (PAN Biotec, Germany) for a gradient separation. Samples were centrifuged at 300 x g for 10 minutes without brake to avoid disturbing of the layers and the upper part, containing all lymphocytes and the great part of leucocytes, was discarded. The layer of high-density neutrophils attached to the bottom was resuspended in distilled water for 30 seconds. After lysis of remaining erythrocytes, the solution was balanced with HBSS containing Ca²⁺ and Mg²⁺ (+/+) and cells were counted at a glass chamber using a confocal microscope (Figure 9).

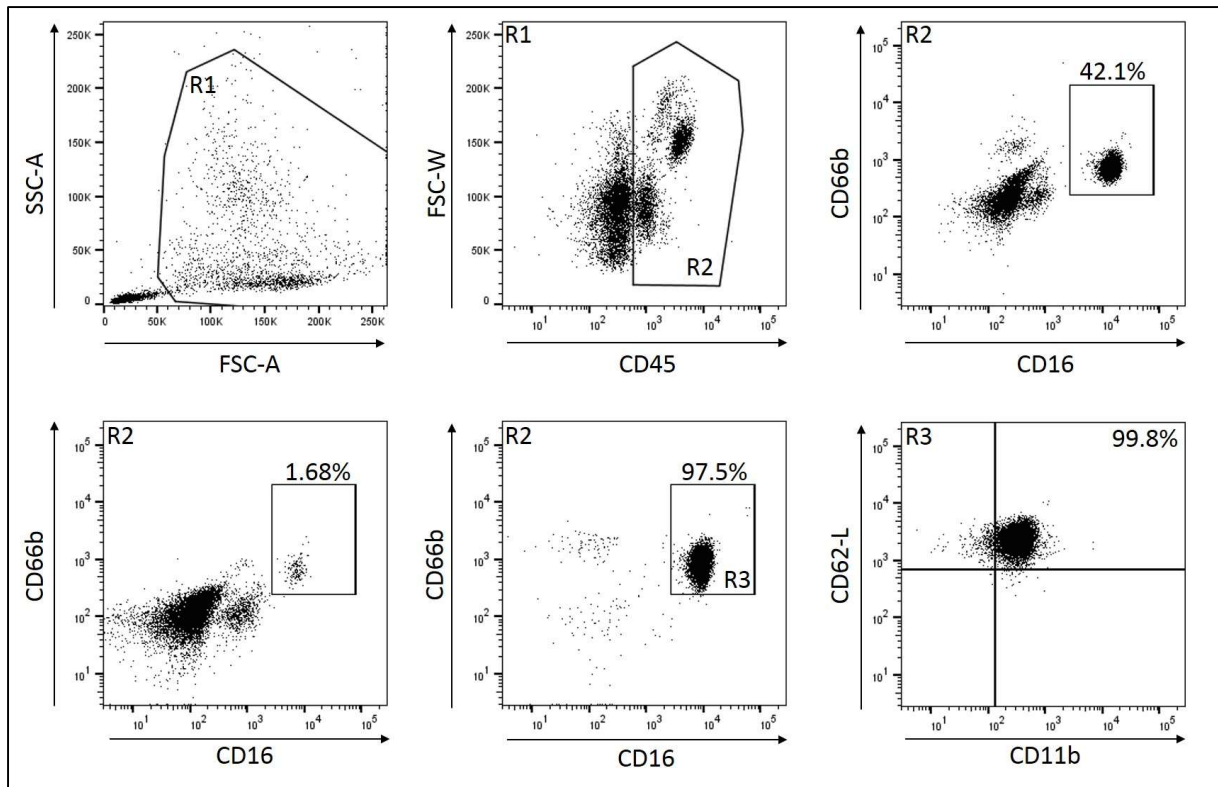


Figure 9: Enrichment of blood-derived human neutrophils. Peripheral blood was used for the isolation of human neutrophils by a density gradient separation. Side scatter (SSC) and forward scatter (FSC) were used for cellular granularity and size analysis, selecting all lymphocytes and leucocytes. CD45⁺ cells were analyzed for typical neutrophil surface markers. Up-right, down-left and down-middle shows the percentage of neutrophils among CD45⁺ cells before enrichment, the negative fraction and the positive fraction of the selection, respectively. Enrichment obtained was superior to 95% neutrophils and cells were further analyzed for typical human neutrophil markers (R3).

3.10. Immunohistochemistry

To characterize the process of NETosis *in vitro*, murine neutrophils or human neutrophils were resuspended in Dulbecco's modified eagle medium (DMEM) solution (Gibco, USA) supplemented with 10% FCS and 1% Penicillin/Streptomycin (Life Technologies, Germany) to a concentration of 1×10^6 cells/mL. 5×10^4 cells were plated on an 8 wells cell chamber (ibidi, Germany) with glass bottom to a total volume of 200 μ L. Cells were let to sediment at a 37°C incubator supplied with 5% CO₂ for 15 minutes before stimulation. In order to understand the role of ADM in the process of NET formation, mouse and human cells were incubated with 0.5 μ M of the hormone-peptide ADM or the substance dilutor at different time-points and stimulated with 100nM or 20nM PMA, respectively. Neutrophils were also stimulated with 500mU/mL glucose oxidase (GO, Sigma-Aldrich Chemie GmbH, USA), as positive control. For a receptor control, 0.5 μ M CGRP (Phoenix Pharmaceuticals, Germany) was used previous

to PMA stimulation. After 14h (mouse) or 4h (human) stimulation, cells were shortly centrifuged and supernatant carefully discarded to avoid disruption of NET structures. Cells were fixed with 3% formalin for 1h at RT. Formalin was carefully discarded and a blocking step was performed with PBS added to 1% BSA, 0.25% Tween and 5% rabbit serum (Sigma-Aldrich Chemie GmbH, USA) for 1h at RT. Blocking solution was discarded and staining was performed with a goat polyclonal antibody against neutrophil elastase (Santa Cruz Biotechnology, USA), AlexaFluor 647-conjugated Phalloidin with 1:200 dilution, for staining of F-actin (Invitrogen, USA), and DAPI. The Alexa488 anti-goat secondary antibody was used against the elastase antibody. Analysis was performed with a phase-contrast microscope for live cell imaging (Zeiss LSM780, Carl Zeiss AG, Germany).

3.11. RNA expression of adrenomedullin receptors

PCR analysis was performed in order to verify the mRNA expression of *Adm* and its receptors in mouse neutrophils. For this purpose, 2×10^6 isolated neutrophils from the BM were cultured in HBSS ++ medium with PMA or left unstimulated for 30 minutes at 37°C with 5% CO₂. After stimulation, cells were centrifuged for 5 minutes at 300 x g and supernatant discarded. Trizol reagent (ThermoFisher Scientific, USA) was added immediately to lyse cells and solution was snap-frozen in liquid nitrogen for later mRNA isolation. Samples were centrifuged at 12000rcf at 4°C for 10 minutes and supernatant collected. Chloroform was added for protein precipitation and vortexed for 15 seconds. After 3 minutes incubation at RT, material was centrifuged at 12000rcf at 4°C for 15 minutes. The upper phase was carefully transferred to a new tube and isopropanol was added for the precipitation of the genetic material. After mixing, samples were centrifuged, supernatant discarded and pellet resuspended in 70% ethanol, which was discarded after centrifugation. RNA pellet was dried under a hood and eluted in distilled water. Complementary DNA (cDNA) was translated from mRNA following instructions from the High Capacity cDNA Reverse Transcription Kit (Applied Biosystems). Shortly, 2µg of mRNA, measured with NanoDrop (ThermoFisher Scientific, USA), was added to 0.5µg/µL Oligo dT primer, 100mM dNTP mix and the kit buffer. Samples were denatured for 5 minutes at 65°C and 50U/µL reverse transcriptase was added at RT. Reverse transcriptase cycle followed 60 minutes at 42°C and 15 minutes at 70°C. cDNA translated was kept at -80°C for further analysis. Real-time quantitative polymerase chain reaction (RT-qPCR) was performed using the I-Cycler IQ detection system (Bio-Rad Laboratories Inc., USA) in combination with the SYBR Green technology (Bio-Rad Laboratories Inc., USA). The PCR conditions included initial denaturation for 10 minutes at 95°C, followed by 40 cycles of 20s at 95°C, 20s at 60°C,

and 20s at 72°C. The relative expressions were calculated as: $2^{-(\Delta CT)} \times 1/\text{mean control PBS group } 2^{-(\Delta CT)}$, where ΔCT is calculated as the $CT_{\text{Gene of interest}} - CT_{\text{Housekeeping gene}}$. PCR was performed with specific primers (Table 1) and β -actin was used as internal “housekeeping” gene control. Relative mRNA expression was quantified after gel electrophoresis analysis.

gene		sequence	Length	Access number
ADM	Forward	GAAGCCCACATTCGTGTCA	138bp	NM009627
	Reverse	TGCCGTCCTTGTCTTTGTC		
CRLR	Forward	GCAGGACCCCATCAACA	185bp	AF209905
	Reverse	GGATGCCGAAACCAGTGT		
RAMP1	Forward	ATGGTGTGACTGGGGAAAGA	205bp	NM031645
	Reverse	CAATGAAAGGGCAGAGGATG		
RAMP2	Forward	TCCCTGAACCAATCTCTTCC	185bp	NM019444
	Reverse	GTCGCTGTAATGCCTGCTAA		
RAMP3	Forward	GCAACGAGACAGGGATGC	312bp	BC024765
	Reverse	GCCACAGTCAGCACGACA		
β -actin	Forward	GTGGGAATGGGTCAGAAGG	299bp	NM007393
	Reverse	GGCATAACAGGGACAGCACA		

Table 1: Primer sequences for Real Time-qPCR. Murine bone marrow (BM)-derived neutrophils were characterized for the mRNA expression of the hormone-peptide *Adm* and its receptors, *Crlr* and *Ramp*. Real-time qPCR was performed with synthesized cDNA and β -actin was used as internal housekeeping gene control for the relative quantification.

3.12. Western Blot

Western blot was used for two independent experiments and two different techniques were applied. For the sample preparation, 2×10^6 isolated human neutrophils, resuspended in DMEM solution were cultured in a 24 wells plate at 37°C with 5% CO₂ for 30 minutes or 1h in the presence of PMA, when specified. ADM was added 1h prior to stimulation. 25 μ M of U-0126 (ChemCruz Biochemicals, USA), an ERK phosphorylation inhibitor, was used as positive control prior to stimulation with PMA. After stimulation, plate was centrifuged with 300 x g for 10 minutes to allow cell sedimentation. Supernatant was discarded and a solution of SBlu containing 6.5mM Tris-HCl (pH 6.8), 2% SDS, 6M Urea, 100mM DTT and 0.1% bromophenol blue was used for cell lysis and protein isolation. Lysate was heated up to 95°C for 10 minutes to accelerate protein denaturation and snap-frozen for later use at the SDS-Page. Samples were applied at a 10% agarose gel or expressPlus PAGE gels (GenScript Biotech, USA), for smaller

protein sizes, and electrophoresis was performed for approximately 1h at 100V with MOPS running buffer (GenScript Biotech, USA). Precision Plus Kaleidoscope ladder (Bio-Rad Laboratories Inc., USA) was used for protein size determination. After electrophoresis, protein transfer to membrane was performed with the semi-dry or wet technique. For the semi-dry technique, nitrocellulose membrane Nitrocell 0.45 μ m pore-sized (Amersham Potran, GE-Healthcare, USA) was pre-incubated in transfer buffer together with paper filters, necessary for the protein transfer. Gel was superposed over the membrane and enclosed by two layers of paper filters. Transfer was performed for 1h with 20V. After transfer, the membrane containing protein was immersed in Ponceau S solution (Sigma-Aldrich Chemie GmbH, USA) for transfer confirmation and washed several times with PBS added to 0.05% Tween 20 for cleaning. Blocking was performed for 1h at RT with pure Odyssey blocking buffer (LI-COR Biosciences, USA). For the analysis of signaling molecules from the MAPK/ERK pathway, the phosphorylated extracellular signal-regulated kinases or p44/42 MAPK (pERK, Cell Signaling, USA) and the molecule phospho-p38 MAPK alpha (Thr180, Tyr 182) (pp38, Cell Signaling, USA) were investigated. Actin was used as internal control for relative protein expression. For the ADM-receptor protein expression analysis, four different primary antibodies were used. An anti-ADM antibody (Cloud-Clone Corp., USA), anti-RAMP1 and anti-RAMP2 (R&D Systems, USA) and an anti-actin (I19) primary antibody (Santa Cruz Biotechnology, USA), used as control, were incubated ON at 4°C. The day after, the membrane was washed several times and incubated with the specific secondary FITC-conjugated anti-rabbit antibody (Rockland Immunochemicals Inc., USA) or the PerCP-conjugated anti-sheep antibody (Rockland Immunochemicals Inc., USA). After several washing steps, protein presence was analyzed for fluorescence signaling with LI-COR Odyssey (LI-COR Biosciences, USA). In order to detect the expression of the ADM receptor CRLR, an enhanced chemiluminescence (ECL) luminol-based technique using wet-transfer western blotting was performed. After running a SDS-Page as previously described, wet transfer to a PVDF 0.45 μ m pore-sized membrane (Bio-Rad Laboratories Inc., USA) was performed. For this goal, gel was superposed over the specified membrane and involved in paper filters. Structure was mounted in a chamber together with sponges and put in a tank with ice cold transfer buffer. Transfer was performed for 1h with 100V. After transfer, blocking and primary antibody binding with CALCRL (biorbyt, United Kingdom) were performed as described with the semi-dry western blot technique. Membrane was washed and a secondary HRP-coupled anti-rabbit antibody (Santa Cruz Biotechnology, USA) diluted in 5% milk (Carl ROTH GmbH, Germany) was added for 1h at RT. Membrane was washed again and the luminol-based Pierce ECL western blotting substrate (Thermofisher

Scientific, USA) or the enzyme-linked Immunosorbent assay kit (Uscn Life Science, China), for lower signal response, was added for 1 or 5 minutes, respectively. After luminol reaction, membrane was superposed with a film slide, allowing detection of luminescence and film was developed and fixed with formalin 4%.

3.13. ROS quantification

To determine ROS production by neutrophils after treatment and stimulation, two different techniques were used. The total amount of neutrophilic ROS was assessed with luminol in a plate reader and the intracellular ROS production could be assessed with the specific ROS fluorescence marker 2'-7' dichlorofluorescein diacetate (DCFH-DA) (Sigma-Aldrich Chemie GmbH, USA) by flow cytometry in the FITC channel with BD FACSCanto™ II. For the luminol assay, 5×10^4 isolated human neutrophils were plated in flat clear-bottom 96-well white plate and incubated for 15 minutes at 37 °C before stimulation. Cells were pre-treated with ADM, 100nM forskolin (Sigma-Aldrich Chemie GmbH, USA) or CGRP prior to stimulation with PMA or 100ng/mL PLY (kindly provided by Prof. Dr. Tim Mitchell, from the University of Birmingham). Before stimulation, 50µM luminol and 1.2U/mL HRP substrate were added to the samples. The stimulus was added right before reading on a SpectraMax L (Molecular Devices, USA), and a kinetic analysis of ROS production was performed at 37°C for 30 minutes with 1-minute interval between reading. For the intracellular analysis of ROS production, 2.5×10^5 human cells were incubated on a glass tube and treated with the substances described previously. 25µM DCFH-DA was added to all tubes before stimulation. Stimulation were performed for 7 minutes at 37°C and cells were washed before staining. Surface staining of specific human neutrophil markers CD11b, CD16 and CD66b were performed parallel to a life/dead cell staining with 7-AAD for 20 minutes and cells were fixed for further analysis.

3.14. NET measurement

a) NETs-sandwich ELISA

BALF samples from the mouse model of pneumonia and samples generated *in vitro* after stimulation with PMA or PLY were analyzed with a highly specific sandwich ELISA for NET detection. This assay quantifies NETs by binding both the core DNA structure and the NET-related protease neutrophil elastase, as previously described by Sayah and colleagues (2015). For this assay, an ELISA 96-well plate was coated ON at 4°C with 0.8µg/mL anti-mouse, anti-human neutrophil elastase antibody (Santa Cruz Biotechnology, USA) diluted in carbonate-bicarbonate buffer. After several wash steps with PBS added to 0.05% Tween, blocking was

performed with PBS and 5% BSA for 2h30 on an orbital shaker at 500rpm at RT. The plate was washed and samples incubated for 2h15 at RT. As negative control, 3 possible conditions were tested, extracted DNA without proteins and a known positive control without addition of the primary or secondary antibody. After several wash steps, a secondary antibody peroxidase-conjugated anti-DNA antibody (Cell death detection ELISA plus, Roche Diagnostic GmbH, Germany) was added and incubated for 2h at RT. The plate was washed again and the TMB substrate added and reaction took 20 minutes at RT before stopping with 2M H₂SO₄ solution. Optical density was measured using a plate reader with 450nm excitation wavelength. For the *in vitro* analysis of NET production by human or murine neutrophils, 1 x 10⁶ isolated cells were plated in a 24-well plate and treated with ADM, previous to stimulation with PMA or 1µg/mL PLY, as specified. After 4h or 14h stimulation, respectively, plate was centrifuged at 300 x g for 5 minutes and a solution containing 0.5U/mL micrococcal nuclease (MNase, ThermoFisher Scientific, USA) was added with the aim of releasing the DNA from the plate without complete degradation of the DNA structure. After 15 minutes, 5mM EDTA was added to stop digestion and solution was centrifuged at 4000 x g and frozen for later quantification.

b) PicoGreen quantification

As a simplified methodology to measure NETs released from neutrophils after stimulation, plasma samples from mice were analyzed for the total cell-free DNA with the Quant-iT PicoGreen Assay (ThermoFisher Scientific, USA). Different from NanoDrop (ThermoFisher Scientific, USA), used as control, PicoGreen technology has a fluorescence-based analysis of specific ds-DNA material. This allows a much more precise quantification of DNA, quantified with the use of ds-DNA standards. Briefly, samples were diluted in Tris-HCl-EDTA buffer and added to the same amount of the PicoGreen fluorescent marker, according to the manufacturer's instructions. Lambda DNA standards and samples were incubated at RT for 5 minutes and measured in a spectrofluorometer with 480nm excitation and 520nm emission wavelength.

c) SYTOX-Green analysis

In order to measure the progressive response of neutrophils and the formation of NETs after different stimulus, the SYTOX-Green Assay (ThermoFisher Scientific, USA) was used. SYTOX-Green is a fluorescent marker that binds highly specifically to DNA, but only penetrates the cell if the plasma membrane is compromised. This allows the temporal analysis of NET generation by neutrophils after stimulation, excluding the DNA staining of living cells. For this assay, human neutrophils and mouse BM-derived neutrophils were plated in 96-well plates and let adhere for 15 minutes at 37°C. Before stimulation, cells were treated with ADM, CGRP or forskolin and pre-treated with 0.5µM of the ADM-receptor blocker olcegepant

(MedChem Express, USA) for receptor control, when indicated. Triton 1% (Sigma-Aldrich Chemie GmbH, USA) was used as positive control for maximal signal. In order to understand the signaling mechanisms involved in NET formation after ADM treatment, 25 μ M of U-0126 was used. Shortly before measurement, 5 μ mol/L SYTOX-Green was added to the wells and followed by stimulus with PMA or PLY. NET generation was analyzed every 15 minutes with a spectrofluorometer with excitation wavelength of 485nm and emission at 525nm at 37°C for 4 or 14h. Released DNA levels was compared to the maximal signal.

d) MPO quantification

To quantify MPO activity present in BALF and blood samples, which could indicate the level of neutrophil activation and the presence of NETs, an MPO quantification assay was performed. This assay quantifies the MPO activity after break of the TMB substrate by MPO itself. Together with the samples, 0.75mM H₂O₂ and TMB were added and incubated for 5 minutes at 37°C. TMB reaction was stopped with 2M H₂SO₄ and the plate was measured with 450nm wavelength using a plate reader.

3.15. Statistical Analysis

Data were analyzed with GraphPad Prism 7 (GraphPad Software, USA). For comparisons of paired samples from the *in vitro* experiments, a student's t-test was used. For the unpaired data of the *in vivo* experiments, one-way ANOVA was used with Tukey's multiple comparisons test. For the *in vivo* experiments for NET degradation, two-way ANOVA with Tukey's multiple comparisons test was used. To facilitate visualization of the results, only comparisons between treated and related non-treated animals at the same time-point per infection group were shown. Data on bacterial burden were compared using Mann-Whitney U test. Data are presented as mean with standard error of mean (SEM). The linear correlation analysis between NETs and the lung permeability in the *in vivo* model of combined pneumococcal pneumonia and MV was performed with the Pearson correlation coefficient test and linear regression is shown.

4. Results

4.1. *Streptococcus pneumoniae* induces NET formation *in vivo*

NET formation was recently described as an alternative effector function of neutrophils to fight infection, helping in the killing of the invading pathogen (Papayannopoulos and Zychlinsky, 2009; Brinkmann et al., 2004; Urban et al., 2009). The Gram-positive bacteria *S.pn.* strain TIGR4 was shown to induce neutrophils to produce NET-like structures, as DNA could be identified in the lung alveoli after infection (Beiter et al., 2006). C57-BL6J mice infected intranasally with 5×10^6 CFU of the highly infectious and invasive *S.pn.* serotype 3, strain PN36 were analyzed in a model of pneumococcus pneumonia for NET formation (Müller-Redetzky et al. 2015). To investigate the presence of NET structures, lung tissue histology was performed at 24h, 36h and 48h post-infection (p.i.). Sections of the lung from infected mice were analyzed by immunohistochemistry with confocal microscopy by staining of the typical NET marker citrullinated histone H3. After 24h p.i., a mild infiltration of neutrophils was seen in the bronchus and alveolar space and citrullinated histone H3 was mainly found in the bronchus. At 36h, more neutrophils were observed in the perivascular space and in the alveoli, with increased presence of the typical NET marker in these areas. Neutrophil infiltration and the presence of citrullinated histone H3 further increased at 48h p.i., mainly in the perivascular space. Notably, no staining of citrullinated histone H3 was detected in the vascular system at all time-points analyzed (Figure 10A). BALF samples were also analyzed for the presence of NETs with the specific NET sandwich ELISA targeting both neutrophil elastase and DNA. The amount of NETs in the alveolar space increased progressively with time, with significant higher levels at 36h and 48h p.i. than the control mock-infected mice. Values obtained for NETs were displayed as OD values, as no standards could be generated. The OD values obtained at 36h and 48h time-points were approximately 4 and 6 times higher than the 24h time-point p.i., respectively (Figure 10B). Lung barrier disruption after infection was investigated with a MSA ELISA assay, measuring the ratio between MSA levels in BALF and plasma. Permeability values were further correlated to the amount of NETs quantified in BALF and a significant positive correlation between these two parameters was found with the Pearson's correlation coefficient (Figure 10C).

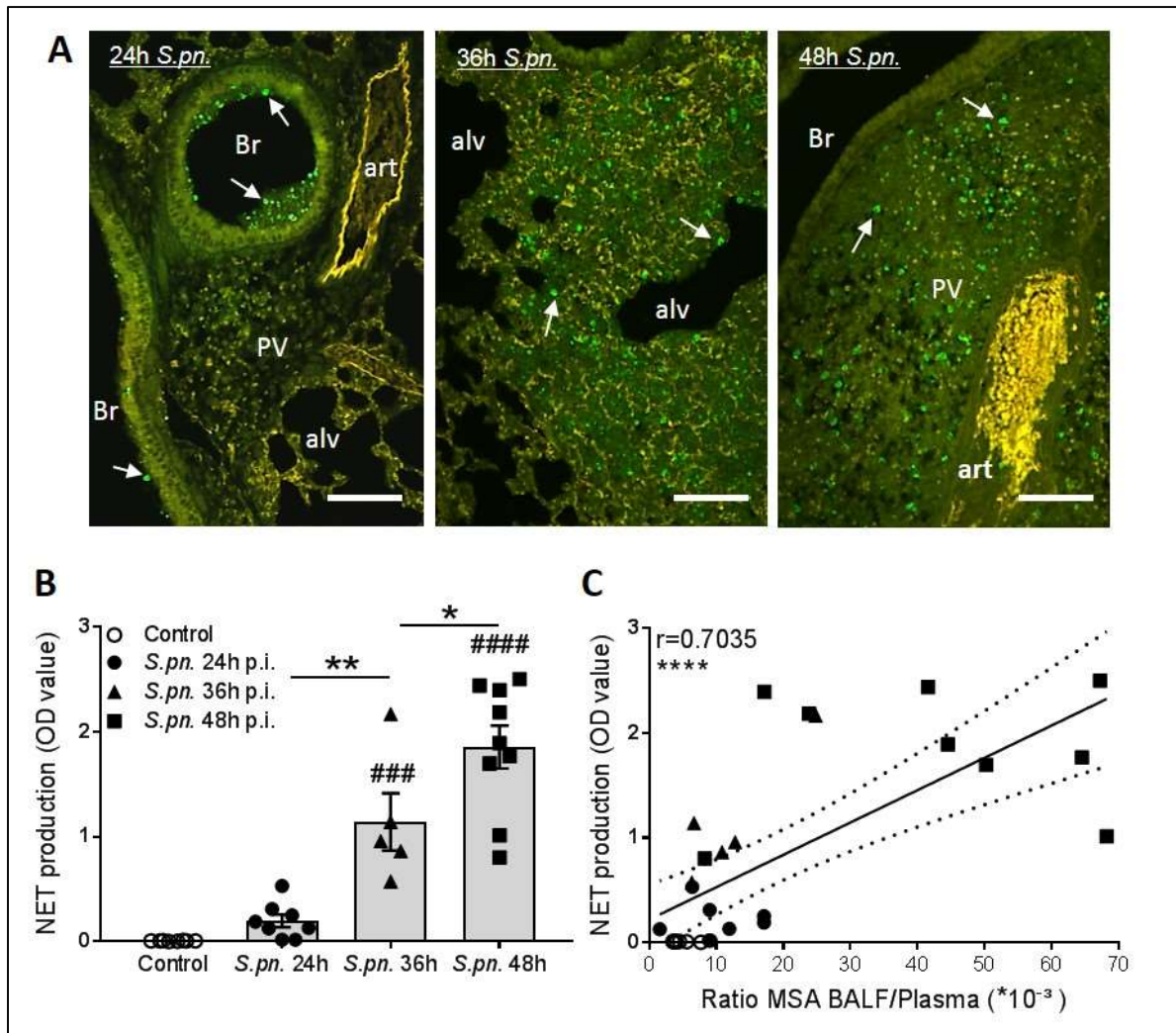


Figure 10: NETs are generated and accumulate in the lungs after *S. pneumoniae* infection. (A) Immunohistochemistry of the lung was performed after infection of the mice for different time-points with *S.pn.* (time-point of 24h, 36h and 48h from left to right). In green, citrullinated histone H3 as a typical NET marker (shown by the arrows); in yellow, CD31 localized at endothelial cell intercellular junctions; artery (art), alveolar space (alv), bronchus (Br) and perivascular space (PV); scale bars: 50 μ m. **(B)** NETs were quantified at different time-points post infection by a sandwich ELISA targeting both elastase and DNA in BALF samples from animals infected with *S.pn.* and compared to PBS-infected mice. **(C)** Correlation of the amount of NETs and the lung permeability (quantified by the ratio between MSA levels in BALF and plasma) was performed with the Pearson's correlation coefficient test and linear regression is shown. One-way ANOVA/Tukey's multiple comparisons test; # shows significance in comparison to PBS; p<0.05 (*), p<0.01 (**), p<0.001 (###), p<0.0001 (****/#####); columns in B represent means and error bars are SEM; n=6-9.

4.2. DNase improves lung barrier function in pneumococcal pneumonia

NETs are generated and accumulate in the lungs after infection with *S.pn*. NETs are important for pathogen control, however, they are also highly cytotoxic to the host and induce endothelial cell death, leading to uncontrolled hyper-inflammation and tissue injury. Targeting NETs with DNase was shown to be effective in the treatment of many distinct pathologies associated with NETs, improving the disease outcome (Cortjens et al., 2016; Narasaraju et al., 2011; Saffarzadeh et al., 2012). In order to reduce the cytotoxic effects of NETs in the lungs, we first targeted their main component, the DNA, with DNase I. Mock-infected and *S.pn*-infected mice were treated with an i.p. application of 5mg/kg bodyweight DNase I or the same volume of NaCl, as control, directly before infection and this application was repeated every 12h until final preparation at the time-points of 24h or 48h p.i. All *S.pn*-infected animals presented typical signs of pneumonia, with strong lung and systemic inflammation, great loss in body weight and temperature and bacteremia.

4.2.1. DNase reduces NETs and lung permeability *in vivo*

At the 24h time-point after infection, levels of NETs were slightly increased in comparison to the mock-infected group. At this time-point, no detectable impact of DNase application was seen in the levels of NETs measured in BALF. At 48h p.i., NET production was considerably higher than in mock-infected mice and around 10-fold greater compared to the levels observed at 24h p.i. The amount of NETs detected in BALF from infected animals treated with DNase at the 48h time-point was significantly reduced in comparison to the non-treated group (Figure 11.1A). Notably, levels of circulating cell free DNA, some of which originated from NETs, were also reduced at 48h p.i. by the DNase treatment (data not shown). Tissue permeability was measured by the total protein amount quantified in BALF and the ratio between the levels of HSA found in BALF and plasma. At the 24h time-point, levels of both total protein and the HSA ratio were slightly higher in the infected groups than the mock-infected animals, but not statistically different. At 48h time-point, permeability levels were considerably higher among the infected animals than the non-infected animals. Animals treated with DNase at the 48h time-point p.i. had a significant reduction in permeability levels, quantified with both assays. At 24h time-point no significant difference was seen after DNase treatment (Figure 11.1B).

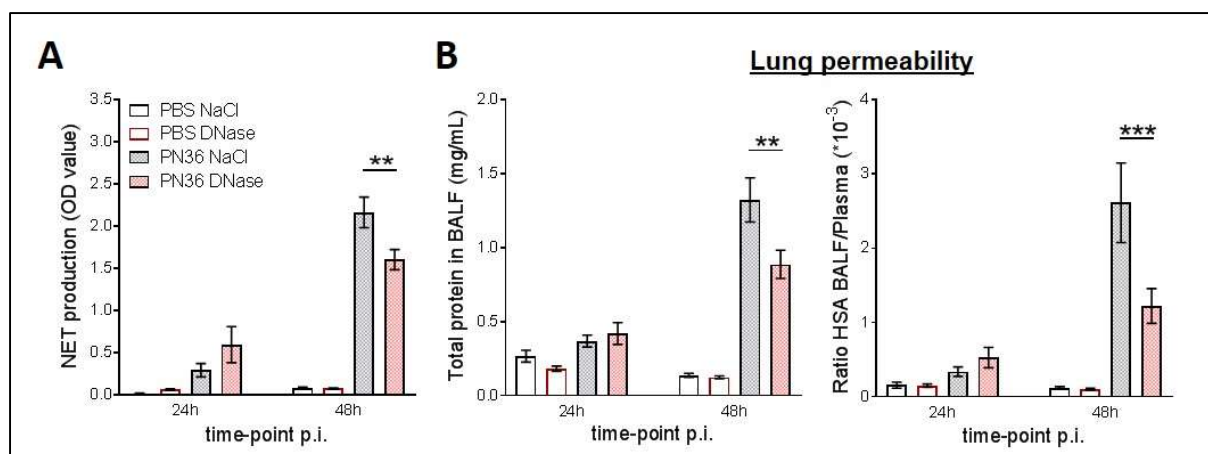


Figure 11.1: DNase reduces NETs and lung permeability. (A) NETs were quantified using a specific sandwich ELISA targeting both neutrophil elastase and DNA in BALF samples from animals infected with *S.pn.* (PN36) and mock-infected (PBS) mice treated with 5mg/kg bodyweight DNase I, when indicated. (B) Lung permeability was measured by two distinct ELISA methodologies. Total protein levels measured in BALF (left) and the HSA concentration ratio between BALF and plasma (right) are shown for the distinct time-points analyzed. Two-way ANOVA/Tukey's multiple comparisons test; only statistical differences between treated and the related non-treated groups are shown; $p < 0.01$ (**), $p < 0.001$ (***) ; columns represent means and error bars are SEM; $n = 5-11$.

4.2.2. DNase does not affect clinical symptoms and bacterial burden

All animals infected with *S.pn.* had a considerable loss of body temperature with time in comparison to the mock-infected mice. No differences in body temperature were seen between DNase-treated and the non-treated control group in both infected and mock-infected mice (Figure 11.2A). Liver injury was assessed by quantification of plasma levels of aspartate transaminase (AST). AST levels among infected animals were slightly higher than the mock-infected animals at 48h time-point, but not statistically significant. No differences were seen after DNase application in both infected and mock-infected groups (Figure 11.2B). Bacterial burden was assessed in BALF, lung tissue, blood, liver and spleen. All animals infected with *S.pn.* showed presence of bacteria in all compartments analyzed at 24h and 48h p.i. The number of CFU increased after 48h, compared to the 24h time-point in lung, blood, liver and spleen, while CFU in BALF were equally high at both time-points. DNase treatment had no effects on CFU count in any of the compartments analyzed (Figure 11.2C).

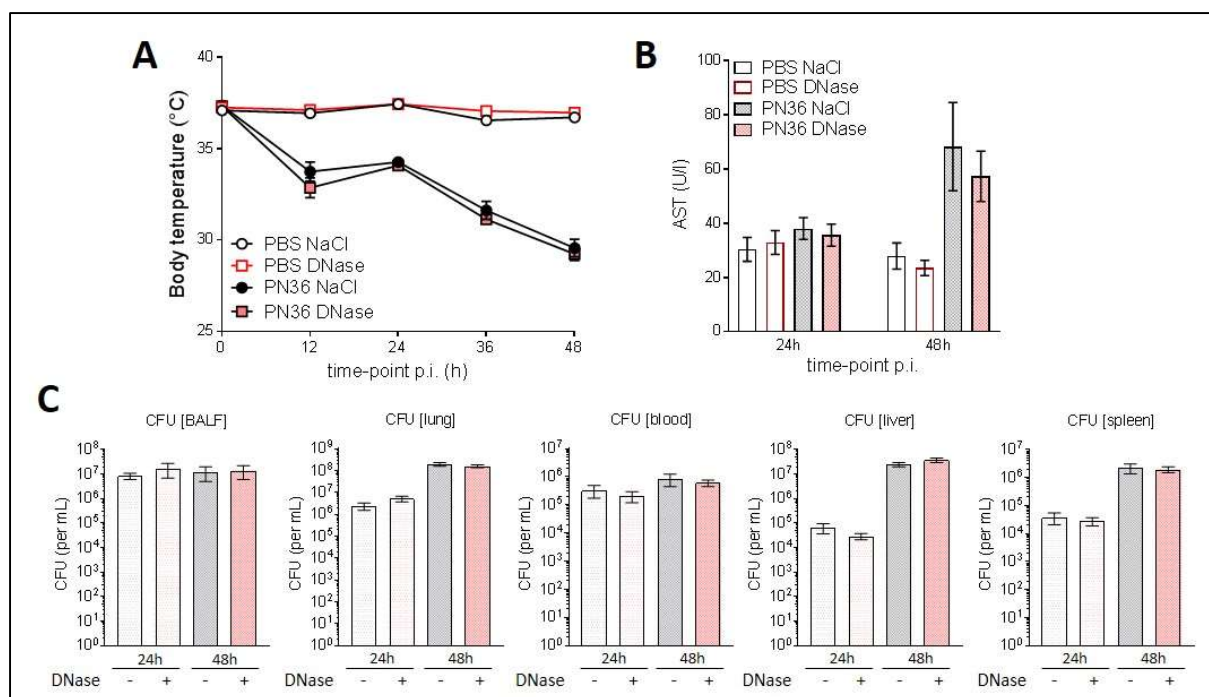


Figure 11.2: DNase treatment does not affect animal clinical symptoms and bacteria burden in pneumococcal pneumonia. (A) Body temperature was measured every 12h for characterization of disease progression and (B) extra-pulmonary organ damage was assessed by measuring aspartate transaminase (AST) levels in plasma samples of *S.pn.*-infected (PN36) and mock-infected (PBS) animals treated with 5mg/kg bodyweight DNase I. (C) Bacterial burden was assessed by quantifying colony-forming units (CFU) in BALF, lung, blood, liver and spleen from infected animals, after growth of the CFU in blood agar plates. Two-way ANOVA/Tukey's multiple comparisons test and Mann-Whitney U test for bacteria CFU between the groups at the same time-point; only statistical differences between treated and the related non-treated groups were analyzed; lines (A) and columns (B and C) represent means and error bars are SEM; n=5-11.

4.2.3. DNase does not affect cellular recruitment and cytokine levels in the lungs and systemically

Neutrophils are normally not seen in BALF of non-infected animals. Here, as seen by flow cytometry analysis of BALF and lung samples, the number of neutrophils increased progressively with time after infection with *S.pn.* No difference in the total number of neutrophils was found between treated and non-treated animals after infection at both time-points analyzed. In blood, a decrease in the number of circulating neutrophils was seen at 48h p.i., which is typically seen after infection. DNase treatment did not affect the cell number at both time-points analyzed after infection, nor at the 48h time-point of the mock-infected group. A significant increase in the number of neutrophils was only seen at 24h p.i. in the mock-infected animals after DNase treatment (Figure 11.3A). Analysis of the activation state of the infiltrating neutrophils was measured in BALF by the median fluorescence intensity (MFI)

expression of the activation markers CD11b and CD18. Only *S.pn.*-infected animals are shown, as mock-infected animals have no significant number of neutrophils in the alveolar space. No differences in the MFI values were found after treatment with DNase at both time-points analyzed (Figure 11.3B). The total number of alveolar macrophages was quantified in BALF and a slight decreased in the number of these cells, simultaneously to the neutrophil infiltration in the alveolar space, is seen. However, DNase application had no impact on the percentage of each cell population among the two main cell groups found in BALF (Figure 11.3C).

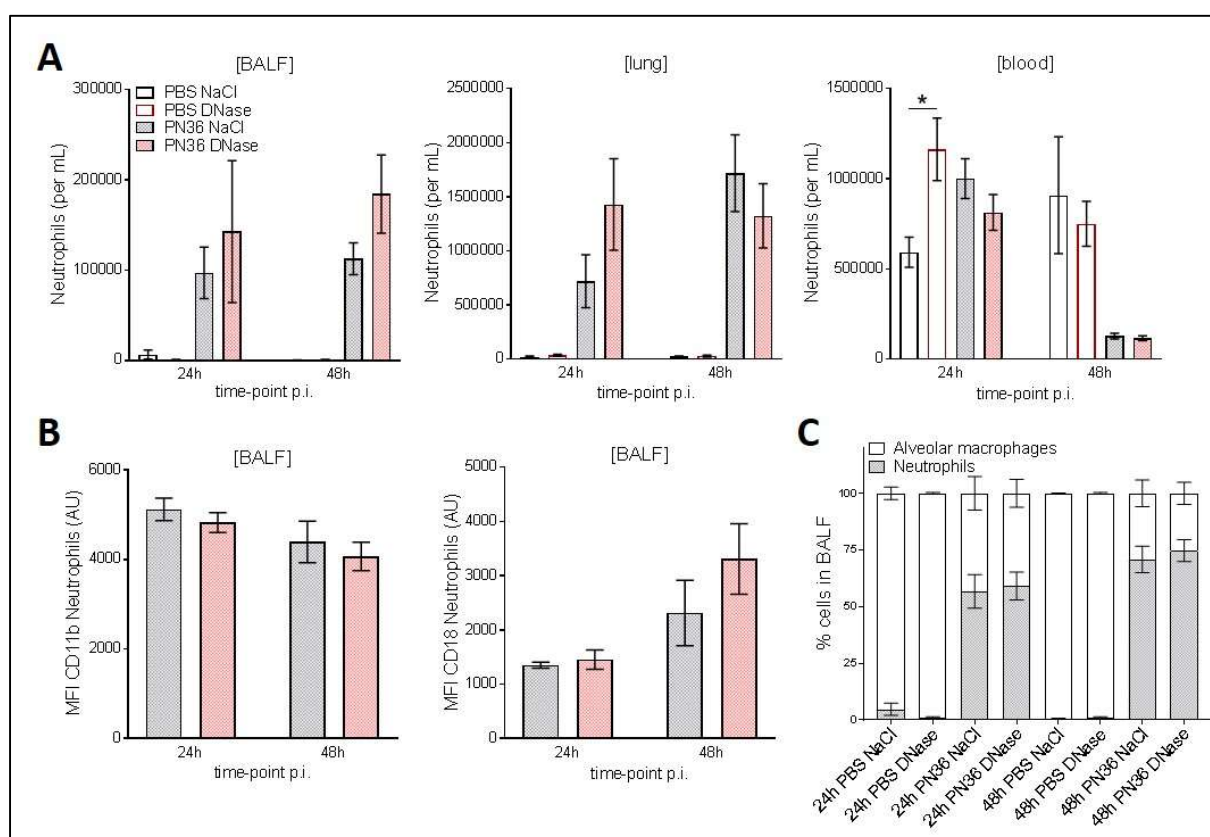


Figure 11.3: DNase treatment does not affect neutrophil recruitment and cellular activation. (A) Neutrophil number was assessed in BALF (left), lung homogenate (middle) and blood (right) of *S.pn.*-infected (PN36) and mock-infected (PBS) animals by flow cytometry. **(B)** BALF neutrophils from infected animals were further characterized for their activation state with the median fluorescence intensity (MFI) value from the activation markers CD11b (left) and CD18 (right). **(C)** Alveolar macrophages were quantified in BALF and cellular frequency of both neutrophils and alveolar macrophages is shown. Two-way ANOVA/Tukey's multiple comparisons test; only statistical differences between treated and the related non-treated groups are shown; $p < 0.05$ (*); columns represent means and error bars are SEM; $n = 5-11$.

Quantification of pro-inflammatory cytokines was performed in BALF (Figure 11.4A) and plasma samples (Figure 11.4B). Concentrations of IL-1 β , GRO- α , IL-6, MIP-1 α , TNF α and MIP-2 were assessed with a multiplex ELISA. Levels of all cytokines increased after infection with *S.pn.* at both time-points in both samples analyzed. In plasma and partially in BALF, cytokine levels were higher at the 48h time-point than the 24h time-point p.i. In BALF, levels of IL-1 β , MIP-1 α and TNF α were higher at 24h p.i. No differences were detected in the cytokine levels between animals treated with DNase and the non-treated mice at both time-points.

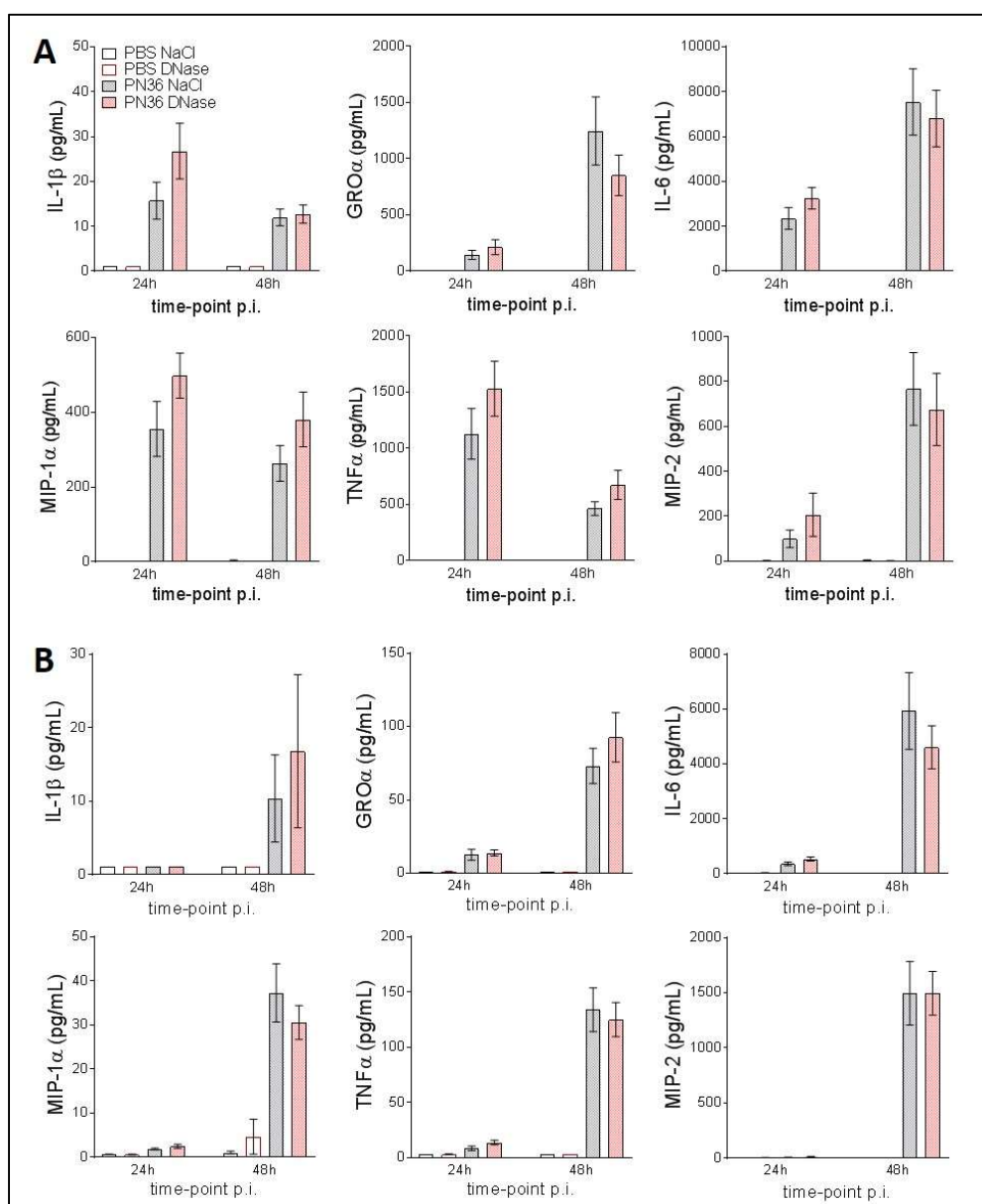


Figure 11.4: DNase treatment does not affect cytokine production. Classical pro-inflammatory cytokines IL-1 β , GRO α , IL-6, MIP-1 α , TNF α and MIP-2 were quantified in BALF (A) and plasma (B) samples from animals infected with *S.pn.* (PN36) or mock-infected (PBS) mice by a multiplex ELISA. Two-way ANOVA/Tukey's multiple comparisons test; only statistical differences between treated and the related non-treated groups were analyzed; columns represent means and error bars are SEM; n=5-11.

4.3. PAD4 inhibition reduces NETs in the lungs and improves the clinical condition of infected mice

The mechanism involved in this process of NETosis is highly dependent on the stimulation pathway being sensed by the neutrophils. A possible common step for NET formation is the citrullination of histones through PAD4, which provide morphological modification of histones, inducing the decondensation of the chromatin in the nucleus, necessary for the process to happen. Inhibition of PAD4 with specific molecules was shown to be efficient in reducing NETs and to have a positive effect in reducing inflammation (Cedervall et al., 2017). Aiming to specifically inhibit the process of NETosis, without affecting other important effector functions of the neutrophils, mice were injected i.p. with 20mg/kg bodyweight of the specific PAD4 inhibitor GSK484. Treatment with GSK484 was performed as previously described for the treatment with DNase. All mice infected with *S.pn.* showed a decrease in body weight and temperature, local and systemic inflammation and bacteremia, typically seen in pneumococcal pneumonia.

4.3.1. PAD4 inhibition efficiently reduces NETs in the lungs

As observed within the experiments of DNase treatment, levels of NETs measured in BALF from *S.pn.*-infected mice were considerably higher at the 48h time-point, when compared to the related mock-infected group and the 24h time-point p.i. The amount of NETs present in BALF after 48h p.i. was efficiently reduced after inhibition of PAD4 with GSK484, when compared to the non-treated group (Figure 12.1A). Contrarily to the experiment of DNase treatment, the levels of cell-free DNA in plasma were increased after treatment with GSK484 at 48h p.i. (data not shown). Permeability levels, assessed by quantification of total protein in BALF and the ratio of HSA quantified in BALF and plasma, showed an increase of permeability after *S.pn.* infection and a further increase at the later time-point. Application of GSK484 led to an apparent reduction in permeability after 48h p.i., but this trend was not statistically different from the non-treated group (Figure 12.1B).

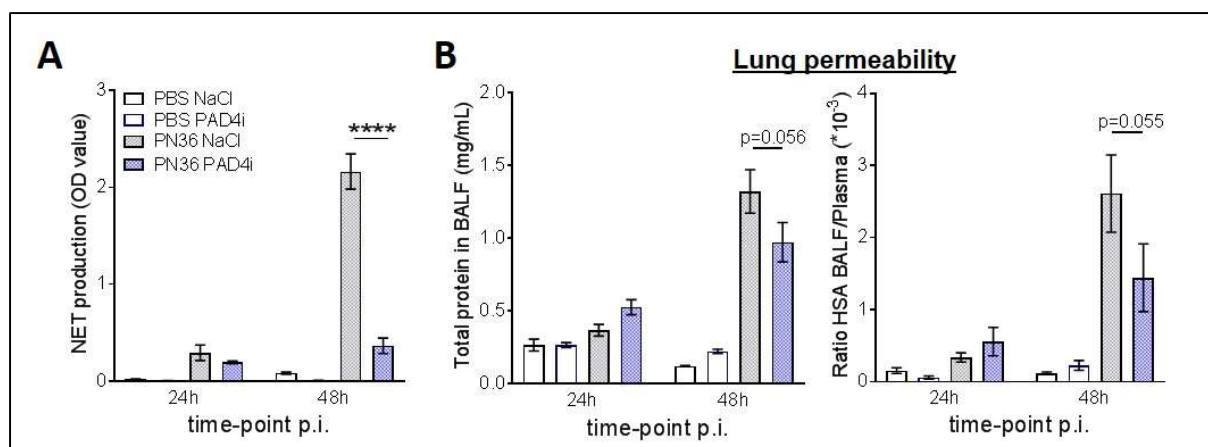


Figure 12.1: PAD4 inhibition reduces NETs in the lungs after pneumococcal pneumonia. (A) NETs were quantified with a specific sandwich ELISA targeting both neutrophil elastase and DNA in BALF samples from animals infected with *S.pn.* (PN36) and mock-infected (PBS) animals treated with 20mg/kg bodyweight of the PAD4 inhibitor GSK484. **(B)** Lung permeability was assessed by total protein levels in BALF (left) and by the ratio between HSA concentrations in BALF and plasma (right). Two-way ANOVA/Tukey's multiple comparisons test; only statistical differences between treated and the related non-treated groups are shown; $p < 0.0001$ (****); columns represent means and error bars are SEM; $n = 5-11$.

4.3.2. GSK484 leads to increased bacteremia in mice

All animals infected with *S.pn.* had a considerable loss of body temperature with time in comparison to the mock-infected mice. Animals treated with the PAD4 inhibitor had improved clinical conditions with significant (at 12h or 36h p.i.) or almost significant (at 24h or 48h p.i.) higher body temperature after infection, when compared to the non-treated control group (Figure 12.2A). Analysis of AST levels in plasma samples showed increased levels of this enzyme in animals after treatment with GSK484 at 48h p.i., while no differences were seen among the mock-infected animals (Figure 12.2B). All infected animals presented bacteremia, with bacteria CFU being count in BALF, lung, blood, liver and spleen. The bacterial burden in BALF was similar at both time-points analyzed and was not affected by the treatment with GSK484. The CFU count in lung, blood, liver and spleen at 48h p.i., was increased in comparison to the 24h time-point. A lower bacteria CFU count was seen in animals treated with GSK484 in lung and liver at 48h p.i. Contrarily to that, a significantly higher bacterial burden was observed in blood at the 48h time-point p.i. after GSK484 treatment. No differences in CFU count were found in any compartment analyzed at the 24h time-point (Figure 12.2C).

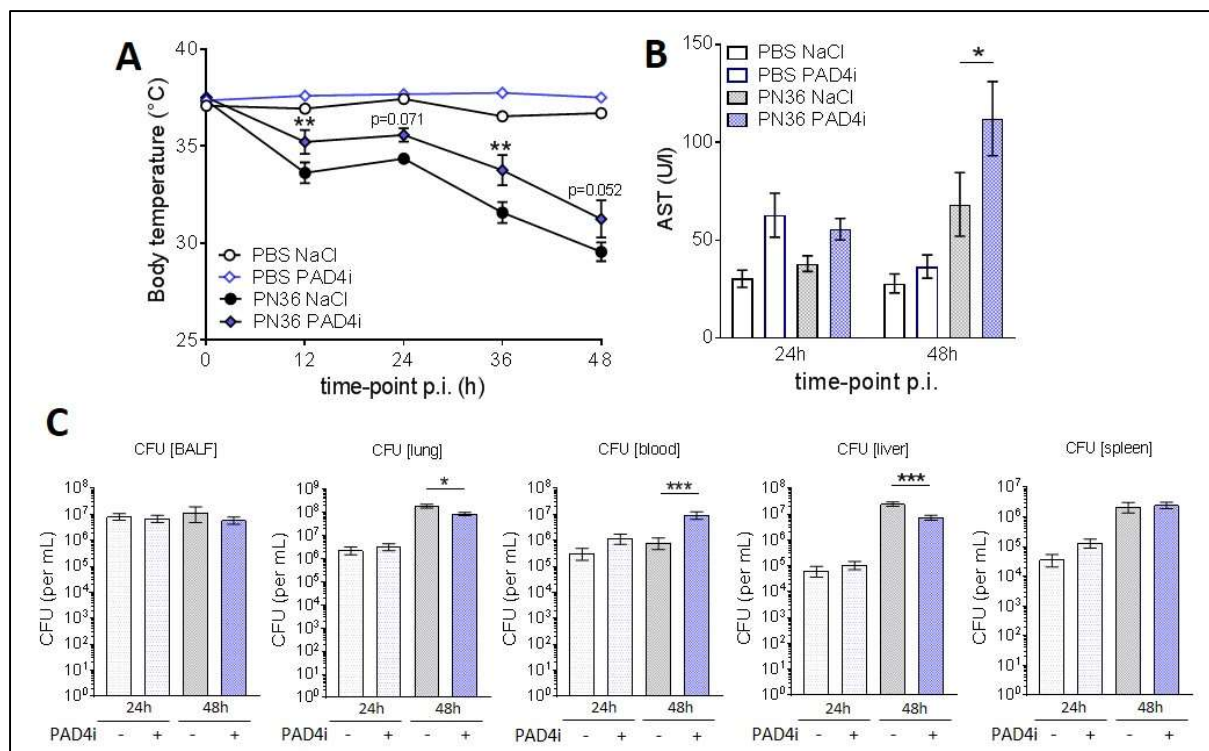


Figure 12.2: PAD4 inhibition leads to increased bacteremia in mice. (A) Body temperature of *S.pn.*-infected (PN36) and mock-infected (PBS) mice treated with 20mg/kg bodyweight PAD4 inhibitor GSK484 was measured every 12h to monitor disease progression. (B) Liver damage was assessed by measuring the aspartate transaminase (AST) concentration in plasma samples. (C) Bacterial burden was quantified in BALF, lung, blood, liver and spleen, respectively. Two-way ANOVA/Tukey's multiple comparisons test and Mann-Whitney U test for bacteria colony-forming unit (CFU) between the groups within same time-point; only statistical differences between treated and the related non-treated groups are shown; $p < 0.05$ (*), $p < 0.01$ (), $p < 0.001$ (***) ; lines (A) and columns (B and C) represent means and error bars are SEM; $n = 5-11$.**

4.3.3. GSK484 affects inflammation and neutrophil recruitment to the lung

FACS analysis of BALF and lung samples showed that all animals infected with *S.pn.* had a substantial increase in the recruitment of neutrophils into the lungs at 24h and 48h p.i. Infected animals treated with GSK484 had a significantly reduced number of infiltrating neutrophils in BALF both at 24h and 48h time-points and in the lung tissue at the 48h time-point. At 24h p.i., only a tendency of reduction in the number of neutrophils in the lungs was seen. A lower number of neutrophils was also found in blood of infected animals after treatment at 24h p.i. and at the 48h time-point of the mock-infected animals. At 48h p.i., the neutrophil number in blood was strongly reduced due to disease progression and no difference in cell number was seen after treatment with GSK484 (Figure 12.3A). Neutrophils present in BALF samples from infected animals had no differences in MFI expression of the activation marker CD11b after

treatment. However, a significant decrease in the MFI of CD18 expression at 48h p.i. was seen after PAD4 inhibition (Figure 12.3B). The total number of alveolar macrophages analyzed in BALF samples was significantly reduced after PAD4 inhibition in almost all groups, with the exception of the 48h *S.pn.*-infected animals, where the number of this cell population was already considerably reduced, due to infection. However, a reduction within the percentage of alveolar macrophages among the two major populations found in BALF was not seen (Figure 12.3C).

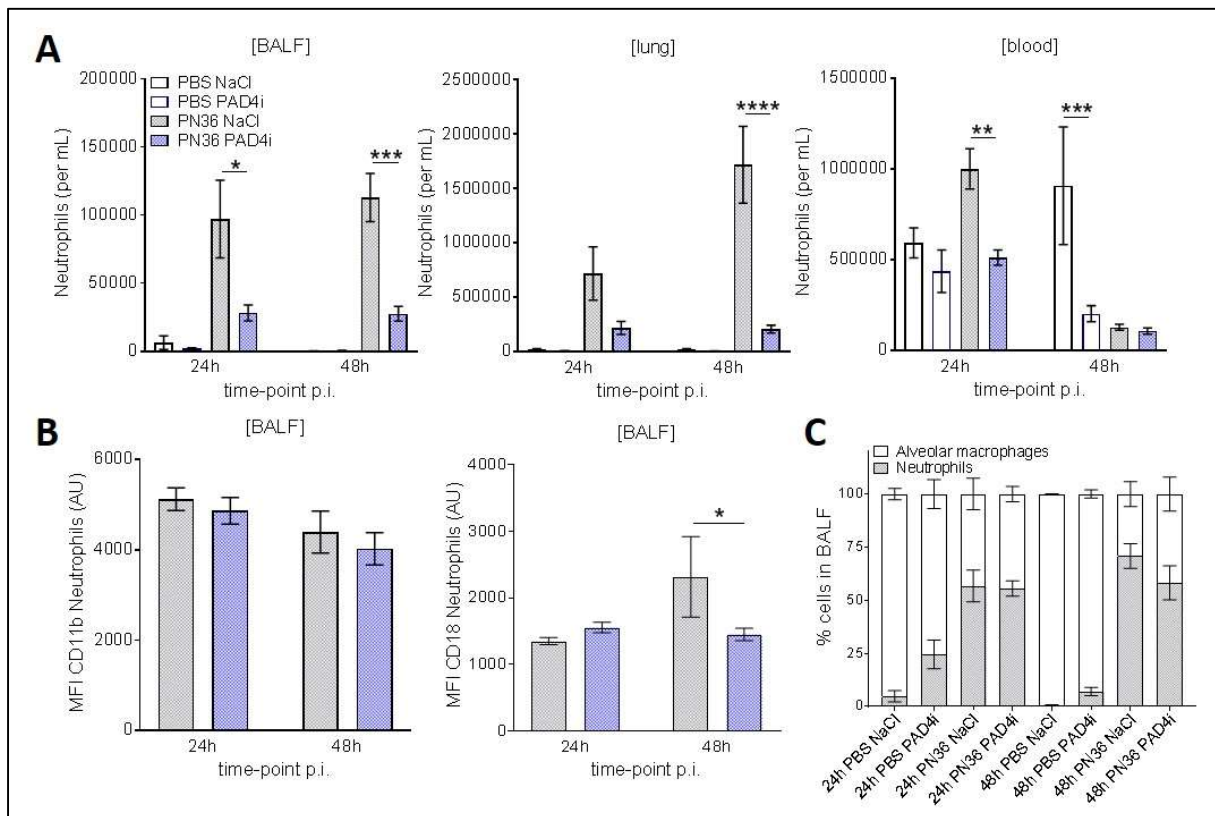


Figure 12.3: GSK484 influences neutrophil recruitment into the lungs. (A) The neutrophil population was characterized in BALF (left), lung homogenate (middle) and blood (right) of *S.pn.*-infected (PN36) and mock-infected (PBS) animals treated with 20mg/kg bodyweight PAD4 inhibitor GSK484 by flow cytometry. (B) BALF neutrophils from the infected groups were further characterized for their activation state with the median fluorescence intensity (MFI) value of the surface markers CD11b (left) and CD18 (right). (C) Alveolar macrophages were quantified in BALF and cellular frequency of the major cell populations found in BALF is shown. Two-way ANOVA/Tukey's multiple comparisons test; only statistical differences between treated and the related non-treated groups are shown; $p < 0.05$ (*), $p < 0.01$ (), $p < 0.001$ (***), $p < 0.0001$ (****); columns represent means and error bars are SEM; $n = 5-11$.**

Concentration of the pro-inflammatory cytokines IL-1 β , GRO- α , IL-6, MIP-1 α , TNF α and MIP-2, assessed in BALF and plasma, increased after *S.pn.* infection, in comparison to non-infected animals. In BALF, higher levels of IL-1 β , MIP-1 α and TNF α were found at 24h p.i. than at the 48h time-point. In plasma, this increase was mainly seen at the 48h p.i. In BALF samples, infected animals had significantly lower levels of TNF α at 24h and of GRO- α at 48h time-point after treatment with GSK484. No further differences in cytokine levels were detected in BALF after PAD4 inhibition (Figure 12.4A). In contrast to the BALF, plasma levels of GRO- α and TNF α were significantly increased at the 48h time-point p.i. after treatment with GSK484, when compared to the non-treated group. All other cytokines showed no differences after treatment with GSK484 between the groups compared (Figure 12.4B).

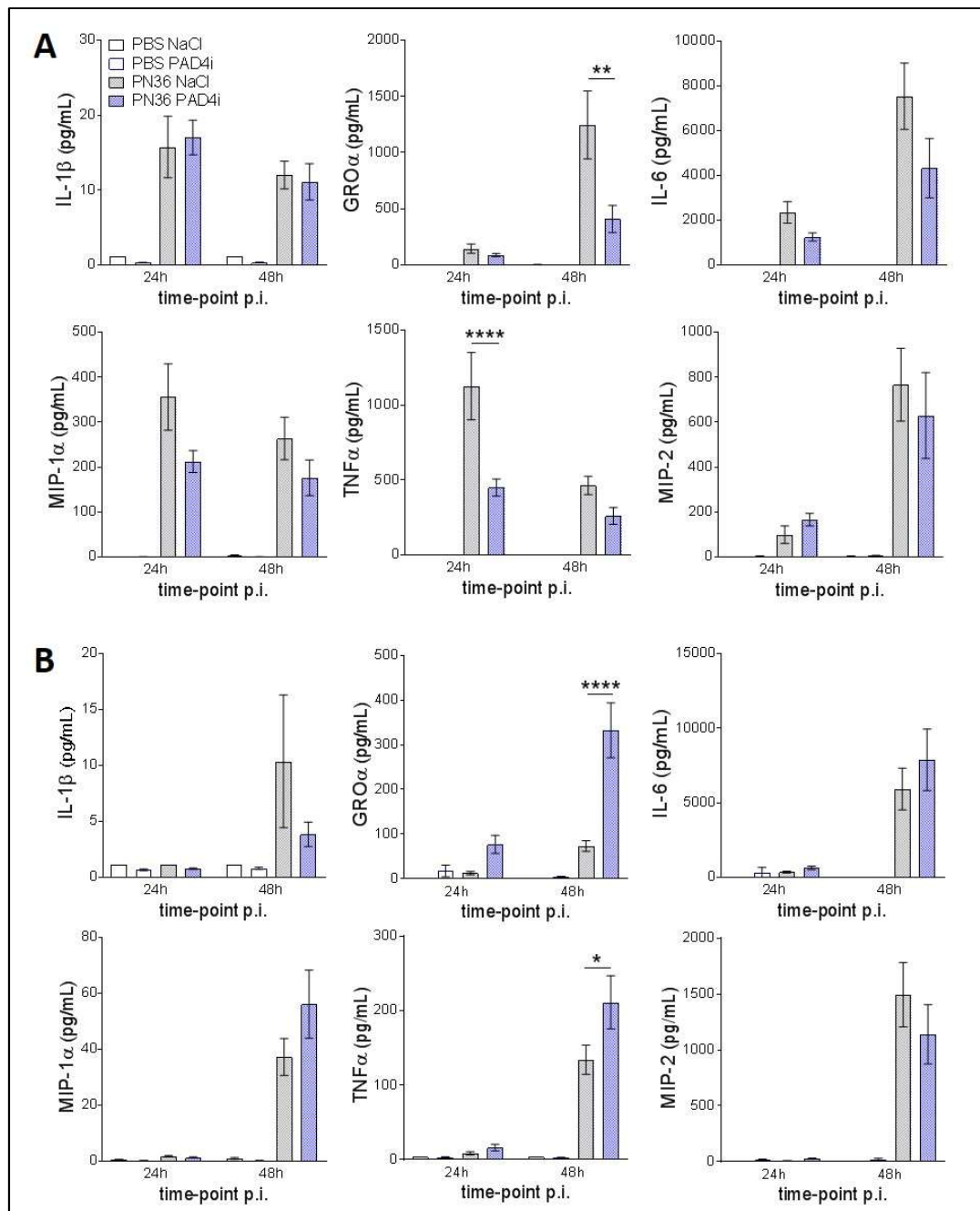


Figure 12.4: GSK484 influences cytokine production in the lungs and systemically. Typical pro-inflammatory cytokines IL-1 β , GRO α , IL-6, MIP-1 α , TNF α and MIP-2 were quantified with a multiplex ELISA in BALF (A) and plasma (B) samples from *S.pn.*-infected (PN36) and mock-infected (PBS) animals after treatment with the potent PAD4 inhibitor GSK484. Two-way ANOVA/Tukey's multiple comparisons test; only statistical differences between treated and the related non-treated groups are shown; $p < 0.05$ (*), $p < 0.01$ (), $p < 0.0001$ (****); columns represent means and error bars are SEM; $n = 5-11$.**

4.4. PSA protects against pneumonia related lung injury

Histones are the second most abundant component of NETs and are highly important for their antimicrobial properties. However, they also play a central role in NET-mediated cytotoxicity, being highly cytotoxic to endothelial and epithelial cells (Saffarzadeh et al., 2012). The third strategy used to minimize the cytotoxicity of NETs in pneumococcal pneumonia was the treatment of mice with PSA, aiming to neutralize the cytotoxic effect of histones. Treatment was performed with an i.p. application of 100mg/kg bodyweight PSA in the mouse model of pneumococcal pneumonia. Treatment with PSA was performed as previously described for the treatment with DNase. Infection of mice with *S.pn.* led to clinical symptoms of pneumococcal pneumonia, with a continuous decrease in body weight and temperature during progression of the disease and bacteremia.

4.4.1. PSA reduces pulmonary NETs during pneumonia

NETs quantified in BALF showed similar results to the previous experiments. Infected animals had significant increased levels of NETs at the 48h time-point p.i. in comparison to the mock-infected animals and to the 24h time-point. PSA treatment led to a significant reduction in NET formation after infection with a 7-fold decrease in NETs levels at 48h p.i. in comparison to the non-treated group (Figure 13.1A). *S.pn.* infection led to an apparent, but not significant, increase in lung permeability in both assays analyzed at the 24h time-point. At 48h p.i., permeability levels were considerably higher in the infected animals than in the non-infected group. Animals treated with PSA had reduced pulmonary permeability levels than the non-treated animals at 48h p.i., measured by total protein extravasation in the alveolar space, as well as by HSA translocation into the lungs. No further differences after treatment were seen among the other compared groups (Figure 13.1B).

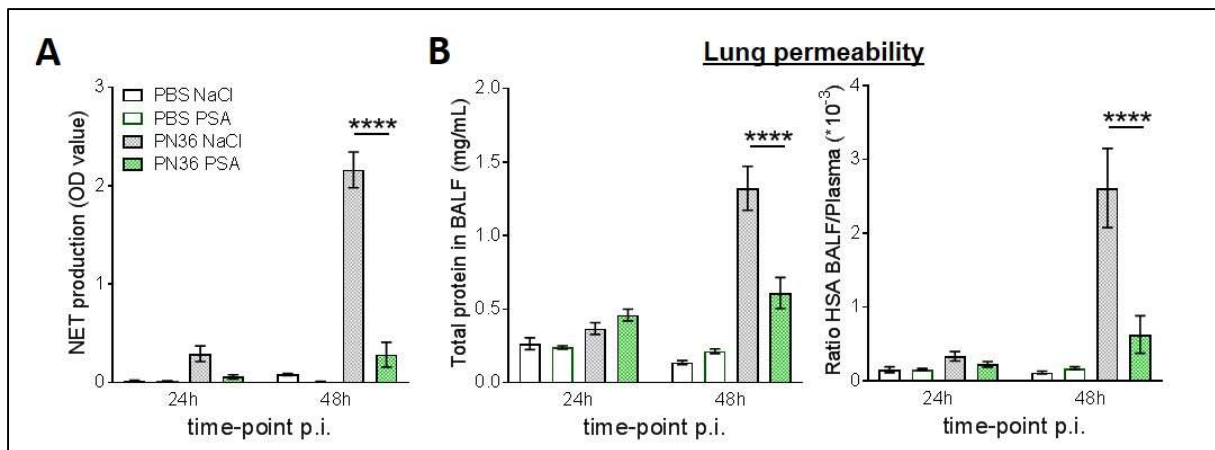


Figure 13.1: PSA reduces NETs and barrier dysfunction of the lungs after pneumococcal pneumonia. (A) NETs were quantified with the specific sandwich ELISA targeting both neutrophil elastase and DNA in BALF samples from animals infected with *S.pn.* (PN36) or mock-infected (PBS) animals treated with 100mg/kg bodyweight PSA, when indicated. **(B)** Lung permeability was assessed by total protein levels, measured in BALF (left) and by the ratio between HSA concentrations in BALF and plasma (right). Two-way ANOVA/Tukey's multiple comparisons test; only statistical differences between treated and the related non-treated groups are shown; $p < 0.0001$ (****); columns represent means and error bars are SEM; $n = 5-11$.

4.4.2. PSA affects bacterial burden in different compartments

All animals infected with *S.pn.* had a considerable loss of body temperature with time in comparison to the mock-infected mice. Animals treated with PSA had higher body temperature at the time-points of 24h and 36h p.i., when compared to the non-treated control group, while at 12h and 48h this difference was not seen (Figure 13.2A). PSA treatment did not affect levels of AST at all time-points analyzed, when compared to the non-treated animals (Figure 13.2B). Analysis of bacterial burden showed presence of bacteria in all compartments analyzed at both time-points after infection. The CFU count in BALF was similar at both time-points analyzed and PSA treatment did not affect the bacterial burden in this compartment. The bacterial burden at 48h p.i. was higher than the 24h time-point in lung, blood, liver and spleen. Animals treated with PSA had significantly lower CFU count in the lungs and in liver at the 48h time-point p.i. and also in blood and in liver at 24h p.i. (Figure 13.2C). To exclude a possible bactericidal effect of PSA, *S.pn.* was cultured with different concentrations of this molecule applied to the growth media. PSA concentrations of 1 μ M, 10 μ M and 100 μ M did not affect bacterial growth, when compared to the PBS control group (Figure 13.2D).

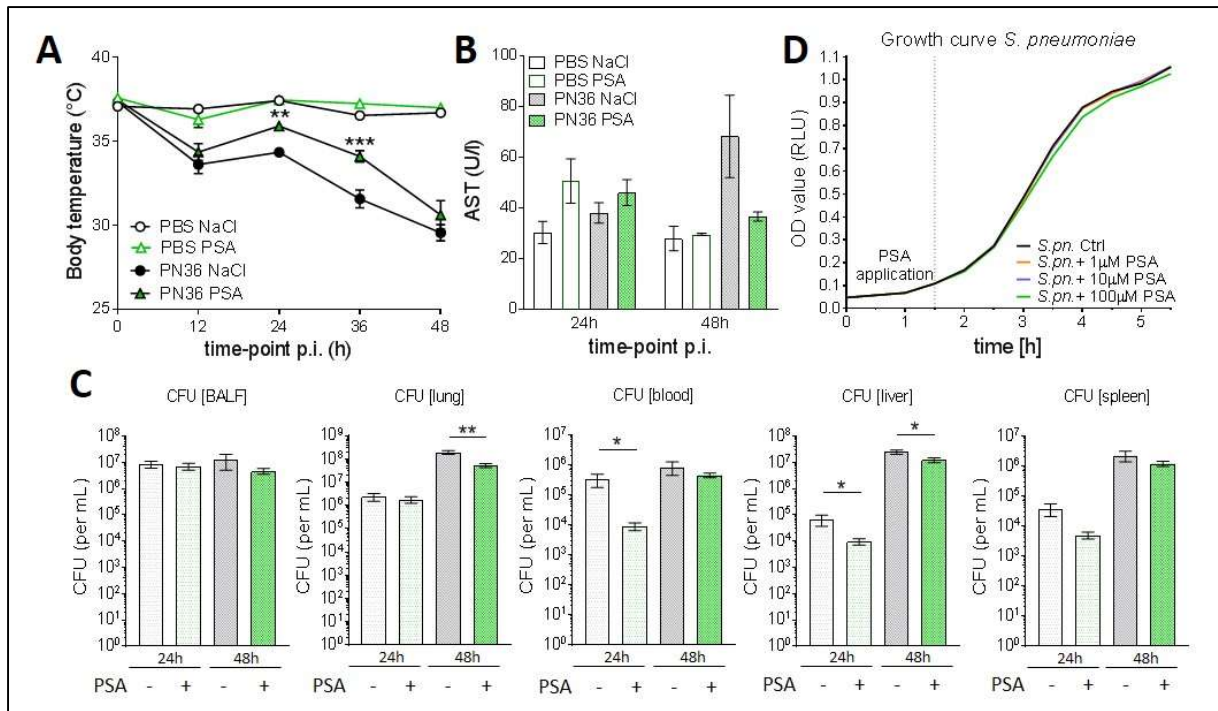


Figure 13.2: PSA delays disease symptoms and affects bacterial burden. (A) Body temperature was measured every 12h in animal infected with *S.pn.* (PN36) or mock-infected (PBS) animals treated with 100mg/kg bodyweight PSA, when indicated. **(B)** Liver damage was quantified by the aspartate transaminase (AST) levels in plasma. **(C)** Bacterial burden was quantified in BALF, lung, blood, liver and spleen, respectively, in colony forming unit (CFU)/mL. **(D)** The effect of PSA on bacteria growth was assessed by culturing *S.pn.* with different PSA concentrations. PSA concentration tested were 1µM, 10 µM and 100 µM, as specified and n=3. Two-way ANOVA/Tukey's multiple comparisons test and Mann-Whitney U test for CFU count between the groups within same time-point; only statistical differences between treated and the related non-treated groups are shown; p<0.05 (*), p<0.01 (**), p<0.001 (***); lines (A) and columns (B and C) represent means and error bars are SEM; n=5-11 for the *in vivo* experiments.

4.4.3. PSA reduces neutrophil recruitment and levels of pro-inflammatory cytokines in the lungs

FACS analysis of BALF and lung homogenate samples showed typical signs of lung tissue inflammation with increased infiltration of neutrophils after *S.pn.* infection. Neutrophil counts were significantly reduced after PSA treatment at 24h and 48h time-point p.i. in BALF and at 48h time-point p.i. in lung homogenate, when compared to solvent treated mice. Analysis of the blood compartment showed that mice had a significantly decreased number of neutrophil at 48h p.i., when compared to the mock-infected animals. At 24h p.i., the number of neutrophils in blood was significantly lower in PSA-treated than in non-treated animals. This PSA-induced reduction was not observed at the 48h time-point. Notably, PSA treatment also led to a lower number of circulating neutrophils in uninfected mice at 48h time-point (Figure 13.3A). Analysis of the activation state of neutrophils in BALF sample from infected animals showed a higher MFI expression of CD18 and CD11b after treatment with PSA at 24h p.i. (Figure 13.3B). In BALF samples, the total number of alveolar macrophages at the 24h time-point of the mock-infected animals was significantly decreased after PSA treatment in comparison to non-treated animals. However, no differences were seen after PSA treatment among the infected animals. Analysis of the percentage of both neutrophils and alveolar macrophages in BALF showed a significant increase in the percentage of alveolar macrophages in comparison to neutrophils after PSA treatment at 48h p.i. (Figure 13.3C). Animals treated with PSA had also alteration on the counting of other cell populations from the immune system. The number of B- and T-cells, NK cells and eosinophils was reduced after PSA treatment at both time-points of the mock-infected groups. However, among the infected animals, only the number of T-cells was significantly reduced at the 24h p.i. (Figure 13.3D).

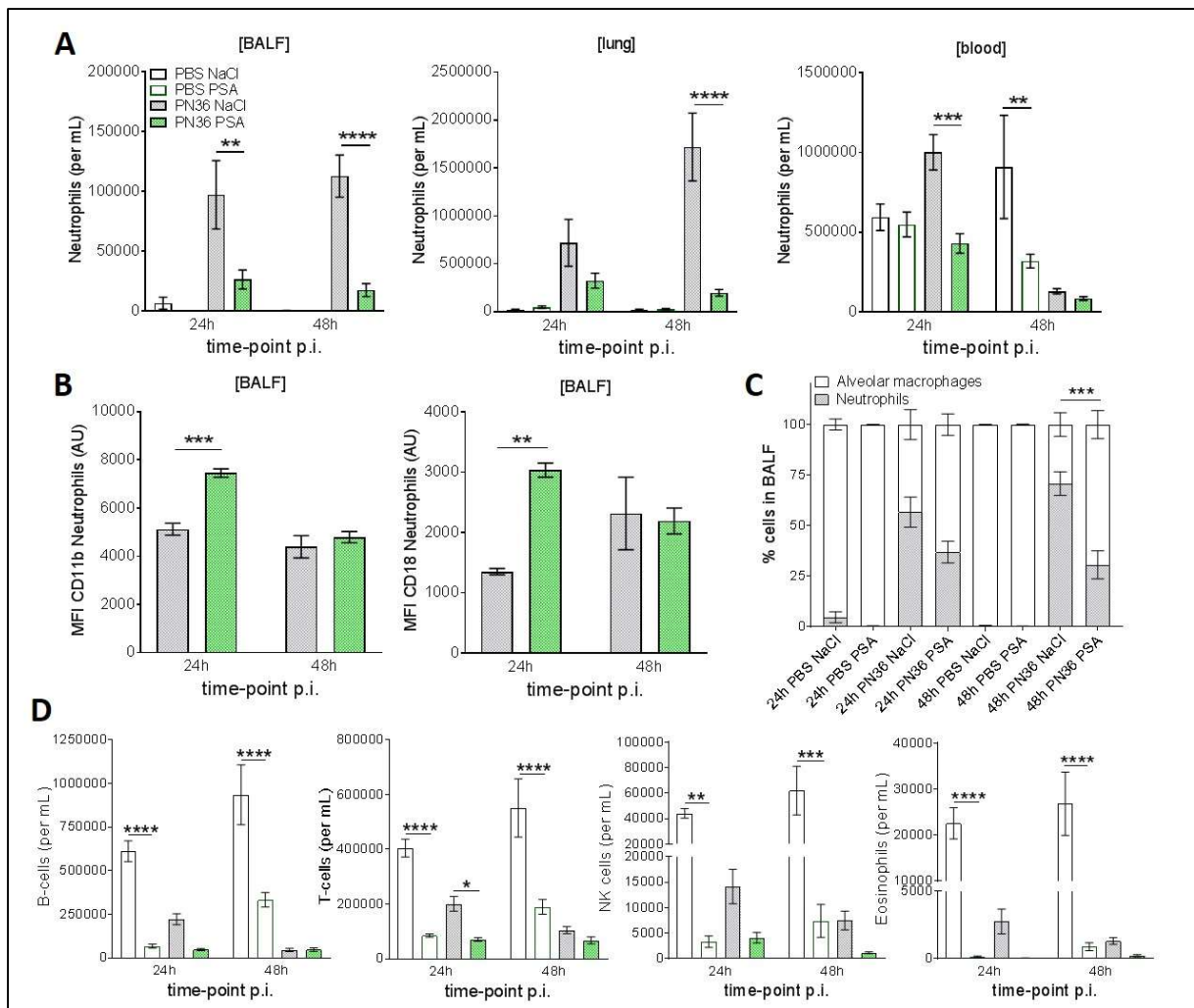


Figure 13.3: PSA influences the cellular recruitment into the lungs. (A) The neutrophil population in BALF (left), lung homogenate (middle) and blood (right) from *S.pn.*-infected (PN36) and mock-infected (PBS) animals treated with 100mg/kg bodyweight PSA was characterized by flow cytometry. (B) BALF neutrophils from *S.pn.*-infected animals were further characterized for their activation state with the median fluorescence intensity (MFI) expression level of CD11b (left) and CD18 (right). (C) Alveolar macrophages were quantified in BALF and cellular frequency of both neutrophils and alveolar macrophages is shown. (D) B-cells, T-cells, NK cells and eosinophils were also quantified in blood samples by flow cytometry. Two-way ANOVA/Tukey's multiple comparisons test; only statistical differences between treated and the related non-treated groups are shown; $p < 0.05$ (*), $p < 0.01$ (), $p < 0.001$ (***), $p < 0.0001$ (****); columns represent means and error bars are SEM; $n = 5-11$.**

Animals infected with *S.pn.* had increased levels of pro-inflammatory cytokines at 24h and 48h time-points, when compared to mock-infected animals. Quantification of pro-inflammatory cytokines after PSA treatment demonstrated profound changes in the inflammatory status both in BALF (Figure 13.4A) and plasma samples (Figure 13.4B). In BALF, $\text{GRO}\alpha$, IL-6, $\text{TNF}\alpha$ and MIP-2 levels were significantly lower in the group receiving PSA at 48h p.i., than the non-treated group. $\text{TNF}\alpha$ levels were also lower in PSA treated mice 24h after infection compared

to solvent treated mice. However, IL-1 β levels were higher after PSA application at the 24h time-point p.i. In plasma, lower levels of IL-6, MIP-1 α , TNF α and MIP-2 were observed at 48h p.i. after PSA treatment. Contrarily, GRO α levels were higher under PSA treatment at both time-points after infection when compared to the non-treated mice.

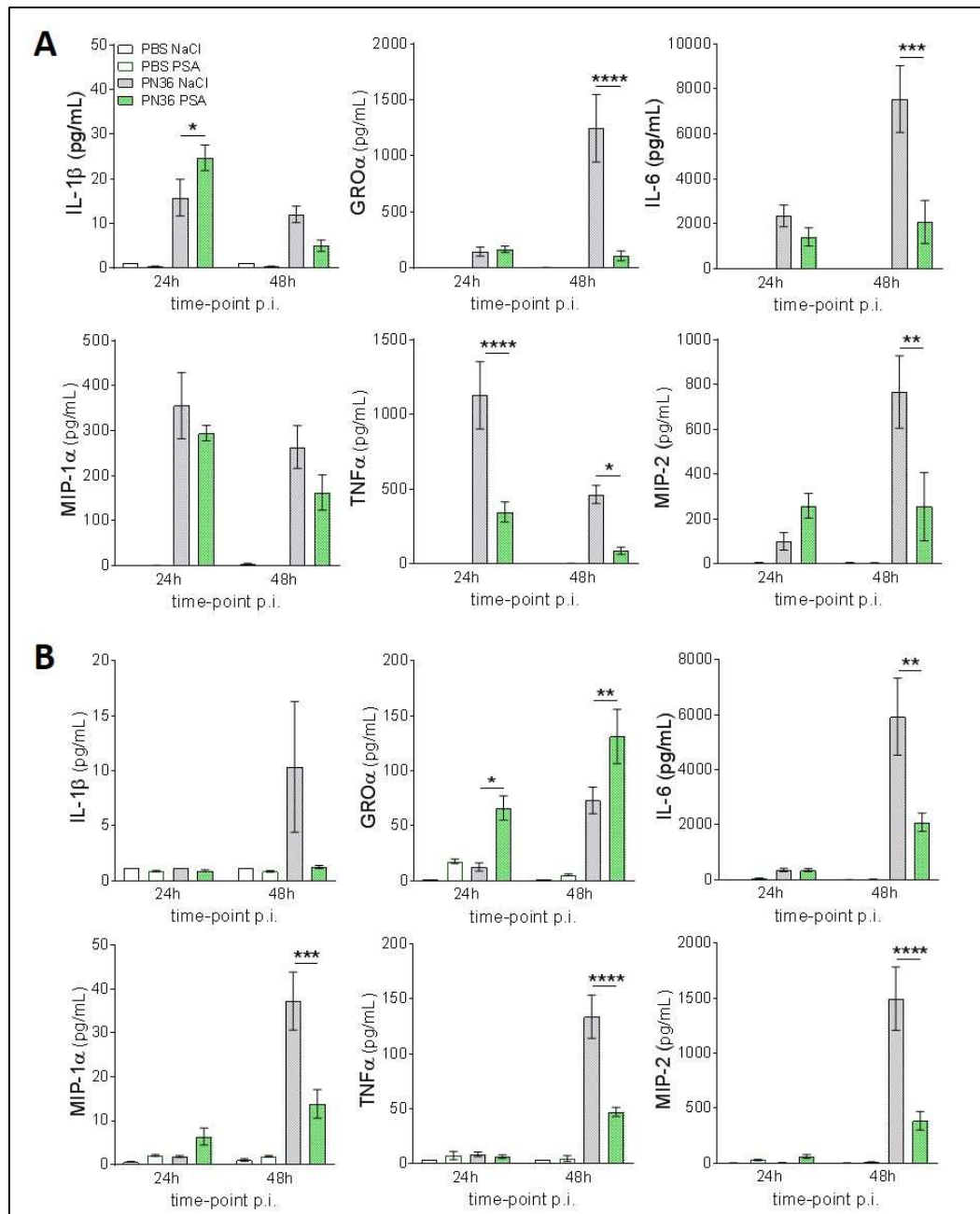


Figure 13.4: PSA influences the inflammatory status of the lungs and systemically. Pro-inflammatory cytokines IL-1 β , GRO α , IL-6, MIP-1 α , TNF α and MIP-2 were quantified in BALF (A) and plasma (B) from *S.pn*-infected (PN36) and mock-infected (PBS) animals treated with 100mg/kg bodyweight PSA, when indicated. Two-way ANOVA/Tukey's multiple comparisons test; only statistical differences between treated and the related non-treated groups are shown; p<0.05 (*), p<0.01 (), p<0.001 (***), p<0.0001 (****); columns represent means and error bars are SEM; n=5-11.**

Histology was performed on lung tissue from mice infected with *S.pn.* for 48h that were treated either with PSA or solvent. Immunohistochemistry was performed by staining of neutrophils with the typical neutrophil marker, neutrophil elastase. Neutrophil infiltration in the lung tissue was seen in both groups analyzed. In non-treated animals, neutrophils were localized both at the alveoli and the perivascular space. However, treatment with PSA prevented neutrophil infiltration into the alveolar space and neutrophils tended to accumulate in the perivascular space (Figure 13.5). Overall the number of pulmonary neutrophils was lower in PSA treated mice.

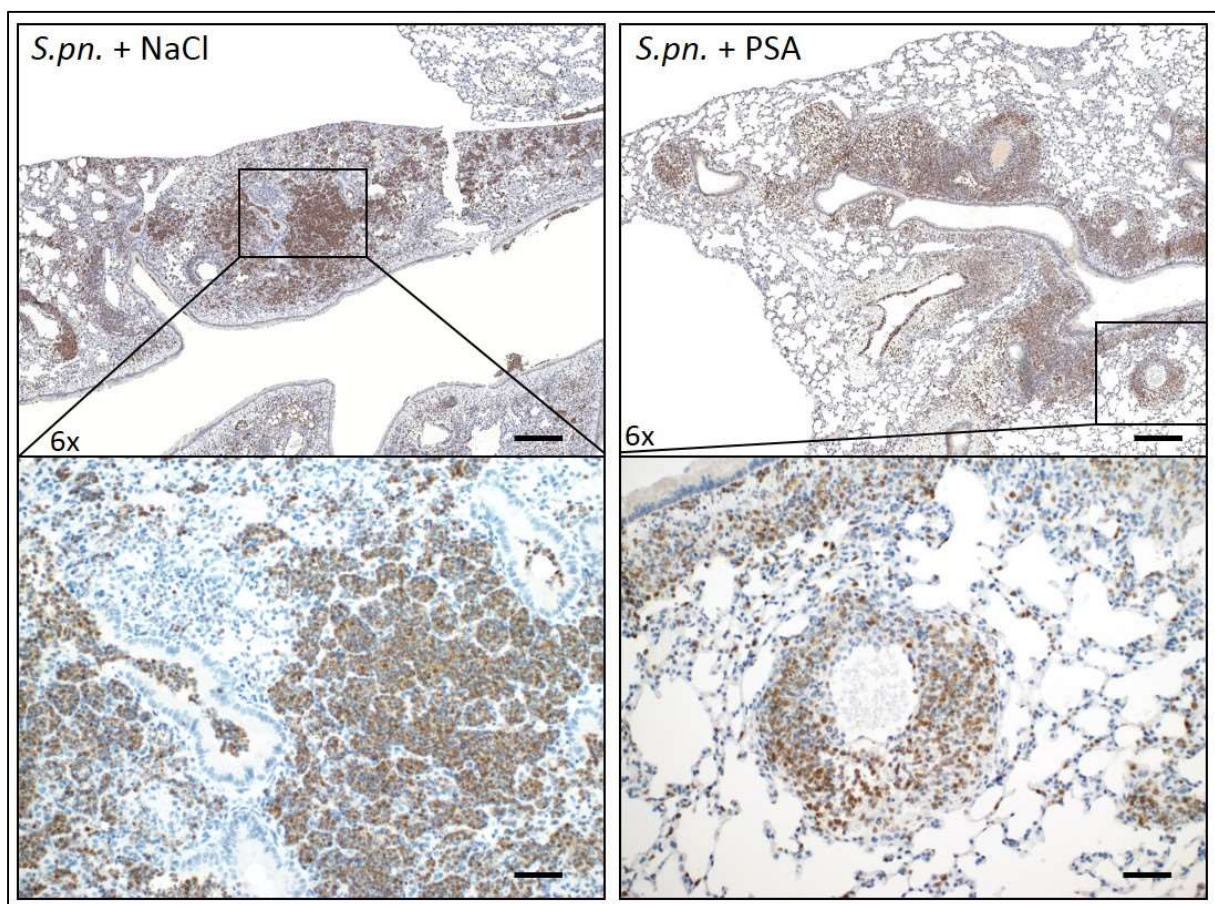


Figure 13.5: PSA affects neutrophil infiltration into the alveolar space. Lung tissue was isolated from animals after 48h infection with *S.pn.* and treated with PSA or NaCl solvent. Histology sections were analyzed under confocal microscopy after staining to neutrophil elastase. Representative images are shown with different magnifications to provide a clear overview of the infiltration process; scale bar 300 μ m (up) and 6x magnification, 50 μ m (down) n=6.

4.5. Reduced NET production upon adrenomedullin treatment is associated with lower pulmonary permeability in pneumonia

Müller-Redetzky et al. (2014) showed that ADM leads to a clear reduction in the vascular barrier breakdown and edema formation during pneumococcal pneumonia. As inhibition of NETosis was effective in reducing pulmonary permeability we questioned if the protective functions of ADM could be at least partially due to an interference with the process of NETosis. Thus, we measured NETs in BALF samples of mice in a combined model of infection with *S. pneumoniae* and MV, as described previously. Infected mice subjected to MV had significantly higher levels of NETs in BALF than the uninfected and non-ventilated control group. Surprisingly, animals treated with 0.05mg/Kg/h ADM showed a significant 3-folds reduction in NETs generated in BALF compared to the non-treated group (Figure 14A). The NET values were further correlated to the permeability levels measured previously by the ratio of HSA quantified in BALF and plasma samples. A positive correlation between these two parameters was found by the Pearson's correlation coefficient, with the higher levels of NETs corresponding to the animals with the greatest values in permeability (Figure 14B).

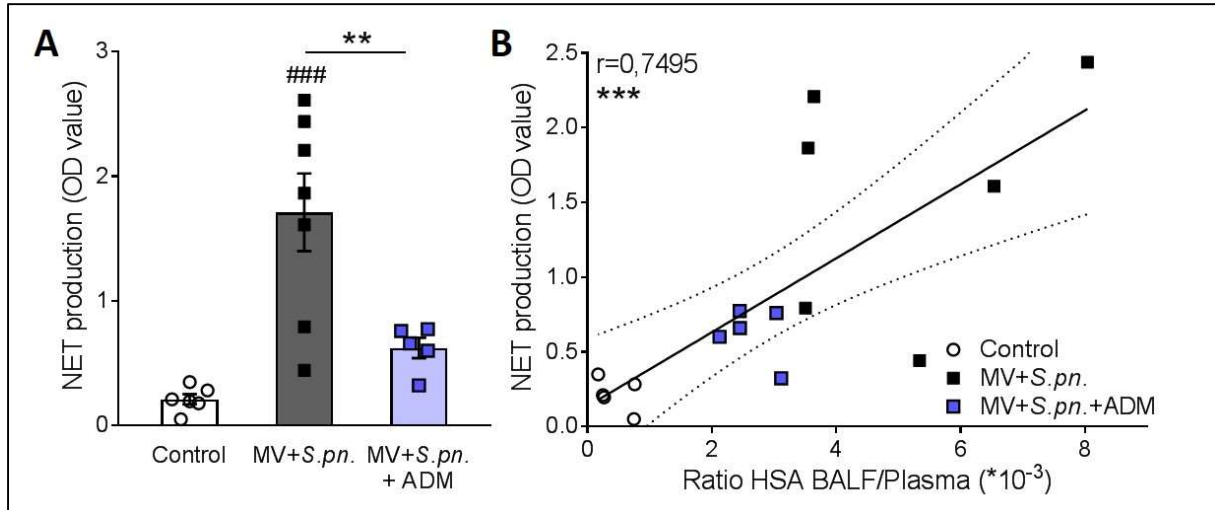


Figure 14: Adrenomedullin reduces NETs in mice infected with *S. pneumoniae*. (A) NETs were measured in BALF samples from animals in a murine model of pneumococcal pneumonia combined with mechanical ventilation (MV) with a specific sandwich ELISA, targeting neutrophil elastase and DNA. Mice were treated intravenously with 0.05mg/Kg/h adrenomedullin (ADM) during the MV or with NaCl and compared to the control non-ventilated and non-infected group. (B) Correlation analysis with the Pearson's correlation coefficient test was performed between values of NETs present in BALF and the permeability levels, measured by the ratio of HSA quantified in BALF and plasma, and linear regression is shown. One-way ANOVA/Tukey's multiple comparisons test, $p < 0.01$ (**), $p < 0.001$ (***/###); # shows significances in comparison to the control group; columns represent means and error bars are SEM; $n = 5-6$.

4.6. Adrenomedullin affects NET formation in murine neutrophils *in vitro*

Since NETs are decreased in the lungs after treatment with ADM, the question raised whether this peptide could directly affect neutrophils and the process of NETosis. For this purpose, murine BM-derived neutrophils were cultured on glass slides, stimulated for 14h with 100nM of the universal stimulator PMA for NET generation and treated with 0.5 μ M ADM, added at different time-points. Confocal microscopic analysis showed that PMA stimulation led to clear morphological changes of the neutrophils. Stimulated cells became strongly attached to the substrate, seen by a difference in cell size, had a strong decondensation of the nuclei and released NET structures with time, confirmed by co-staining of DNA and neutrophil elastase. ADM treatment resulted in a weaker attachment of the cells to the substrate and a lower number of cells actively expelling NETs (Figure 15A). Quantification of NETosis, seen by the externalization of the nucleus content after the staining of DAPI and elastase, showed a 4-fold increase in the amount of NETotic cells after PMA stimulation compared to PBS-treated cells. This increase was subrogated in about 50% by the simultaneous treatment of the stimulated cells with ADM. A delay in the application of ADM of 1h, 2h and 4h after start of stimulation was also sufficient to diminish the number of NETotic cells, whereas by this last time-point, the reduction was not statistically significant. ADM alone, used as negative control, had no effect on NETosis and was comparable to the PBS control group (Figure 15B). NETs were also quantified with the specific NET sandwich ELISA, targeting both neutrophil elastase and DNA, after stimulation of 1×10^6 neutrophils with PMA or 1 μ g/mL of the *S.pn.* cytotoxin, PLY. Stimulation with PMA and PLY led to a significant increase in the release of NETs, when compared to PBS-treated cells. The amount of NETs, generated after stimulation with PMA was higher than after stimulation with PLY. Treatment with ADM was sufficient to reduce significantly the amount of NETs generated after stimulation with both PMA and PLY (Figure 15C). Kinetic analysis of NET formation analyzed by quantification with SYTOX-Green showed a progressive increase of NETs generation after PMA stimulation, with the peak of fluorescence reaching a plateau after 7h of stimulation. Treatment of the cells with ADM was also sufficient to reduce NET formation in stimulated murine cells, seen with the peak of fluorescence signal and the area under the curve (AUC) analysis (Figure 15D).

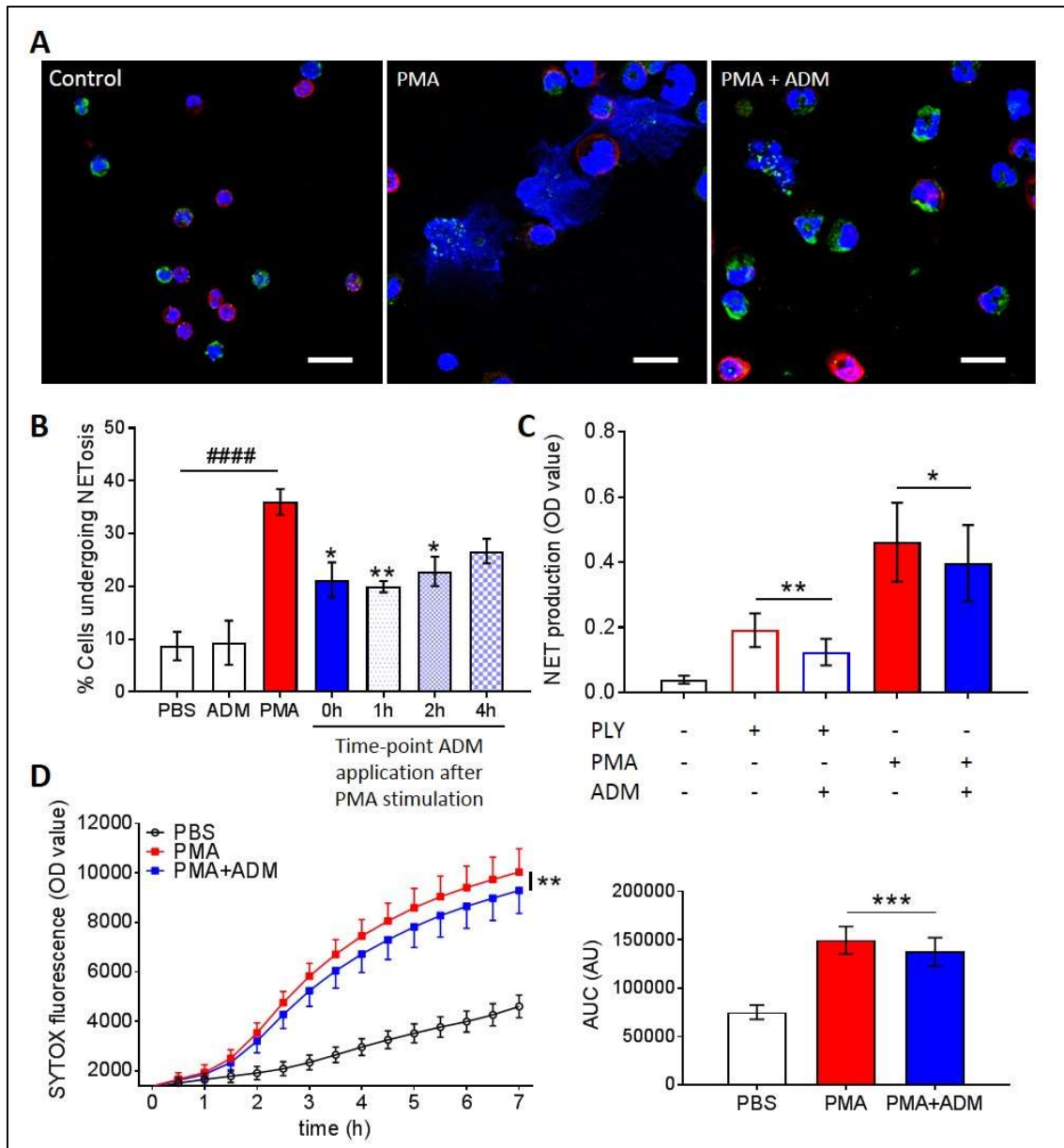


Figure 15: Adrenomedullin affects NET formation in murine neutrophils. (A) Murine bone-marrow-derived neutrophils were cultured on glass slides and analyzed by confocal microscopy. Cells were treated with 0.5 μ M adrenomedullin (ADM) at different time-points and stimulated with 100nM PMA for 14h. NETotic cells were analyzed by co-staining DAPI (blue) with neutrophil elastase (green). F-actin shows intact cells (red); scale bars: 20 μ m. The number of cells undergoing NETosis was calculated after fixation (B). (C) Isolated neutrophils were treated with ADM, when specified, and stimulated with PMA or 1 μ g/mL pneumolysin (PLY) for 14h. Cell culture supernatant was assessed for NETs with the specific NET sandwich ELISA targeting both elastase and DNA. (D) The kinetic quantification of NET formation after PMA stimulation and ADM treatment was also verified with the SYTOX-Green assay, by measuring the peak of fluorescence after 7h of stimulation (left) and the area under the curve (AUC) analysis (right). One-way ANOVA/Tukey's multiple comparisons test in B and Student's t-test for paired data in C and D; p<0.05 (*), p<0.01 (**), p<0.001 (***), p<0.0001 (####); *shows difference to the PMA-treated group; columns represent means and error bars are SEM; SEM in D are represented differently among the groups to facilitate visualization; n=5-13.

4.7. Adrenomedullin treatment affects NET formation in human neutrophils

BM-derived murine neutrophils represent a heterogeneous population, containing cells with different degree of maturation and activation state. Neutrophil progenitor cells and cells with a lower degree of maturation were not excluded from the experimental set used. Blood neutrophils represent a more homogeneous population. Therefore, the subsequent experiments were performed with human neutrophils isolated from peripheral blood. Stimulation of human neutrophils with 20nM PMA also led to the release of NET structures, as observed with murine cells. Differently from mice, human NETs were released much earlier, with the maximal signal occurring after 4h stimulation. The area occupied by the DNA backbone structure was considerably larger than what was seen with murine neutrophils, not allowing the quantification of NETs by the counting of NETotic neutrophils under the microscope. Therefore, confocal microscopy was only used to identify and confirm NET structures after PMA stimulation, by co-staining DNA (DAPI, shown in red to facilitate visualization) and the typical NET-markers citrullinated histones or neutrophil elastase (green) (Figure 16A). Evaluation of the role of ADM in NET formation was performed with the SYTOX-Green assay after stimulation of human neutrophils with PMA. PMA stimulation led to a significant increase in NET formation, with a signal stagnation being reached after 4h. Treatment with ADM led to a significant decrease in the amount of NETs being released, quantified by the fluorescence signal peak and analysis of the AUC (Figure 16B). PLY was used to verify if *S.pn.* can also induce human neutrophils to form NETs. Differently from PMA, PLY induced NET formation in a much faster manner, with higher levels of NETs being reached already after 1h stimulation. Treatment with ADM significantly reduced NET formation after stimulation with PLY, as seen by analysis of the peak of fluorescence and the AUC (Figure 16C).

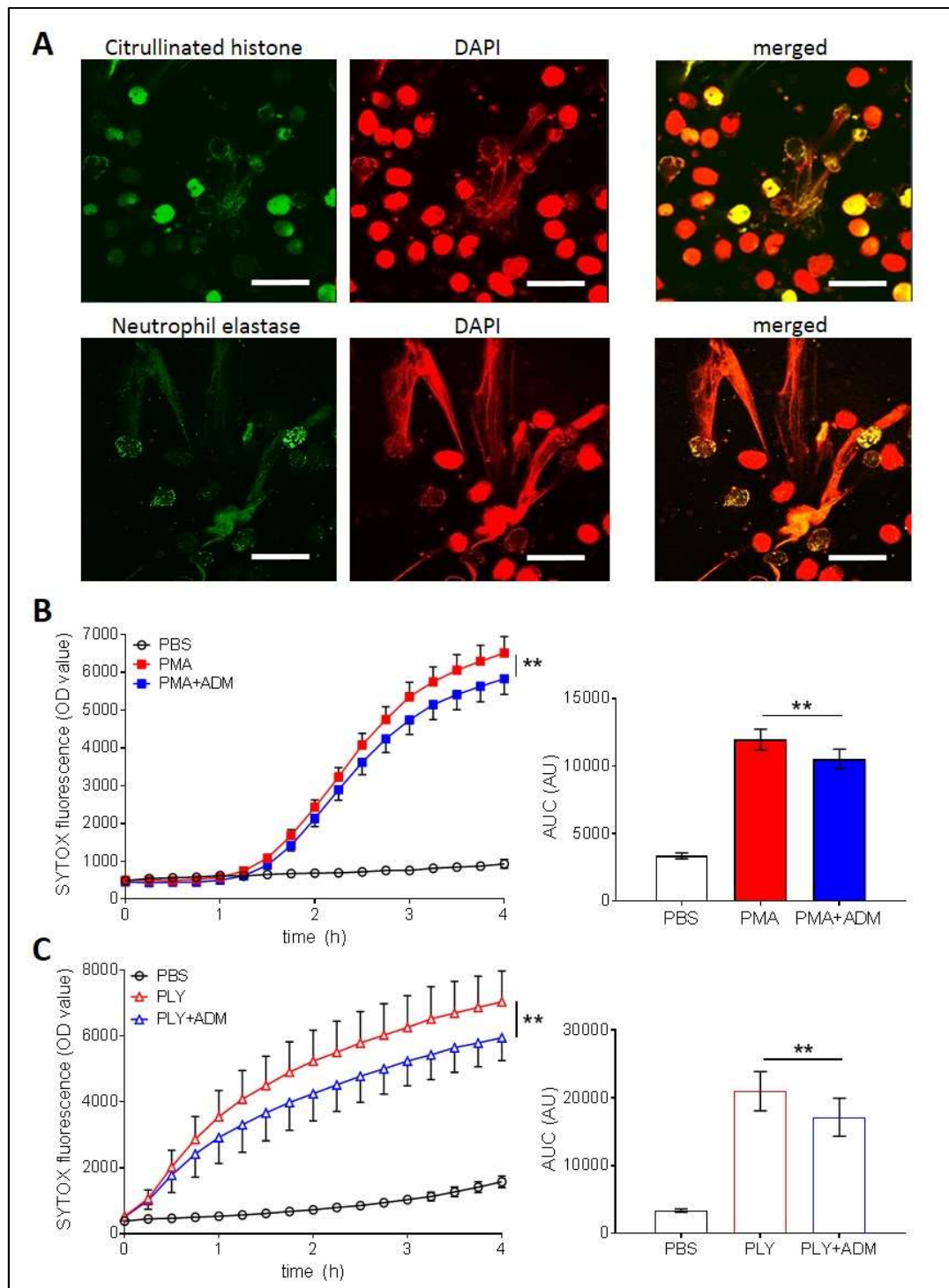


Figure 16: Adrenomedullin affects NET formation in human neutrophils. (A) Human blood-derived neutrophils were analyzed by confocal microscopy after stimulation of the cells with 20nM PMA. NETotic cells were stained with DAPI (red) and the typical NET markers citrullinated histones (upper row) or neutrophil elastase (lower row; green); scale bars: 50 μ m. **(B and C)** The kinetic quantification of NET formation by the signal peak (left) and the area under the curve (AUC) analysis (right) were performed with SYTOX-Green after cell treatment with adrenomedullin (ADM) and stimulation with PMA or 100ng/mL pneumolysin (PLY) for 4h. Student's t-test for paired data; * shows difference to the PMA/PLY group; $p < 0.01$ (**); columns represent means and error bars are SEM; SEM in B and C are represented differently among the groups to facilitate visualization; $n = 5-13$.

4.8. Adrenomedullin receptors are expressed in murine and human neutrophils

Murine BM-derived neutrophils were further analyzed for the presence of mRNA and proteins of the typical ADM receptors, CRLR and RAMP, in order to investigate whether ADM directly influences the process of NETosis via receptor recognition. Therefore, cDNA from 2×10^6 murine BM-derived neutrophils was synthesized from extracted mRNA and PCR was performed to verify the expression of the receptors *Crlr*, *Ramp1*, *Ramp2* and *Ramp3*. mRNA quantification showed that murine neutrophils express the *Crlr* receptor and the CGRP-specific receptor *Ramp1*. However, no expression of *Ramp2* or *Ramp3* was detected. Notably, mRNA expression of *Adm* was also found in murine cells. Relative mRNA expression was calculated by comparison to the internal house-keeping gene β -actin (Figure 17A). *Adm*, *Crlr* and *Ramp1* mRNA expression did not show any further increase after stimulation of the cells with PMA (data not shown). In order to verify whether the mRNA is translated into proteins, we quantified the expression of ADM, CRLR and RAMP proteins on murine neutrophils by western blot. In agreement with results obtained by the mRNA expression analysis, murine BM-derived neutrophils also presented protein levels of ADM, CRLR and RAMP1. Expression of RAMP2 in murine neutrophils was not detected and RAMP3 protein expression was not investigated. Stimulation of the cells with PMA did not affect levels of protein expression. Additionally, we investigated for the receptor protein levels in a mature population of neutrophils isolated from human peripheral blood. 2×10^6 neutrophils were acquired from human blood and used for protein expression analysis with specific antibodies by western blot. Protein levels of CRLR and RAMP1 were present in all three replicates analyzed, similarly to murine neutrophils. The protein RAMP2 was also not detected in human cells. Beta-actin was used as an internal control for relative quantification. Interestingly, the peptide ADM was also found to be expressed in human neutrophils (Figure 17B). Neutrophils stimulated with PMA or treated with ADM had similar levels of protein expression compared to the control group (data not shown).

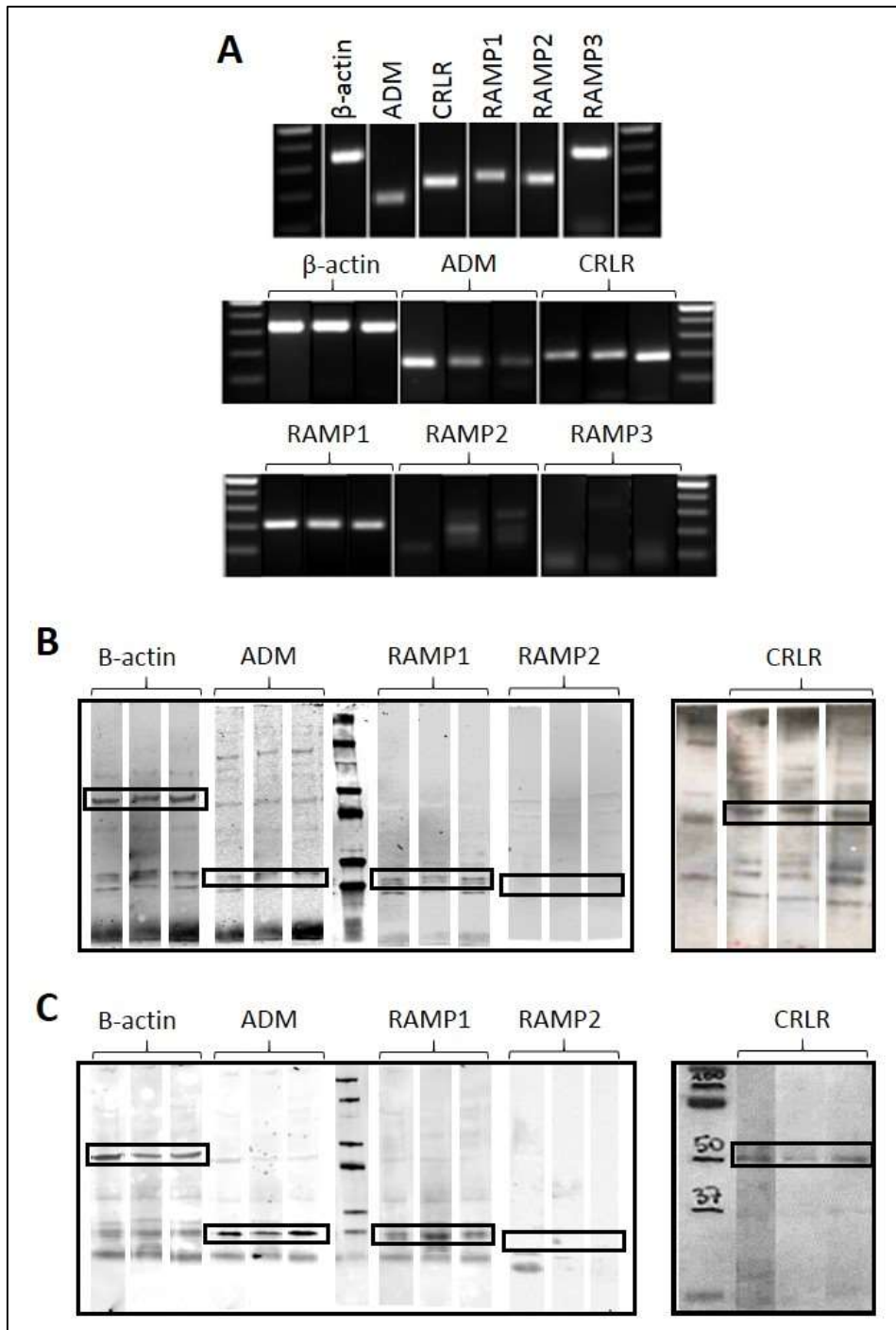


Figure 17: The adrenomedullin receptors, CRLR and RAMP, are expressed in murine and human neutrophils. (A) PCR was performed with specific primers targeting *Adm*, the receptor *Crlr* and the three distinct *Ramp* receptors in murine BM-derive neutrophils. *Beta-actin* was used as internal control for relative quantification. Positive controls are shown (upper row). (B and C) Protein levels of adrenomedullin (ADM) and its receptors CRLR, RAMP1 and RAMP2 were analyzed by western blot in mice cells and in human blood-derived neutrophils. Beta-actin was used as internal control for protein quantification. Bars shows expected band size; n=3.

4.9. Adrenomedullin reduces NET formation via CRLR-RAMP receptor complex ligation and cAMP production

To verify that ADM acts via receptor ligation and not via another mechanistic pathway within the process of NETosis, the specific CRLR/RAMP inhibitor olcegepant was used to block the activity of this receptor complex. NET formation was quantified with SYTOX-Green after treatment of the cells with ADM and blockage of the receptor complex with olcegepant. As described previously, PMA stimulation of human neutrophils led to the formation of NETs within 4h of stimulation and ADM significantly reduced the amount of DNA being released. Olcegepant was able to prevent the inhibitory effect of the peptide ADM on NETosis, as the amount of NETs measured after receptor blockage was similar to the amount found after PMA stimulation alone. As CRLP/RAMP1 is the described receptor complex for CGRP, cells were further treated with CGRP, as a positive control, and it was found that CGRP also reduced NET formation after cellular stimulation in similar levels to ADM, when compared to the control PMA group. Comparison in the level of NET formation was made by the peak of fluorescence after 4h stimulation and the AUC analysis (Figure 18A). Previous studies have shown that ADM recognition by the CRLR/RAMP complex leads to the activation of a G-protein, which is directly connected to the enzyme adenylyl cyclase (Kitamura et al., 1993). To verify whether cAMP levels were affected by stimulation of the cells with this peptide and interfere within the process of NETosis, NET formation was analyzed with the SYTOX-Green assay after stimulating neutrophils with the specific cAMP-inducer, forskolin. Interestingly, forskolin also led to a significant reduction in the amount of NET formation after PMA stimulation, similarly to the levels obtained after treatment of the cells with ADM or CGRP (Figure 18B).

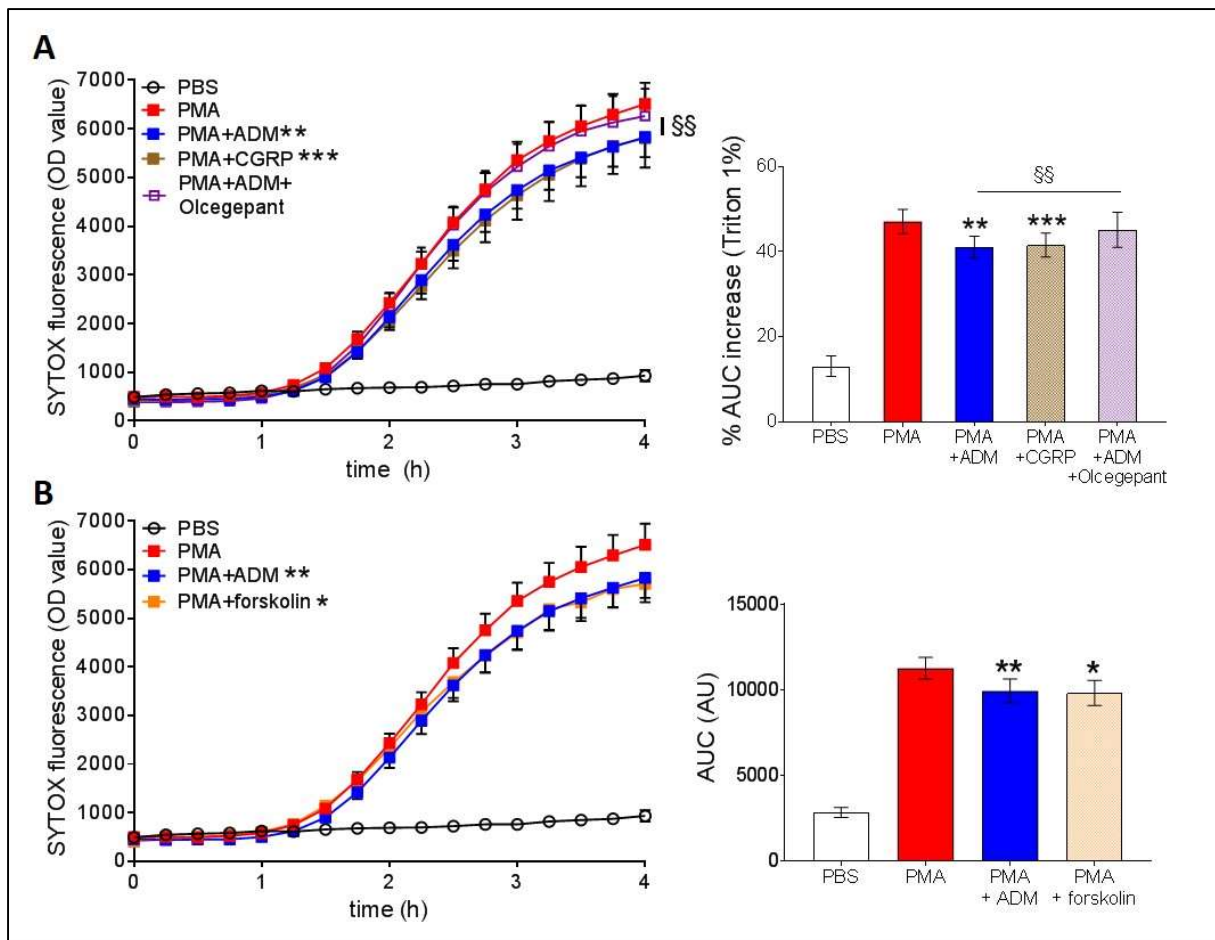


Figure 18: Adrenomedullin affects NET formation via receptor activation and subsequent cAMP production. (A) Human neutrophils were stimulated with 20nM PMA and NET formation was quantified for 4h with the SYTOX-Green assay. Before stimulation, cells were treated with 0.5 μ M of adrenomedullin (ADM), CGRP or the receptor blocker olcegepant, as indicated. (B) 100nM forskolin was also added previously to stimulation of the neutrophils for comparison. NET formation was quantified by the peak of fluorescence signal after 4h stimulation (left) or by the area under the curve (AUC) analysis (right). Student's t-test for paired data; * shows difference to the PMA-treated group; § shows difference to the group PMA+ADM; p<0.05 (*), p<0.01 (/§§), p<0.001 (***)**; columns represent means and error bars are SEM; n=13-15.

4.10. Adrenomedullin affects NET production via ROS inhibition

To test the mechanistic pathway by which ADM suppresses NET formation in neutrophils after stimulation, we analyzed if ADM affects the ROS production in human neutrophils, as this step is central for the process of NETosis. Total ROS and intracellular ROS levels were measured by two distinct methodologies. Kinetic analysis of total ROS production in neutrophils, assessed by the luminol reaction assay, showed that PMA stimulation led to a fast response of the cells to release ROS, with a peak of production occurring after 7 minutes of stimulation. After this peak, ROS levels tended to decrease until a plateau slightly lower than the peak. ADM treatment led to a significant inhibition of ROS production after PMA stimulation, demonstrated by the analysis of the peak of luminescence (Figure 19A). The kinetic curve of ROS production from the treated and non-treated cells, obtained with the luminol assay, was compared by the receiver operating characteristic (ROC) curve and also showed significant differences between the curves of ROS production analyzed (Figure 19B). The AUC of the kinetic analysis of ROS production was also analyzed and used for comparison between the groups and a significant reduction in ROS production after ADM treatment was found (Figure 19C). Flow cytometry was used to quantify intracellular ROS generation through the MFI levels of the fluorescent dye DCFH-DA, which change conformation after contact with ROS. Intracellular levels of ROS were significantly reduced after treatment with ADM when compared to the PMA control group. Analysis with FACS showed that CGRP was also able to inhibit ROS production in human neutrophils (data not shown), and olcegepant could partially inhibit the effect of ADM in the reduction of ROS production (Figure 19D).

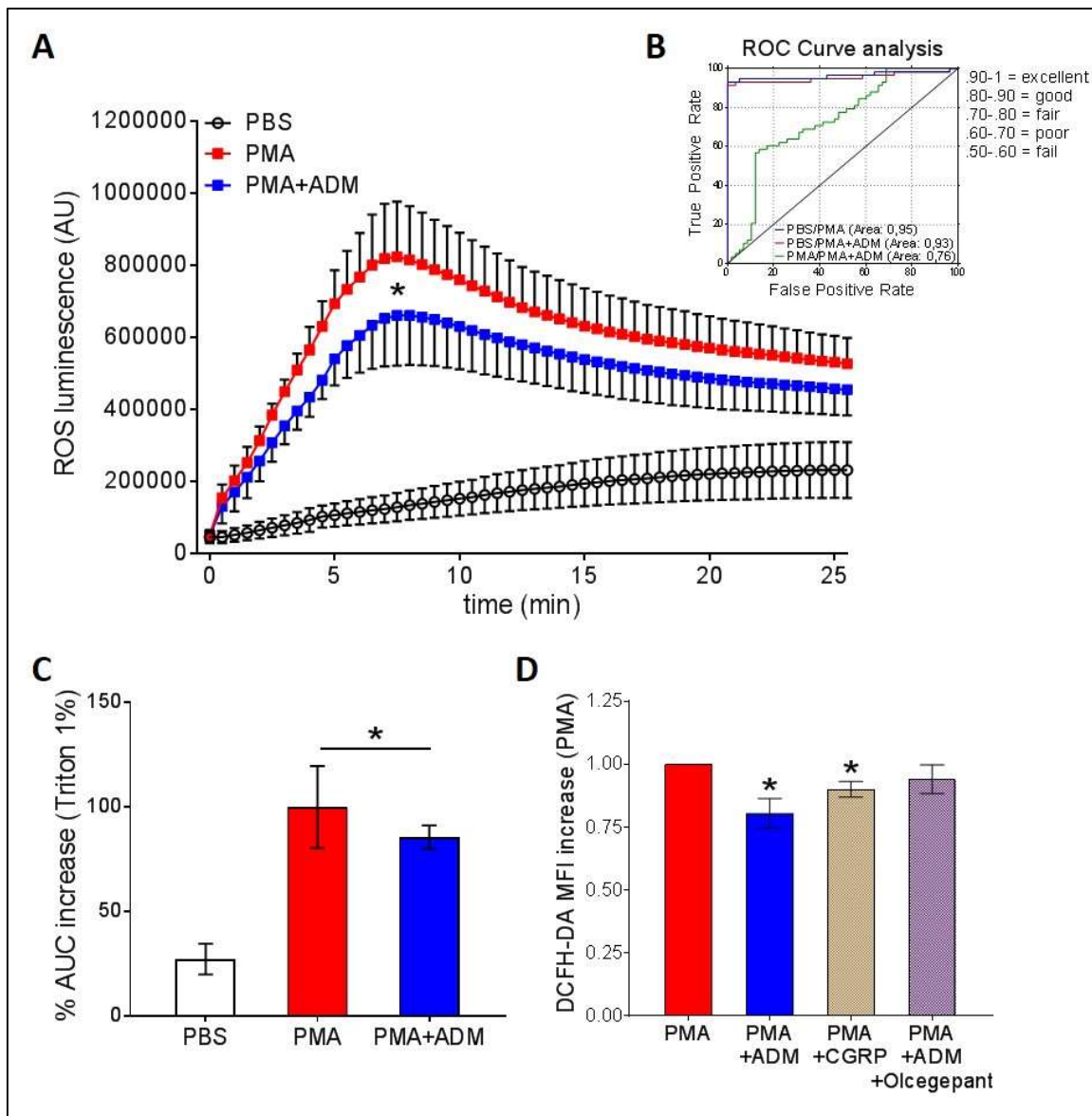


Figure 19: ROS production is reduced after treatment of neutrophils with adrenomedullin. (A) Blood-derived human neutrophils were incubated with luminol and total ROS production was measured with a kinetic luminescence assay. Cells were stimulated with 20nM PMA and treated with 0.5 μ M adrenomedullin (ADM), as indicated. **(B)** The kinetic curves of ROS production from the treated and non-treated groups were compared using the receiver operating characteristic (ROC) curve analysis. **(C)** Area under the curve (AUC) of the luminol kinetic assay was calculated for comparison. **(D)** The intracellular ROS quantified by the median fluorescence intensity (MFI) of DCFH-DA expression on neutrophils was analyzed by flow cytometry. CGRP was used as positive control and receptor complex blocker, olcegepant, as receptor control. Values obtained are relative to the PMA-stimulated group. Student's t-test for paired data; $p < 0.05$ (*); * shows difference between the treated group and the PMA group; columns represent means and error bars are SEM; SEM in A are represented differently among the groups to facilitate visualization; $n = 15$.

4.11. ERK phosphorylation is diminished after adrenomedullin treatment

PMA stimulation triggers many different signaling pathways in neutrophils, among them, PKC activation, which leads to further activation of MAPK members of the canonical Raf-MEK-ERK pathway by phosphorylation. MAPK pathway activation is upstream of NOX activation and the superoxide formation, which is necessary for NETosis (Hakkim et al., 2011; Keshari et al., 2013). To understand the role of ADM in the MAPK pathway, protein expression from members of this pathway was measured. For this purpose, 2×10^6 isolated human neutrophils were treated with $0.5 \mu\text{M}$ ADM and subsequently stimulated for 1h with 20nM PMA. Upon stimulation with PMA, neutrophils strongly increased levels of the phosphorylated ERK version (pERK) and p-38 molecule (p-p38), when compared to the PBS control group. ERK phosphorylation after PMA stimulation is completely subrogated when using the general ERK phosphorylation inhibitor, U-0126. For quantification analysis, β -actin was used as internal control (Figure 20A). Cells stimulated with PMA and treated previously with ADM for 1h had significantly reduced levels of phosphorylated ERK than PMA-stimulated cells (Figure 20B). Phosphorylation and activation of the signaling molecule p-p38 was not affected by ADM treatment or by pERK inhibition (Figure 20C). NET generation after stimulation of neutrophils with PMA and PLY, quantified with SYTOX-Green, was strongly reduced by application of U-0126. This inhibitory effect was temporary with an increase in fluorescence signal observed at later time-points (Figure 20D and E, respectively).

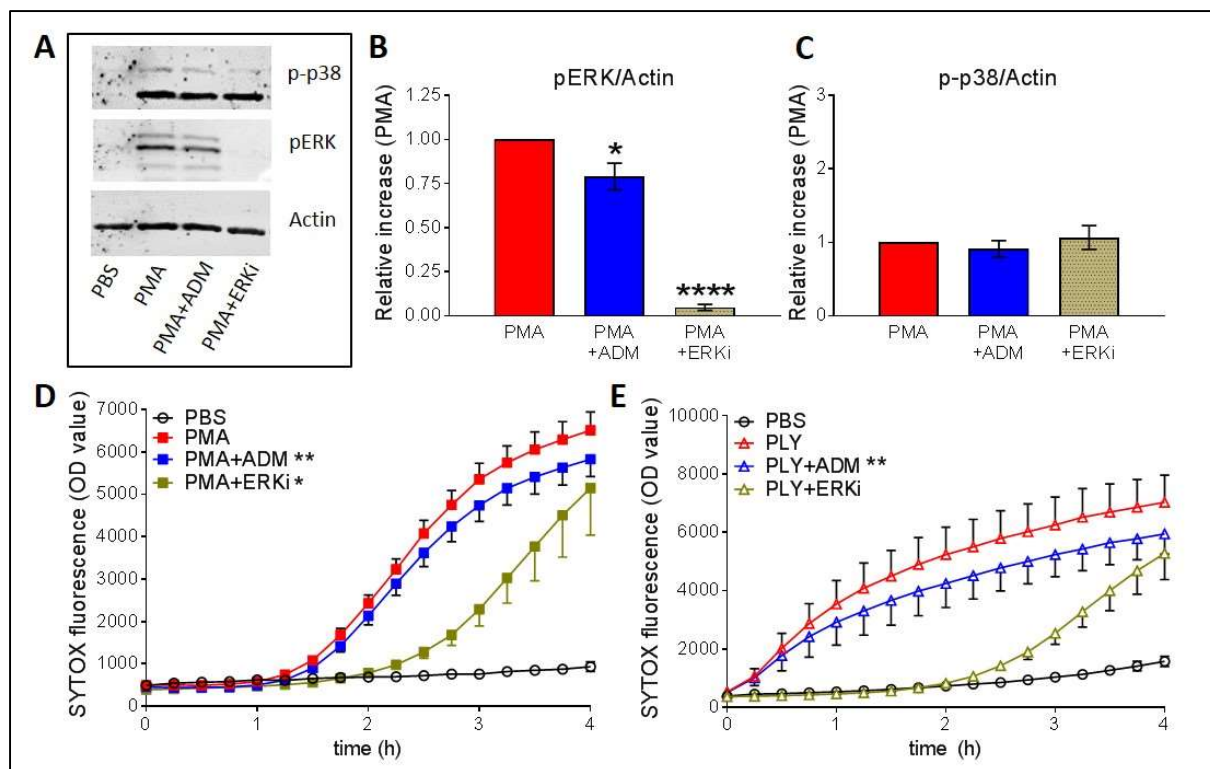


Figure 20: Adrenomedullin inhibits ERK phosphorylation in human neutrophils. (A) Western blot was performed with specific primers against typical members of the MAPK pathway. Protein levels of pERK and p-p38 were measured in human neutrophils after 1h stimulation with 20nM PMA and pre-treatment for 1h with 0.5 μ M adrenomedullin (ADM). The ERK inhibitor U-0126 was used as negative control and β -actin as internal control. (B and C) Protein levels of pERK and p-p38, relative to the internal control β -actin are shown. Protein quantification is relative to the PMA group. (D and E) NET formation measured with the SYTOX-Green assay was quantified after inhibition of ERK phosphorylation with U-0126. PMA and 100ng/mL of pneumolysin (PLY) were used for stimulation of the cells and ADM was used when indicated. Student's t-test for paired data; * shows difference to the PMA-treated group; $p < 0.05$ (*); $p < 0.01$ (**), $p < 0.0001$ (****); columns represent means and error bars are SEM; SEM in D and E are represented differently among the groups to facilitate visualization; $n = 7$ for A, B and C and $n = 7-13$ for D and E.

5. Discussion

5.1. NETs are produced in the lungs upon pneumococcal infection

Upon bacterial infection of the upper respiratory tract, neutrophils are recruited to the infected site in order to fight the harmful pathogen. After infiltration and recognition of the invading microorganism, intracellular signaling cascades are initiated, enhancing phagocytosis and inducing cytokine production. Another effector function of neutrophils for pathogen clearance is the formation NETs, which is released through the active process of NETosis. The large surface of the NET structures helps to prevent pathogen dissemination to other tissues, trapping the microorganisms via charge interactions, and their highly cytotoxic components can prolong the antimicrobial activity of neutrophils (Brinkmann et al., 2004). Here, in a murine model of pneumococcal pneumonia, quantification of NETs with the specific sandwich ELISA, targeting both neutrophil elastase and DNA, showed that NETs are produced by activated neutrophils after infection of the lung with the Gram-positive bacterium *S.pn*. NETs gradually accumulate in the alveolar space during the development of disease with a significant increase of 5 and 7-fold, respectively, at 36h and 48h time-points p.i., when compared to the 24h time-point. Histology of the lungs after staining with the typical NET marker, citrullinated histone H3, showed that NET structures are initially released at the bronchus at 24h p.i., where the neutrophils have the first contact with the pathogens. At later time-points, NETs were also detected in the alveolar space and the perivascular space. The accumulation of NETs in the lung tissue occurs in parallel with the increased cellular infiltration into the tissue. This is probably due to an increase in the amounts of potent pro-inflammatory components in the tissue after infection, which is likely to be enhanced by NETs. The increase in NET levels in the alveolar space was related to the increase in lung permeability, suggesting an association between these two factors. As the decrease of NETs via ADM application or PAD4 inhibition led to a significant reduction in pulmonary permeability, it was proposed that NETs are involved in the breakdown of the endothelial barrier function, leading to edema formation. This could be due to the highly cytotoxic components of NETs that can be recognized as DAMPs by the host, triggering inflammation and that are sufficient to induce lung injury and alveolar-capillary damage, as described by Cortjens et al. (2016) and Narasaraju et al. (2011). The deleterious role of NETs was further confirmed by the results obtained after treatment of the infected animals with DNase, which was efficient in reducing the amount of NETs in BALF. This reduction led to a concomitantly reduction of lung permeability but had no effect on the inflammatory status

and cell recruitment into the lungs. We further observed an increase in cell-free DNA levels in plasma of animals after *S.pn.* infection, which also decreased after DNase treatment. These DNA structures found in the blood are not necessarily NETs, as cell death and tissue injury can also lead to the release of DNA in the vascular system. Here, it can only be assumed that NETs are present in the vascular system, as observed by Clark and colleagues (2015), as no specific detection of NETs could be performed. Some *S.pn.* antigens have already been shown to be capable of triggering NET formation in neutrophils (McDonald et al., 2012; Apel et al., 2018; Yipp et al., 2012). Here, we show with two different specific methods for NET detection *in vitro* that neutrophils undergo NETosis after stimulation with the main cytotoxic component of *S.pn.*, PLY. NET formation after PLY stimulation was as efficient as after stimulation with PMA, a well-known universal stimulator of NETs, as previously described by different studies and measured here *in vitro*. Müller-Redetzky et al. (2014) showed in a mouse model of pneumococcal pneumonia, in which animals were subjected to MV, that mice had increased lung injury after infection and developed VILI over time. The amount of NETs quantified in the infected animals subjected to MV was substantially higher than in the non-ventilated mice at the same time-point. Therefore, MV could also trigger NET formation and exacerbate the inflammation in the lungs after infection. However, pneumonia is a complex inflammatory disease and, in addition to the pathogen, neutrophils are probably activated simultaneously by many distinct pro-inflammatory mediators or immune cells involved in this pathology. An increase in NET production could therefore be the result of many simultaneous factors, activating neutrophils during the development of pneumonia. Therefore, we show that NETs are generated in lungs after infection with the highly invasive *S.pn.* serotype 3, strain PN36 and that they are at least partially originated by the direct activation of neutrophils after pathogen recognition. Similarly to previous studies, where NETs were generated after infections with *Salmonella enterica*, *Shigella flexneri*, *S. aureus* and *Candida albicans* (Beiter, et al. 2006; Halverson et al., 2015; Moorthy et al., 2013; Papayannopoulos and Zychlinsky, 2009). We cannot exclude the possibility of an indirect stimulation of the neutrophils by other agents during the development of pneumonia that could trigger further NET formation, as pro-inflammatory mediators released after lung tissue damage or other cell populations. To further elucidate this question, further *in vitro* experiments with specific stimulators are necessary.

5.2. Hindering NET formation is beneficial in pneumococcal pneumonia

Neutrophils are of great importance for the control of the invading microorganism. However, its excessive recruitment into the tissue and activation can lead to the disproportionate inflammation of the lungs, with alveolar epithelial cell damage and breakdown of the endothelial vascular barrier (Matthay et al., 2012; Grailer et al., 2014). On one hand, NETs are essential for the immune defense of the body, trapping and killing the pathogen, but on the other hand, if over-produced or not precisely removed, they may play a central role in the associated tissue damage. To avoid this damage, a perfect balance in the amount of NETs being generated is necessary for the immune system to protect the organism against the pathogens without promoting further collateral damage (Lefrancais et al. 2018; Weiser et al., 2018). In the murine model of pneumococcal pneumonia with PN36 used in the present study, mice develop many typical symptoms of pneumonia after infection, as decreased body temperature and weight and extra-pulmonary organ damage. At early time-points, as 24h p.i., mice already had bacteremia, with spread of the pathogen in blood, liver and spleen. Moreover, we could show that infection with *S.pn.* led to an abrupt increase in neutrophil infiltration into the lungs, with enhanced NET formation and release of pro-inflammatory mediators. The correlation between NETs released in the alveolar space by infiltrating neutrophils upon infection and permeability, indicates that an increase in NETs is associated with the severity of lung injury and vascular barrier breakdown, leading to edema formation. Therefore, we targeted NETs, produced after infection with *S.pn.*, with the aim of reducing the main structure of NETs, the DNA. Applying DNase was shown to be efficient, as the amount of NETs in BALF samples and the cell-free DNA levels in plasma were reduced. Moreover, the NET breakdown in the alveolar space mediated by DNase treatment led to tissue protection against pulmonary barrier failure, measured here with two distinct techniques. We expected that reducing the presence of NETs in the lungs would possibly affect the inflammatory status of the tissue, once NETs, composed of DNA, are recognized as DAMPs by the immune system. Therefore, its release could trigger inflammation, further activating different cells from the immune system. Differently to what was expected, the reduction of NETs in this compartment did not affect cellular infiltration in the tissue and cytokine production, both in the alveolar space and systemically. However, as discussed, pneumonia is a complex disease in which the many pro-inflammatory signals released and the activation of distinct cell populations can lead to inflammation and further cell activation. Therefore, even with a significant decrease in the amount of NETs in the lung and a correlated decrease in lung permeability, the inflammatory players were already compromised, and the inflammatory status measured was not altered. Previous publications showed that the use of

DNase could promote the release of the histones and proteases previously attached to the DNA-backbone structure, worsening the scenario of acute tissue pathology during systemic infection. Moreover, these proteases were also found to be more active after release from NETs (Kolaczowska et al., 2015). Here, we found no detrimental effects of DNase treatment regarding extra-pulmonary organ injury, as no significant differences in AST levels were detected. Probably, with the breakdown of the NET structures with DNase, the released NET-related proteins could induce further tissue inflammation and, by this way, prevent the reduction of the inflammatory process after decrease in DNA levels. We further hypothesized that disrupting NETs with DNase could eventually lead to an increased bacterial spread towards extra-pulmonary compartments. However, no differences in respect to the bacterial burden in lung, BALF and the other compartments analyzed were seen after DNase treatment. This could rely on the fact that *S.pn.*, as seen in *S. aureus* and *P. aeruginosa* infection, developed mechanisms to evade NETs. Modifications of the bacterial cell surface, as presence of the polysaccharide capsule, secretion of catalases and endonucleases, as EndA, are known strategies of these pathogens to rapidly avoid NET toxicity and evade NETs, inducing further tissue damage (Beiter et al., 2006; Halverson et al., 2015; Moorthy et al., 2013; Papayannopoulos and Zychlinsky, 2009). Altogether, we can postulate that NETs are directly involved in lung tissue damage, influencing the breakdown of the vascular barrier, as treatment with DNase only affected the levels of NETs in the tissue and not the inflammatory parameters, neutrophil recruitment and bacterial burden. Therefore, disrupting NETs with DNase could prevent their cytotoxic effect on lung tissue after infection with pneumococci. However, different strategies should be evaluated to verify the accuracy of this hypothesis. It is planned to test a localized application of DNase *in vivo* (e.g. with aerosol application), which could affect NET accumulation directly in the alveolar space, and not systemically, as seen in the i.p. application used here. This could lead to a more efficient and precise degradation of NET structure in the lungs, clarifying the role of NETs in lung tissue damage. This strategy, however, would not affect the increasing amounts of NETs observed in the perivascular space after infection, which could also be an important aspect for disease progression in pneumococcal pneumonia.

To further elucidate the role of NETs in pneumococcal pneumonia, we applied another strategy that directly targeted the process of NETosis and does not only disrupt the DNA structure after its generation. Inhibiting PAD4 and therefore preventing neutrophils to release NETs would not affect further effector functions of neutrophils and their capacity to control pathogen infection. Neutrophils would still play an important role in controlling pathogens mainly via

phagocytosis, degranulation and cytokine release. We used the specific PAD4 inhibitor, GSK484, since it is a specific inhibitor of PAD4 and may not affect other cellular mechanisms, as it may occur with the pan-PAD inhibitor, Cl-amidine. The latter has already been described to induce inflammatory cells into apoptosis, affecting the immune response and the control of pathogens (Zhao et al., 2016; Chumanevich et al., 2011). Many authors have stated that histone citrullination by PAD4 may not be a common step of NET formation and may occur only after specific stimulatory pathways. Here we show that PAD4 is also involved in the process of NETosis in pneumococcal pneumonia, since we could see a significant reduction in the amount of NETs released in BALF after PAD4 inhibition. The decrease in NET formation was even clearer than observed after treatment with DNase. In our model, we cannot precisely clarify if the substance GSK484 interferes in the process of NETosis initiated after pathogen activation or by any different stimulatory pathway that influences neutrophils infiltration in the lungs. An indirect stimulation provided by pro-inflammatory mediators released by different cell types or immune cells activated in the infected tissue could also lead to neutrophil activation and NET release. Different mechanistic pathways could be involved simultaneously, as pneumonia is a complex inflammatory disease, and PAD4 inhibition could partially affect neutrophils in many of the pathways being activated, which are dependent on PAD4 activation. Furthermore, the reduction in NETs measured in BALF samples could be further explained by a reduction in the infiltration of neutrophils into the alveolar space. This probably occurs due to a positive feedback loop in which reduction in NET formation led to a reduction in the release of pro-inflammatory mediators in the tissue, as seen in the reduction of important cytokines measured in BALF. This reduced inflammation led to a reduction in neutrophils recruitment, affecting further the formation of NETs. To elucidate this question, we correlated the amount of NETs measured in BALF with the total number of infiltrating neutrophils in the lung. By this analysis we would be able to see a relation between the amount of NETs accumulated in the lungs and the number of neutrophils found in the tissue. Interestingly, in the infected animals, no differences in the ratio between NETs being generated and the number of infiltrating neutrophils after treatment with GSK484 could be seen. With this result, we can assume that the reduction in neutrophil infiltration into the lungs is an important factor in the reduction of NETs, as less neutrophils would simply lead to less NETs. PAD4 inhibition also led to an apparent reduction of lung injury, measured by lung permeability with two different assays. This decrease in permeability was not as substantial as observed by treatment with DNase and not statistically significant. This could be explained by the fact the PAD4 inhibition could be partially affecting a fundamental function of NETs, which is the entrapment of the bacteria in

its structures. The importance of NETs for bacteria control at early time-points of infection was already shown in mice models of sepsis with NET degradation. With NET removal, an enhanced bacterial spread would take place, leading to increased inflammation and organ injury, as observed by Meng and colleagues (2012). Even if bacteria could be evading these structures with endonucleases, as described before, NETs could be providing a physical barrier, reducing further bacterial spread. Without this bacterial trapping provided by NETs, a significant increase in the bacterial burden after treatment with GSK484 was seen in blood. This could also explain the increase in cell-free DNA in the vascular system, which could be partially derived by NET structures. More NETs in the blood could lead to the retention of the *S.pn.* in the vasculature, controlling its spread towards other tissues, as seen in liver. However, increased levels of AST were obtained in plasma from infected animals after treatment with GSK484. We suggest that a) GSK484 could possibly have a hepatotoxic effect, not analyzed here, or b) that neutrophils would be more activated after GSK484 treatment and have increased cytotoxic effect on liver cells or c) that an increase in NETs, as seen by the cell-free DNA levels, could be leading to occlusion of the microvasculature of extra-pulmonary organs with thrombosis formation and tissue injury, as previously observed by Kolaczowska et al. (2015). Altogether, clinical condition and body temperature showed that mice presented reduced clinical symptoms of the disease. Therefore, controlling the amount of NETs accumulating in the lungs may reduce inflammation and improve the animal clinical conditions after infection. Application of GSK484 could supplement the important functions of antibiotics, which is of extreme importance in the elimination of the invading pathogen, interfering with the inflammatory process already initiated in the lung. Therefore, PAD4 inhibition may be exploited as a novel adjunctive treatment, controlling the process of NETosis and the hyper-inflammatory conditions of the lung, attenuating tissue damage. However, we should consider its application at later time-points or in combined therapy strategies. Further experiments should be performed aiming the inhibition in NET formation during pneumococcal pneumonia, however, avoiding possible complications generated by reducing the desired role of NETs in pathogen entrapment and killing.

In addition to DNA, histones and the many proteases attached to NETs have an important role in NET-mediated cytotoxicity. Histones, specially histone H3 and H4, were shown to be important in promoting cytotoxicity to endothelial and epithelial cells, due to their ability to compromise cell membrane integrity (Narasaraju et al., 2011; Saffarzadeh et al., 2012; Cortjens et al., 2016). Treatment of sepsis and other inflammatory diseases aiming to neutralize histones toxicity was already shown to be highly effective in different disease models, minimizing organ

damage and mortality (Xu et al., 2009; Wen et al., 2013; Monestier et al., 1993; Grailer et al., 2014; Saffarzadeh et al., 2012; Chaput and Zychlinsky, 2009; Abrams et al., 2013). The substance used here, PSA, which aims to reduce the cytotoxicity of histones, showed remarkable results in our model of pneumococcal pneumonia, affecting simultaneously many of the parameters analyzed. Treatment with PSA affected primarily the recruitment of innate cells into the blood and their infiltration into the alveolar space. A huge drop in the number of NK cells and eosinophils was observed in the blood and BALF. PSA is known to modify the protein NCAM, typically found in NK cells, regulating cell adhesion, migration and cytokine response (Costantini et al., 2010). This could potentially have a direct impact on the recruitment and activation of neutrophils, as it has already been shown that neutrophils and NK cells can modulate each other, thereby modifying their activity and survival. Furthermore, PSA was shown to be an important innate immunomodulatory compound, preventing among others the activation of macrophages and by this way bacterial clearance (Drake et al., 2008; Karlstetter et al., 2017; Shahraz et al., 2015; Stamatou et al., 2014). This could possibly explain the reduction in alveolar macrophage numbers in the lungs in the mock-infected animals at 24h p.i. Neutrophil recruitment from the BM towards circulation and into the lungs was also profoundly affected, with a reduced number of cells being found in blood, lung tissue and BALF. PSA is expressed in early hematopoietic cells, concomitantly with c-kit expression and tends to decrease upon maturation of these cells, modulating myeloid maturation in mice (Drake et al., 2008). Therefore, the presence of PSA could affect the recruitment of important primary inflammatory cells from the BM or promote its regression from the circulation prematurely and affect the activation state of these cells. Immunohistochemistry analysis of lung tissue from infected animals showed that PSA impacted the process of neutrophil infiltration into the infection site, as they accumulated in the perivascular space and did not further migrate into the alveolar space. This shows the modulatory functions of PSA, affecting the process of neutrophil migration, activation and recruitment to the inflammatory site. This reduced number of neutrophils in the alveolar space is probably correlated to the concomitant reduction in NETs in BALF, as a reduced number of cells would be actively releasing NETs after pathogen recognition. PSA did not directly affect the neutrophils in the process of NETosis, as no effect in NET formation was seen with the SYTOX-Green assay after PSA application (data not shown). With a decrease in neutrophil infiltration and therefore in NET accumulation in the lungs, a reduction in inflammation would follow, affecting further the recruitment of neutrophils. This positive feedback loop would explain the expressive reduction in NETs, in cell counts and in lung injury measured by the permeability assays. Most likely, the reduction

of neutrophil infiltration in the alveolus by prevention of trafficking through the epithelial barrier is the main underlying mechanism of the decreased NET formation and the reduced permeability seen here. However, we cannot exclude the possibility that the decrease in lung epithelial damage is simultaneously caused by a decrease in histone cytotoxicity provided by PSA, as seen in previous studies. To clarify this questions, further experiments should be performed with the use of more specific neutralizing agents that affect specifically histone cytotoxicity and not distinct components of the immune system, as observed with PSA. With an increase in the proportion of bacteria in relation to neutrophils infiltrating the lungs, a stronger activation of this cell population could be seen, measured by the activation markers CD11b and CD18. Possibly, more activated neutrophils would be more effective in the clearance of the invading bacteria after evasion of the alveolar space. This could explain the decrease in bacteremia in blood, lung and liver, seen after PSA treatment, as this substance did not affect bacteria growth directly. Tsuchiya et al. (2014) showed that PSA is necessary for embryonic liver development and has a major role in tissue regeneration after damage, which could affect AST levels, seen by a trend in decrease in plasma. Altogether, PSA treatment was sufficient to improve the general clinical conditions of the mice after infection with *S.pn.*, with a substantial decrease in the amount of NETs accumulating in the alveolar space after infection and in tissue injury. PSA was shown to be an important modulatory factor of cellular activity, interfering in the process of migration from the BM towards the circulation and infiltration in the lung tissue of distinct immune cells. Considering that in pneumococcal pneumonia the uncontrolled cellular infiltration in the lungs and the associated hyper-inflammatory state is the main cause for the breakdown of the epithelial-vascular barrier and the increased leakage of protein-enriched plasma, the inhibition of neutrophil infiltration and NET formation is of great interest for the control of the inflammatory process and the progression of the disease. This molecule could be an interesting target for the treatment of the acute inflammatory process observed in pneumococcal pneumonia. However, the fact that we could not explain the exact mechanism of action of PSA, since it could concomitantly affect other cell types, and the fact that mock-infected mice had an abnormal body weight lost over time (weight loss of approximately 15% after 48h after PBS infection and statistically different to the non-treated mock-infected group at the 24h, 36h and 48h time-points with a probability of $p < 0.0001$), indicates that further studies with PSA should be conducted before its application in a combinatory therapeutic model.

5.3. Adrenomedullin affects NETosis via ERK phosphorylation and NOX inhibition

There is an increasing interest in the development of adjuvant therapies for bacterial infections, since it is known that a combinatory therapy can be more efficient in the control of the disease than single therapies (Dockrell et al., 2012; Weiser et al., 2018). This applies for infections with *S.pn.*, as this pathogen demonstrates a high rate of genome variation, which facilitates evasion of vaccine-induced immunity and the raise of antibiotic resistant microorganisms. ADM is a hormone-peptide produced in many different tissues, by many distinct cell types. It is known to promote stabilization of the endothelial barrier functions by preventing inter-endothelial gap formation, thus reducing organ dysfunction in acute inflammation after infection. ADM administration also affects secretion of pro-inflammatory mediators in the tissue, reducing inflammation and protecting the lung, liver and gut in ARDS/ALI and sepsis (Kato and Kitamura, 2015; Temmesfeld-Wollbruck et al., 2009). Müller-Redetzky and colleagues (2014) showed in a mouse model of severe pneumonia adapted to the life-saving strategy of MV that ADM is protective against vascular barrier breakdown and edema formation. We measured NETs in this model of pneumococcal pneumonia with exacerbated tissue damage provoked by MV and showed that ADM application also led to a reduction in the amount of NETs accumulating in the alveolar space. Interestingly, the decrease in NETs could not be explained by a reduced inflammatory state of the tissue, as no differences in neutrophil recruitment into the lungs and cytokine production were seen. Moreover, the reduction in NETs was shown to have an important association to the decrease of the pulmonary barrier failure. The receptors for ADM, namely CRLR and RAMP, were shown to be expressed on murine neutrophils. Further characterization using mature blood cells showed that the receptors CRLR and RAMP1 are also found in human neutrophils. Interestingly, only expression of the CGRP-specific receptor RAMP1 was seen and not of the typical ADM receptor RAMP2. It is possible that, due to the many structural similarities between these two RAMP receptors, we could have a degenerated recognition and receptor activation of RAMP1 by ADM, as previously described (Kuwasako et al., 2012). Moreover, ADM also presents structural similarities to CGRP, as both belong to the CGRP-family. By this way ADM could be efficiently recognized by neutrophils via CRLR-RAMP ligation and influence cellular functions of this innate cell population. Using two distinct assays, we were able to show that both murine and human neutrophils are responsive to ADM, leading to a significant reduction in the amounts of NET being generated *in vitro* after stimulation with PMA and the *S.pn.* major toxin PLY. In murine cells, the effect of this peptide was also sensed after application of ADM at later time-points. The process of

NETosis in murine cells takes much longer than in humans, where NET production is first seen after around 4h to 5h and reaches a peak after 7h stimulation. Therefore, the late application of ADM, of 1h or 2h was efficiently in inhibiting the process of NET formation. Treatment of the cells with ADM 4h after start of stimulation, however, could not rescue cells from this suicidal NETotic fate and the number of cells undergoing NETosis was not significantly different from the untreated group. We confirmed that the structures seen after stimulation of the cells with PMA were indeed NETs after staining DNA with typical NET proteins, citrullinated histones and neutrophil elastase. Altogether, ADM is sensed by neutrophils and affects the process of NETosis after cellular recognition via receptor ligation. We were able to corroborate this statement by analyzing NET formation after blocking of the receptor complex CRLR-RAMP with olcegepant. This substance was sufficient to prevent ligation of ADM, affecting NET reduction, measured with SYTOX-Green. As previously described, after ADM binding, the CRLR-RAMP complex activates a G-protein, further activating different regulatory mechanisms in the cells. It is known that calcium ion concentrations and cAMP levels are increased upon ADM binding, showing a connection between G-proteins to adenylyl cyclase. Eby and colleagues (2014) showed in a study with the Gram-negative bacteria *Bordetella pertussis* that the adenylate cyclase toxin (ACT), secreted by this bacteria can impair neutrophil functions, converting ATP into cAMP, which accumulates in the cells. The supraphysiologic levels of cAMP are important in mediating suppression of NET formation and apoptosis in neutrophils, by inhibition of the caspase3/7 activity and the oxidative burst. Increase in cAMP and inhibition of NET formation could also be achieved at similar levels to ACT by cellular induction with prostaglandin E₂, a cAMP inducer, and phosphodiesterase inhibition (mainly PDE4) (Hakkim et al., 2011). Here, we also showed that an intracellular increase in cAMP, seen after application of the specific adenylyl-cyclase activator forskolin, could also lead to the inhibition of the process of NETosis. PMA is known to activate many different pathways in the cell, including PKC, which is of great importance for NET formation. PKC triggers activation of MAPK members of the canonical Raf-MEK-ERK pathway by phosphorylation. cAMP is a known inhibitor of ERK phosphorylation, which is upstream of NOX2 activation and ROS production, necessary for NET formation (Hakkim et al., 2011; Keshari et al., 2013). We further showed here that the process of NETosis after stimulation with PMA is dependent on the Raf-MEK-ERK pathway, as inhibition of ERK phosphorylation with U-0126 led to a great delay in DNA release, seen with SYTOX-Green. Treatment of the cells with ADM, before PMA stimulation, also affected ERK phosphorylation, probably via the increase in cAMP levels. Increased cAMP levels and the concomitantly inhibition of ERK phosphorylation, seen here

after treatment of neutrophils with ADM, could explain the reduction in ROS production and NET formation. However, we cannot exclude the possibility that cAMP acts independently in different cellular pathways that could lead to suppression of ROS production, as via calcium influx or alteration of gene expression. We can infer that ADM could at least partially affect the mechanistic pathways activated after neutrophil stimulation with PMA. Altogether, treatment with ADM may be recognized by the receptor complex CRLR-RAMP, leading to the activation of adenylyl cyclase. With increased intracellular levels of cAMP, ERK phosphorylation might be inhibited, leading to the reduction in NOX2 activation and the generation of ROS, necessary for the process of NETosis (Figure 21). Although the levels of NET reduction seen *in vitro* after treatment of the cells with ADM is significant, it is minimal when compared to the *in vivo* model used before. *In vivo*, the number of neutrophils infiltrating the tissue is much larger and continuous throughout infection, as neutrophils are constantly replenished by new cells recruited to the inflamed tissue. Moreover, in the animal model we had a continuous application of ADM during the 4h ventilation, while *in vitro*, a single dose of the peptide was used. The half-life of the peptide after stimulation *in vitro* was not tested, and ADM could have been rapidly degraded with time, as shown by other groups. Moreover, we used a known concentration of ADM, described previously by other authors and did not test any different concentration of ADM that could provide a more significant effect on the process of NETosis. An important factor that could also explain this reduced effect of ADM *in vitro*, lies in the fact that *in vivo*, ADM may modulate simultaneously different cell types and cellular mechanisms, reducing the inflammation of the tissue, promoting homeostasis and by this way having greater influence in reducing NET formation. By this way, the reduced effects in NET inhibition seen *in vitro* could be escalated *in vivo*, as seen in the mouse model. Another important factor that could explain this reduced effect of ADM on neutrophils *in vitro* is that we used the potent universal stimulator PMA for most of our experiments. This molecule is known to induce simultaneously many distinct intracellular pathways, including PKC, which is involved in the process of NETosis. Differently, ADM specifically acts through receptor activation and cAMP production, and therefore could have a minimal impact against the strong effects of PMA on neutrophils. Therefore, further experiments with different and more specific stimulators are necessary to confirm this statement.

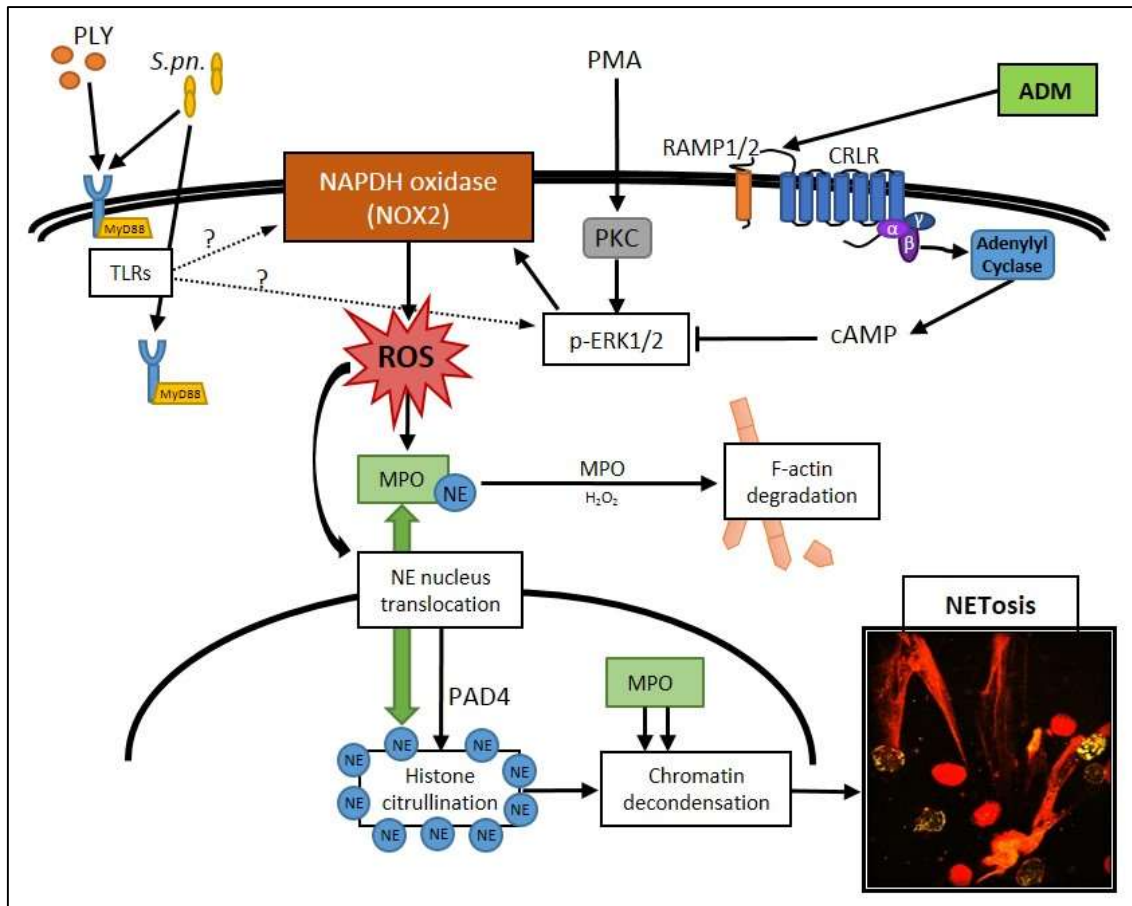


Figure 21: Possible mechanistic pathway of adrenomedullin interference in NET formation. Adrenomedullin (ADM) is recognized by the neutrophil receptors CRLR/RAMP, activating a G-protein, which is connected to the enzyme adenylyl cyclase. Increased cAMP levels lead to the inhibition of ERK phosphorylation and subsequent decrease of the NAPDH oxidase (NOX2) activation. A reduction in ROS production directly affects NET formation, as ROS are essential for the process of NETosis. The use of more physiological stimulators, as the Gram-positive bacterium *S. pneumoniae* and its major cytotoxic component pneumolysin (PLY) can also lead to NET formation. However, the mechanistic pathway involved may be different than the observed after stimulation with PMA. Toll-like Receptors (TLRs), Reactive Oxygen Species (ROS), Myeloperoxidase (MPO), Neutrophil Elastase (NE).

5.4. Targeting NETs is effective against pneumococcal pneumonia

Altogether, this study showed that NETs are produced in the lungs by infiltrating neutrophils after infection with the Gram-positive bacterium *S.pn.* and that NET accumulation is associated with an increase in barrier damage, leading to edema formation in the tissue. We demonstrated that reducing the amount of NETs in the lungs is protective in pneumococcal pneumonia. NETs are pro-inflammatory structures and cytotoxic to the host and may lead to worsening of the disease outcome. Anti-NET therapies might be beneficial as adjuvant therapies to antibiotics for patients with pneumonia and sepsis. This treatment should aim a controlled decrease in NETs generation in the tissue, not affecting their important anti-microbial properties. ADM was shown to have a great potential as adjuvant agent, inhibiting NET formation in the alveolar space and reducing the amount of the pro-inflammatory molecules in the tissue. In addition to its positive effects on reducing NET formation, ADM could further provide its many known important functions in tissue homeostasis, such as stabilization of the lung barrier. Together, this would be of great importance in the reduction of tissue damage. Pneumonia is a very complex disease with many different parts of the organism being affected simultaneously and influencing each other. The multiple positive functions provided by ADM could influence the many cell types inflicted in this acute uncontrolled inflammatory disease, ameliorating the inflammatory condition and the outcome of the disease. In this broad view of the disease, ADM emerges as an ideal complementary therapeutic agent for the treatment of severe inflammation and autoimmune diseases, influencing not only NET formation, but concomitantly other cellular functions.

6. Bibliography

- Abi Abdallah, Delbert S., Changyou Lin, Carissa J. Ball, Michael R. King, Gerald E. Duhamel, and Eric Y. Denkers. 2012. “Toxoplasma Gondii Triggers Release of Human and Mouse Neutrophil Extracellular Traps.” Edited by J. H. Adams. *Infection and Immunity* 80 (2): 768–77. <https://doi.org/10.1128/IAI.05730-11>.
- Abrams, Simon T., Nan Zhang, Joanna Manson, Tingting Liu, Caroline Dart, Florence Baluwa, Susan Siyu Wang, et al. 2013. “Circulating Histones Are Mediators of Trauma-Associated Lung Injury.” *American Journal of Respiratory and Critical Care Medicine* 187 (2): 160–69. <https://doi.org/10.1164/rccm.201206-1037OC>.
- Agorreta, J, J J Zulueta, L M Montuenga, and M Garayoa. 2005. “Adrenomedullin Expression in a Rat Model of Acute Lung Injury Induced by Hypoxia and LPS.” *Am J Physiol Lung Cell Mol Physiol* 288 (3): L536-45. <https://doi.org/10.1152/ajplung.00314.2004>.
- Akong-Moore, Kathryn, Ohn A. Chow, Maren von Köckritz-Blickwede, and Victor Nizet. 2012. “Influences of Chloride and Hypochlorite on Neutrophil Extracellular Trap Formation.” Edited by Jan Wehkamp. *PLoS ONE* 7 (8): e42984. <https://doi.org/10.1371/journal.pone.0042984>.
- Albiger, Barbara, Sofia Dahlberg, Andreas Sandgren, Florian Wartha, Katharina Beiter, Hiroaki Katsuragi, Shizuo Akira, Staffan Normark, and Birgitta Henriques-Normark. 2007. “Toll-like Receptor 9 Acts at an Early Stage in Host Defence against Pneumococcal Infection.” *Cellular Microbiology* 9 (3): 633–44. <https://doi.org/10.1111/j.1462-5822.2006.00814.x>.
- Ampofo, Krow, and Carrie L. Byington. 2018. “Streptococcus Pneumoniae.” In *Principles and Practice of Pediatric Infectious Diseases*, Fifth Edit, 737-746.e4. Elsevier. <https://doi.org/10.1016/B978-0-323-40181-4.00123-7>.
- Amulic, Borko, Christel Cazalet, Garret L. Hayes, Kathleen D. Metzler, and Arturo Zychlinsky. 2012. “Neutrophil Function: From Mechanisms to Disease.” *Annual Review of Immunology* 30 (1): 459–89. <https://doi.org/10.1146/annurev-immunol-020711-074942>.
- Apel, F, A Zychlinsky, and E F Kenny. 2018. “The Role of Neutrophil Extracellular Traps in Rheumatic Diseases.” *Nat Rev Rheumatol* 14 (8): 467–75. <https://doi.org/10.1038/s41584->

018-0039-z.

- Bals, R., and P.S. Hiemstra. 2004. "Innate Immunity in the Lung: How Epithelial Cells Fight against Respiratory Pathogens." *European Respiratory Journal* 23 (2): 327–33. <https://doi.org/10.1183/09031936.03.00098803>.
- Beiter, K, F Wartha, B Albiger, S Normark, A Zychlinsky, and B Henriques-Normark. 2006. "An Endonuclease Allows Streptococcus Pneumoniae to Escape from Neutrophil Extracellular Traps." *Curr Biol* 16 (4): 401–7. <https://doi.org/10.1016/j.cub.2006.01.056>.
- Beiter, Katharina, Florian Wartha, Barbara Albiger, Staffan Normark, Arturo Zychlinsky, and Birgitta Henriques-Normark. 2006. "An Endonuclease Allows Streptococcus Pneumoniae to Escape from Neutrophil Extracellular Traps." *Current Biology* 16 (4): 401–7. <https://doi.org/10.1016/j.cub.2006.01.056>.
- Bekkering, Siroon. 2013. "Another Look at the Life of a Neutrophil." *World Journal of Hematology* 2 (2): 44. <https://doi.org/10.5315/wjh.v2.i2.44>.
- Bianchi, Matteo, Abdul Hakkim, Volker Brinkmann, Ulrich Siler, Reinhard A. Seger, Arturo Zychlinsky, and Janine Reichenbach. 2009. "Restoration of NET Formation by Gene Therapy in CGD Controls Aspergillosis." *Blood* 114 (13): 2619–22. <https://doi.org/10.1182/blood-2009-05-221606>.
- Björnsdóttir, Halla, Amanda Welin, Erik Michaëlsson, Veronica Osla, Stefan Berg, Karin Christenson, Martina Sundqvist, Claes Dahlgren, Anna Karlsson, and Johan Bylund. 2015. "Neutrophil NET Formation Is Regulated from the inside by Myeloperoxidase-Processed Reactive Oxygen Species." *Free Radical Biology and Medicine* 89 (December): 1024–35. <https://doi.org/10.1016/j.freeradbiomed.2015.10.398>.
- Black, R.E., Cousens, S., Johnson, H.L., Lawn, J.E., Rudan, I., Bassani, D.G., Jha, P., Campbell, H., Walker, C.F., Cibulskis, R., Eisele, T., Liu, L. and Mathers, C. 2010. "No TitleGlobal, Regional, and National Causes of Child Mortality in 2008: A Systematic Analysis." *The Lancet* 375: 1969–87.
- Branzk, N, A Lubojemska, S E Hardison, Q Wang, M G Gutierrez, G D Brown, and V Papayannopoulos. 2014. "Neutrophils Sense Microbe Size and Selectively Release Neutrophil Extracellular Traps in Response to Large Pathogens." *Nat Immunol* 15 (11): 1017–25. <https://doi.org/10.1038/ni.2987>.

- Branzk, Nora, and Venizelos Papayannopoulos. 2013. "Molecular Mechanisms Regulating NETosis in Infection and Disease." *Seminars in Immunopathology* 35 (4): 513–30. <https://doi.org/10.1007/s00281-013-0384-6>.
- Brinkmann, V, U Reichard, C Goosmann, B Fauler, Y Uhlemann, D S Weiss, Y Weinrauch, and A Zychlinsky. 2004. "Neutrophil Extracellular Traps Kill Bacteria." *Science* 303 (5663): 1532–35. <https://doi.org/10.1126/science.1092385>.
- Brinkmann, V, and A Zychlinsky. 2012. "Neutrophil Extracellular Traps: Is Immunity the Second Function of Chromatin?" *J Cell Biol* 198 (5): 773–83. <https://doi.org/10.1083/jcb.201203170>.
- Brinkmann, Volker, and Arturo Zychlinsky. 2007. "Beneficial Suicide: Why Neutrophils Die to Make NETs." *Nature Reviews Microbiology* 5 (8): 577–82. <https://doi.org/10.1038/nrmicro1710>.
- Caudrillier, Axelle, Kai Kessenbrock, Brian M. Gilliss, John X. Nguyen, Marisa B. Marques, Marc Monestier, Pearl Toy, Zena Werb, and Mark R. Looney. 2012. "Platelets Induce Neutrophil Extracellular Traps in Transfusion-Related Acute Lung Injury." *Journal of Clinical Investigation* 122 (7): 2661–71. <https://doi.org/10.1172/JCI61303>.
- Cedervall, J, A Dragomir, F Saupe, Y Zhang, J Arnlov, E Larsson, A Dimberg, A Larsson, and A K Olsson. 2017. "Pharmacological Targeting of Peptidylarginine Deiminase 4 Prevents Cancer-Associated Kidney Injury in Mice." *Oncoimmunology* 6 (8): e1320009. <https://doi.org/10.1080/2162402X.2017.1320009>.
- Cedervall, Jessica, Anca Dragomir, Falk Saupe, Yanyu Zhang, Johan Ärnlov, Erik Larsson, Anna Dimberg, Anders Larsson, and Anna-Karin Olsson. 2017. "Pharmacological Targeting of Peptidylarginine Deiminase 4 Prevents Cancer-Associated Kidney Injury in Mice." *OncoImmunology* 6 (8): e1320009. <https://doi.org/10.1080/2162402X.2017.1320009>.
- Chaput, Catherine, and Arturo Zychlinsky. 2009. "Sepsis : The Dark Side of Histones." *Nature Medicine* 15 (11): 1245–46. <http://dx.doi.org/10.1038/nm1109-1245>.
- Clark, Stephen R., Adrienne C. Ma, Samantha A. Tavener, Braedon McDonald, Zahra Goodarzi, Margaret M. Kelly, Kamala D. Patel, et al. 2007. "Platelet TLR4 Activates Neutrophil Extracellular Traps to Ensnare Bacteria in Septic Blood." *Nature Medicine* 13

(4): 463–69. <https://doi.org/10.1038/nm1565>.

Colley, Karen J., Ken Kitajima, and Chihiro Sato. 2014. “Polysialic Acid: Biosynthesis, Novel Functions and Applications.” *Critical Reviews in Biochemistry and Molecular Biology* 49 (6): 498–532. <https://doi.org/10.3109/10409238.2014.976606>.

Cortjens, B., O.J. De Boer, R. De Jong, A.F.G Antonis, Y.S. Sabogal Pineros, R. Lutter, and J.B.M Van Woensel. 2016. “Neutrophil Extracellular Traps Cause Airway Obstruction during Respiratory Syncytial Virus Disease.” *Journal of Pathology* 238 (3): 401–11.

Cortjens, B, J B van Woensel, and R A Bem. 2017. “Neutrophil Extracellular Traps in Respiratory Disease: Guided Anti-Microbial Traps or Toxic Webs?” *Paediatr Respir Rev* 21: 54–61. <https://doi.org/10.1016/j.prrv.2016.03.007>.

Costantini, Claudio, Alessandra Micheletti, Federica Calzetti, Omar Perbellini, Giovanni Pizzolo, and Marco A. Cassatella. 2010. “Neutrophil Activation and Survival Are Modulated by Interaction with NK Cells.” *International Immunology* 22 (10): 827–38. <https://doi.org/10.1093/intimm/dxq434>.

Dackor, R, and K Caron. 2007. “Mice Heterozygous for Adrenomedullin Exhibit a More Extreme Inflammatory Response to Endotoxin-Induced Septic Shock.” *Peptides* 28 (11): 2164–70. <https://doi.org/10.1016/j.peptides.2007.08.012>.

Daigo Nakazawa, Santosh Kumar VR, Jyaysi Desai, and Hans-Joachim Anders. 2017. “Neutrophil Extracellular Traps in Tissue Pathology.” *Histology and Histopathology*, 203–13. <https://doi.org/10.14670/HH-11-816>.

Dessing, Mark C., Sandrine Florquin, James C. Paton, and Tom van der Poll. 2007. “Toll-like Receptor 2 Contributes to Antibacterial Defence against Pneumolysin-Deficient Pneumococci.” *Cellular Microbiology*, August, 070817225835002-??? <https://doi.org/10.1111/j.1462-5822.2007.01035.x>.

Dockrell, D. H., H. M. Marriott, L. R. Prince, V. C. Ridger, P. G. Ince, P. G. Hellewell, and M. K. B. Whyte. 2003. “Alveolar Macrophage Apoptosis Contributes to Pneumococcal Clearance in a Resolving Model of Pulmonary Infection.” *The Journal of Immunology* 171 (10): 5380–88. <https://doi.org/10.4049/jimmunol.171.10.5380>.

Dockrell, David H., Moira K.B. Whyte, and Timothy J. Mitchell. 2012. “Pneumococcal Pneumonia: Mechanisms of Infection and Resolution.” *Chest* 142 (2): 482–91.

<https://doi.org/10.1378/chest.12-0210>.

Drake, P. M., J. K. Nathan, C. M. Stock, P. V. Chang, M. O. Muench, D. Nakata, J. R. Reader, et al. 2008. "Polysialic Acid, a Glycan with Highly Restricted Expression, Is Found on Human and Murine Leukocytes and Modulates Immune Responses." *The Journal of Immunology* 181 (10): 6850–58. <https://doi.org/10.4049/jimmunol.181.10.6850>.

Drijkoningen, J. J.C., and G. G.U. Rohde. 2014. "Pneumococcal Infection in Adults: Burden of Disease." *Clinical Microbiology and Infection* 20 (S5): 45–51. <https://doi.org/10.1111/1469-0691.12461>.

Eby, Joshua C., Mary C. Gray, and Erik L. Hewlett. 2014. "Cyclic AMP-Mediated Suppression of Neutrophil Extracellular Trap Formation and Apoptosis by the Bordetella Pertussis Adenylate Cyclase Toxin." Edited by S. R. Blanke. *Infection and Immunity* 82 (12): 5256–69. <https://doi.org/10.1128/IAI.02487-14>.

Ermert, D, C F Urban, B Laube, C Goosmann, A Zychlinsky, and V Brinkmann. 2009. "Mouse Neutrophil Extracellular Traps in Microbial Infections." *J Innate Immun* 1 (3): 181–93. <https://doi.org/10.1159/000205281>.

Ermert, David, Constantin F. Urban, Britta Laube, Christian Goosmann, Arturo Zychlinsky, and Volker Brinkmann. 2009. "Mouse Neutrophil Extracellular Traps in Microbial Infections." *Journal of Innate Immunity* 1 (3): 181–93. <https://doi.org/10.1159/000205281>.

Fuchs, T A, A Brill, D Duerschmied, D Schatzberg, M Monestier, D D Myers Jr., S K Wroblewski, T W Wakefield, J H Hartwig, and D D Wagner. 2010. "Extracellular DNA Traps Promote Thrombosis." *Proc Natl Acad Sci U S A* 107 (36): 15880–85. <https://doi.org/10.1073/pnas.1005743107>.

Fuchs, Tobias A., Ulrike Abed, Christian Goosmann, Robert Hurwitz, Ilka Schulze, Volker Wahn, Yvette Weinrauch, Volker Brinkmann, and Arturo Zychlinsky. 2007. "Novel Cell Death Program Leads to Neutrophil Extracellular Traps." *The Journal of Cell Biology* 176 (2): 231–41. <https://doi.org/10.1083/jcb.200606027>.

Gonzalez-Rey, E, A Chorny, N Varela, G Robledo, and M Delgado. 2006. "Urocortin and Adrenomedullin Prevent Lethal Endotoxemia by Down-Regulating the Inflammatory Response." *Am J Pathol* 168 (6): 1921–30. <https://doi.org/10.2353/ajpath.2006.051104>.

- Gould, T J, Z Lysov, and P C Liaw. 2015. “Extracellular DNA and Histones: Double-Edged Swords in Immunothrombosis.” *J Thromb Haemost* 13 Suppl 1: S82-91. <https://doi.org/10.1111/jth.12977>.
- Grailer, J. J., B. A. Canning, M. Kalbitz, M. D. Haggadone, R. M. Dhond, A. V. Andjelkovic, F. S. Zetoune, and P. A. Ward. 2014. “Critical Role for the NLRP3 Inflammasome during Acute Lung Injury.” *The Journal of Immunology* 192 (12): 5974–83. <https://doi.org/10.4049/jimmunol.1400368>.
- Gray, R D. 2018. “NETs in Pneumonia: Is Just Enough the Right Amount?” *Eur Respir J* 51 (4). <https://doi.org/10.1183/13993003.00619-2018>.
- Gray, R D, C D Lucas, A MacKellar, F Li, K Hiersemenzel, C Haslett, D J Davidson, and A G Rossi. 2013. “Activation of Conventional Protein Kinase C (PKC) Is Critical in the Generation of Human Neutrophil Extracellular Traps.” *J Inflamm (Lond)* 10 (1): 12. <https://doi.org/10.1186/1476-9255-10-12>.
- Grommes, J, and O Soehnlein. 2011. “Contribution of Neutrophils to Acute Lung Injury.” *Mol Med* 17 (3–4): 293–307. <https://doi.org/10.2119/molmed.2010.00138>.
- Hakim, A., B. G. Furnrohr, K. Amann, B. Laube, U. A. Abed, V. Brinkmann, M. Herrmann, R. E. Voll, and A. Zychlinsky. 2010. “Impairment of Neutrophil Extracellular Trap Degradation Is Associated with Lupus Nephritis.” *Proceedings of the National Academy of Sciences* 107 (21): 9813–18. <https://doi.org/10.1073/pnas.0909927107>.
- Hakim, A, T A Fuchs, N E Martinez, S Hess, H Prinz, A Zychlinsky, and H Waldmann. 2011. “Activation of the Raf-MEK-ERK Pathway Is Required for Neutrophil Extracellular Trap Formation.” *Nat Chem Biol* 7 (2): 75–77. <https://doi.org/10.1038/nchembio.496>.
- Halverson, Tyler W.R., Mike Wilton, Karen K. H. Poon, Björn Petri, and Shawn Lewenza. 2015. “DNA Is an Antimicrobial Component of Neutrophil Extracellular Traps.” Edited by David Weiss. *PLOS Pathogens* 11 (1): e1004593. <https://doi.org/10.1371/journal.ppat.1004593>.
- Hamid, Shabaz A., Matthias Totzeck, Christina Drexhage, Iain Thompson, Robert C. Fowkes, Tienush Rassaf, and Gary F. Baxter. 2010. “Nitric Oxide/CGMP Signalling Mediates the Cardioprotective Action of Adrenomedullin in Reperfused Myocardium.” *Basic Research in Cardiology* 105 (2): 257–66. <https://doi.org/10.1007/s00395-009-0058-7>.

- Hazeldine, Jon, Phillipa Harris, Iain L. Chapple, Melissa Grant, Hannah Greenwood, Amy Livesey, Elizabeth Sapey, and Janet M. Lord. 2014. "Impaired Neutrophil Extracellular Trap Formation: A Novel Defect in the Innate Immune System of Aged Individuals." *Aging Cell* 13 (4): 690–98. <https://doi.org/10.1111/accel.12222>.
- Hippenstiel, Stefan, Martin Witzernath, Bernd Schmeck, Andreas Hocke, Mathias Krisp, Matthias Krüll, Joachim Seybold, et al. 2002. "Adrenomedullin Reduces Endothelial Hyperpermeability." *Circulation Research* 91 (7): 618–25. <https://doi.org/10.1161/01.RES.0000036603.61868.F9>.
- Hirst, R. A., A. Kadioglu, C. O'Callaghan, and P. W. Andrew. 2004. "The Role of Pneumolysin in Pneumococcal Pneumonia and Meningitis." *Clinical and Experimental Immunology* 138 (2): 195–201. <https://doi.org/10.1111/j.1365-2249.2004.02611.x>.
- Iba, T, M Murai, I Nagaoka, and Y Tabe. 2014. "Neutrophil Extracellular Traps, Damage-Associated Molecular Patterns, and Cell Death during Sepsis." *Acute Med Surg* 1 (1): 2–9. <https://doi.org/10.1002/ams2.10>.
- Iba, Toshiaki, Miwa Murai, Isao Nagaoka, and Yoko Tabe. 2013. "Neutrophil Extracellular Traps (NETs), Damage-Associated Molecular Patterns (DAMPs) and Cell-Death during Sepsis." *Nihon Kyukyu Igakukai Zasshi* 24 (10): 827–36. <https://doi.org/10.3893/jjaam.24.827>.
- Idrovo, Juan-Pablo, Weng-Lang Yang, Asha Jacob, Michael A. Ajakaiye, Cletus Cheyuo, Zhimin Wang, Jose M. Prince, Jeffrey Nicastro, Gene F. Coppa, and Ping Wang. 2015. "Combination of Adrenomedullin with Its Binding Protein Accelerates Cutaneous Wound Healing." Edited by Utpal Sen. *PLOS ONE* 10 (3): e0120225. <https://doi.org/10.1371/journal.pone.0120225>.
- Janoff, Edward N. and Musher, Daniel M. 2014. *Streptococcus Pneumoniae. Streptococcus Pneumonia, Part III Infectious Diseases and Their Etiologic Agents*. Eighth Edi. Vol. 2. Elsevier Inc. <https://doi.org/10.1016/B978-1-4557-4801-3.00201-0>.
- Jorch, Selina K., and Paul Kubes. 2017. "An Emerging Role for Neutrophil Extracellular Traps in Noninfectious Disease." *Nature Medicine* 23 (3): 279–87. <https://doi.org/10.1038/nm.4294>.
- Kaczmarek, Agnieszka, Peter Vandenabeele, and Dmitri V. Krysko. 2013. "Necroptosis: The

- Release of Damage-Associated Molecular Patterns and Its Physiological Relevance.” *Immunity* 38 (2): 209–23. <https://doi.org/10.1016/j.immuni.2013.02.003>.
- Kantrow, S P, Z Shen, T Jagneaux, P Zhang, and S Nelson. 2009. “Neutrophil-Mediated Lung Permeability and Host Defense Proteins.” *Am J Physiol Lung Cell Mol Physiol* 297 (4): L738–45. <https://doi.org/10.1152/ajplung.00045.2009>.
- Kaplan, M J, and M Radic. 2012. “Neutrophil Extracellular Traps: Double-Edged Swords of Innate Immunity.” *J Immunol* 189 (6): 2689–95. <https://doi.org/10.4049/jimmunol.1201719>.
- Karlstetter, Marcus, Jens Kopatz, Alexander Aslanidis, Anahita Shahraz, Albert Caramoy, Bettina Linnartz-Gerlach, Yuchen Lin, et al. 2017. “Polysialic Acid Blocks Mononuclear Phagocyte Reactivity, Inhibits Complement Activation, and Protects from Vascular Damage in the Retina.” *EMBO Molecular Medicine* 9 (2): 154–66. <https://doi.org/10.15252/emmm.201606627>.
- Kato, J, and K Kitamura. 2015. “Bench-to-Bedside Pharmacology of Adrenomedullin.” *Eur J Pharmacol* 764: 140–48. <https://doi.org/10.1016/j.ejphar.2015.06.061>.
- Kerr, A. R. 2002. “Role of Inflammatory Mediators in Resistance and Susceptibility to Pneumococcal Infection.” *Infection and Immunity* 70 (3): 1547–57. <https://doi.org/10.1128/IAI.70.3.1547-1557.2002>.
- Keshari, Ravi S., Anupam Verma, Manoj K. Barthwal, and Madhu Dikshit. 2013. “Reactive Oxygen Species-Induced Activation of ERK and P38 MAPK Mediates PMA-Induced NETs Release from Human Neutrophils.” *Journal of Cellular Biochemistry* 114 (3): 532–40. <https://doi.org/10.1002/jcb.24391>.
- Kessenbrock, Kai, Markus Krumbholz, Ulf Schönemarker, Walter Back, Wolfgang L Gross, Zena Werb, Hermann-Josef Gröne, Volker Brinkmann, and Dieter E Jenne. 2009. “Netting Neutrophils in Autoimmune Small-Vessel Vasculitis.” *Nature Medicine* 15 (6): 623–25. <https://doi.org/10.1038/nm.1959>.
- Kitamura, K., K. Kangawa, M. Kawamoto, Y. Ichiki, S. Nakamura, H. Matsuo, and T. Eto. 1993. “Adrenomedullin: A Novel Hypotensive Peptide Isolated from Human Pheochromocytoma.” *Biochemical and Biophysical Research Communications* 192 (2): 553–60. <https://doi.org/10.1006/bbrc.1993.1451>.

- Kolaczowska, E, C N Jenne, B G Surewaard, A Thanabalasuriar, W Y Lee, M J Sanz, K Mowen, G Opendakker, and P Kubes. 2015. “Molecular Mechanisms of NET Formation and Degradation Revealed by Intravital Imaging in the Liver Vasculature.” *Nat Commun* 6: 6673. <https://doi.org/10.1038/ncomms7673>.
- Koppe, Uwe, Norbert Suttorp, and Bastian Opitz. 2012. “Recognition of Streptococcus Pneumoniae by the Innate Immune System.” *Cellular Microbiology* 14 (4): 460–66. <https://doi.org/10.1111/j.1462-5822.2011.01746.x>.
- Kubo, Keishi, Mariko Tokashiki, Kenji Kuwasako, Masaji Tamura, Shugo Tsuda, Shigeru Kubo, Kumiko Yoshizawa-Kumagaye, Johji Kato, and Kazuo Kitamura. 2014. “Biological Properties of Adrenomedullin Conjugated with Polyethylene Glycol.” *Peptides* 57 (July): 118–21. <https://doi.org/10.1016/j.peptides.2014.05.005>.
- Kusunoki, Yoshihiro, Daigo Nakazawa, Haruki Shida, Fumihiko Hattanda, Arina Miyoshi, Sakiko Masuda, Saori Nishio, Utano Tomaru, Tatsuya Atsumi, and Akihiro Ishizu. 2016. “Peptidylarginine Deiminase Inhibitor Suppresses Neutrophil Extracellular Trap Formation and MPO-ANCA Production.” *Frontiers in Immunology* 7 (JUN): 1–7. <https://doi.org/10.3389/fimmu.2016.00227>.
- Kuwasako, Kenji, Debbie L. Hay, Sayaka Nagata, Tomomi Hikosaka, Kazuo Kitamura, and Johji Kato. 2012. “The Third Extracellular Loop of the Human Calcitonin Receptor-like Receptor Is Crucial for the Activation of Adrenomedullin Signalling.” *British Journal of Pharmacology* 166 (1): 137–50. <https://doi.org/10.1111/j.1476-5381.2011.01803.x>.
- Lefrancais, E, B Mallavia, H Zhuo, C S Calfee, and M R Looney. 2018. “Maladaptive Role of Neutrophil Extracellular Traps in Pathogen-Induced Lung Injury.” *JCI Insight* 3 (3). <https://doi.org/10.1172/jci.insight.98178>.
- Lewis, H D, J Liddle, J E Coote, S J Atkinson, M D Barker, B D Bax, K L Bicker, et al. 2015. “Inhibition of PAD4 Activity Is Sufficient to Disrupt Mouse and Human NET Formation.” *Nat Chem Biol* 11 (3): 189–91. <https://doi.org/10.1038/nchembio.1735>.
- Lewis, Megan L., and Bas G. J. Surewaard. 2018. “Neutrophil Evasion Strategies by Streptococcus Pneumoniae and Staphylococcus Aureus.” *Cell and Tissue Research* 371 (3): 489–503. <https://doi.org/10.1007/s00441-017-2737-2>.
- Li, Pingxin, Ming Li, Michael R. Lindberg, Mary J. Kennett, Na Xiong, and Yanming Wang.

2010. "PAD4 Is Essential for Antibacterial Innate Immunity Mediated by Neutrophil Extracellular Traps." *The Journal of Experimental Medicine* 207 (9): 1853–62. <https://doi.org/10.1084/jem.20100239>.
- Liang, Yingjian, Baihong Pan, Hasan B. Alam, Qiufang Deng, Yibing Wang, Eric Chen, Baoling Liu, et al. 2018. "Inhibition of Peptidylarginine Deiminase Alleviates LPS-Induced Pulmonary Dysfunction and Improves Survival in a Mouse Model of Lethal Endotoxemia." *European Journal of Pharmacology* 833 (April): 432–40. <https://doi.org/10.1016/j.ejphar.2018.07.005>.
- Maas, Sanne L., Oliver Soehnlein, and Joana R. Viola. 2018. "Organ-Specific Mechanisms of Transendothelial Neutrophil Migration in the Lung, Liver, Kidney, and Aorta." *Frontiers in Immunology* 9 (November). <https://doi.org/10.3389/fimmu.2018.02739>.
- Macanovic, M., D. SINICROPI, S. SHAK, S. BAUGHMAN, S. THIRU, and P. J. LACHMANN. 1996. "The Treatment of Systemic Lupus Erythematosus (SLE) in NZB/W F1 Hybrid Mice; Studies with Recombinant Murine DNase and with Dexamethasone." *Clinical and Experimental Immunology* 106 (2): 243–52. <https://doi.org/10.1046/j.1365-2249.1996.d01-839.x>.
- Mackenzie, Grant. 2016. "The Definition and Classification of Pneumonia." *Pneumonia* 8 (1): 14. <https://doi.org/10.1186/s41479-016-0012-z>.
- Makni-Maalej, Karama, Viviana Marzaioli, Tarek Boussetta, Sahra Amel Belambri, Marie-Anne Gougerot-Pocidalo, Margarita Hurtado-Nedelec, Pham My-Chan Dang, and Jamel El-Benna. 2015. "TLR8, but Not TLR7, Induces the Priming of the NADPH Oxidase Activation in Human Neutrophils." *Journal of Leukocyte Biology* 97 (6): 1081–87. <https://doi.org/10.1189/jlb.2A1214-623R>.
- Martinod, K., T. Witsch, K. Farley, M. Gallant, E. Remold-O'Donnell, and D. D. Wagner. 2016. "Neutrophil Elastase-Deficient Mice Form Neutrophil Extracellular Traps in an Experimental Model of Deep Vein Thrombosis." *Journal of Thrombosis and Haemostasis* 14 (3): 551–58. <https://doi.org/10.1111/jth.13239>.
- Matthay, Michael A., Lorraine B. Ware, and Guy A. Zimmerman. 2012. "The Acute Respiratory Distress Syndrome." *Journal of Clinical Investigation* 122 (8): 2731–40. <https://doi.org/10.1172/JCI60331>.

- Matthay, Michael A., and Guy A. Zimmerman. 2005. "Acute Lung Injury and the Acute Respiratory Distress Syndrome." *American Journal of Respiratory Cell and Molecular Biology* 33 (4): 319–27. <https://doi.org/10.1165/rcmb.F305>.
- Maueröder, Christian, Deborah Kienhöfer, Jonas Hahn, Christine Schauer, Bernhard Manger, Georg Schett, Martin Herrmann, and Markus H Hoffmann. 2015. "How Neutrophil Extracellular Traps Orchestrate the Local Immune Response in Gout." *Journal of Molecular Medicine* 93 (7): 727–34. <https://doi.org/10.1007/s00109-015-1295-x>.
- McDonald, Braedon, Rossana Urrutia, Bryan G. Yipp, Craig N. Jenne, and Paul Kubes. 2012. "Intravascular Neutrophil Extracellular Traps Capture Bacteria from the Bloodstream during Sepsis." *Cell Host & Microbe* 12 (3): 324–33. <https://doi.org/10.1016/j.chom.2012.06.011>.
- Medzhitov, Ruslan, and Charles Janeway. 2000. "Innate Immunity." Edited by Ian R. Mackay and Fred S. Rosen. *New England Journal of Medicine* 343 (5): 338–44. <https://doi.org/10.1056/NEJM200008033430506>.
- Medzhitov, Ruslan, and Charles A Janeway. 1997. "Innate Immunity: Impact on the Adaptive Immune Response." *Current Opinion in Immunology* 9 (1): 4–9. [https://doi.org/10.1016/S0952-7915\(97\)80152-5](https://doi.org/10.1016/S0952-7915(97)80152-5).
- Menegazzo, Lisa, Valentina Scattolini, Roberta Cappellari, Benedetta Maria Bonora, Mattia Albiero, Mario Bortolozzi, Filippo Romanato, et al. 2018. "The Antidiabetic Drug Metformin Blunts NETosis in Vitro and Reduces Circulating NETosis Biomarkers in Vivo." *Acta Diabetologica* 55 (6): 593–601. <https://doi.org/10.1007/s00592-018-1129-8>.
- Meng, Wei, Adnana Paunel-Görgülü, Sascha Flohé, Almuth Hoffmann, Ingo Witte, Colin MacKenzie, Stephan E. Baldus, Joachim Windolf, and Tim T. Lögters. 2012. "Depletion of Neutrophil Extracellular Traps in Vivo Results in Hypersusceptibility to Polymicrobial Sepsis in Mice." *Critical Care* 16 (4): R137. <https://doi.org/10.1186/cc11442>.
- Metzler, Kathleen D., Christian Goosmann, Aleksandra Lubojemska, Arturo Zychlinsky, and Venizelos Papayannopoulos. 2014. "A Myeloperoxidase-Containing Complex Regulates Neutrophil Elastase Release and Actin Dynamics during NETosis." *Cell Reports* 8 (3): 883–96. <https://doi.org/10.1016/j.celrep.2014.06.044>.
- Meyer, Simon F. De, Georgette L. Suidan, Tobias A. Fuchs, Marc Monestier, and Denisa D.

- Wagner. 2012. "Extracellular Chromatin Is an Important Mediator of Ischemic Stroke in Mice." *Arteriosclerosis, Thrombosis, and Vascular Biology* 32 (8): 1884–91. <https://doi.org/10.1161/ATVBAHA.112.250993>.
- Mikacenic, Carmen, Richard Moore, Victoria Dmyterko, T. Eoin West, William A. Altemeier, W. Conrad Liles, and Christian Lood. 2018. "Neutrophil Extracellular Traps (NETs) Are Increased in the Alveolar Spaces of Patients with Ventilator-Associated Pneumonia." *Critical Care* 22 (1): 358. <https://doi.org/10.1186/s13054-018-2290-8>.
- Mócsai, Attila. 2013. "Diverse Novel Functions of Neutrophils in Immunity, Inflammation, and Beyond." *The Journal of Experimental Medicine* 210 (7): 1283–99. <https://doi.org/10.1084/jem.20122220>.
- Monestier, Marc, Thomas M. Fasy, Michele J. Losman, Kristine E. Novick, and Sylviane Muller. 1993. "Structure and Binding Properties of Monoclonal Antibodies to Core Histones from Autoimmune Mice." *Molecular Immunology* 30 (12): 1069–75. [https://doi.org/10.1016/0161-5890\(93\)90153-3](https://doi.org/10.1016/0161-5890(93)90153-3).
- Mori, Yuka, Masaya Yamaguchi, Yutaka Terao, Shigeyuki Hamada, Takashi Ooshima, and Shigetada Kawabata. 2012. "α-Enolase of Streptococcus Pneumoniae Induces Formation of Neutrophil Extracellular Traps." *Journal of Biological Chemistry* 287 (13): 10472–81. <https://doi.org/10.1074/jbc.M111.280321>.
- Müller-Redetzky, H. C., S. M. Wienhold, J. Berg, A. C. Hocke, S. Hippenstiel, K. Hellwig, B. Gutbier, et al. 2015. "Moxifloxacin Is Not Anti-Inflammatory in Experimental Pneumococcal Pneumonia." *Journal of Antimicrobial Chemotherapy* 70 (3): 830–40. <https://doi.org/10.1093/jac/dku446>.
- Müller-Redetzky, Holger C, Daniel Will, Katharina Hellwig, Wolfgang Kummer, Thomas Tschernig, Uwe Pfeil, Renate Paddenberg, et al. 2014. "Mechanical Ventilation Drives Pneumococcal Pneumonia into Lung Injury and Sepsis in Mice: Protection by Adrenomedullin." *Critical Care* 18 (2): R73. <https://doi.org/10.1186/cc13830>.
- Muller, H C, M Witzernath, T Tschernig, B Gutbier, S Hippenstiel, A Santel, N Suttorp, and S Rosseau. 2010. "Adrenomedullin Attenuates Ventilator-Induced Lung Injury in Mice." *Thorax* 65 (12): 1077–84. <https://doi.org/10.1136/thx.2010.135996>.
- Nakazawa, Daigo, Haruki Shida, Yoshihiro Kusunoki, Arina Miyoshi, Saori Nishio, Utano

- Tomaru, Tatsuya Atsumi, and Akihiro Ishizu. 2016. "The Responses of Macrophages in Interaction with Neutrophils That Undergo NETosis." *Journal of Autoimmunity* 67 (February): 19–28. <https://doi.org/10.1016/j.jaut.2015.08.018>.
- Narasaraju, Teluguakula, Edwin Yang, Ramar Perumal Samy, Huey Hian Ng, Wee Peng Poh, Audrey-Ann Liew, Meng Chee Phoon, Nico van Rooijen, and Vincent T. Chow. 2011. "Excessive Neutrophils and Neutrophil Extracellular Traps Contribute to Acute Lung Injury of Influenza Pneumonitis." *The American Journal of Pathology* 179 (1): 199–210. <https://doi.org/10.1016/j.ajpath.2011.03.013>.
- Narayana Moorthy, Anandi, T. Narasaraju, Prashant Rai, R. Perumalsamy, K. B. Tan, Shi Wang, Bevin Engelward, and Vincent T. K. Chow. 2013. "In Vivo and in Vitro Studies on the Roles of Neutrophil Extracellular Traps during Secondary Pneumococcal Pneumonia after Primary Pulmonary Influenza Infection." *Frontiers in Immunology* 4 (March): 1–13. <https://doi.org/10.3389/fimmu.2013.00056>.
- Nathan, C. 2006. "Neutrophils and Immunity: Challenges and Opportunities." *Nat Rev Immunol* 6 (3): 173–82. <https://doi.org/10.1038/nri1785>.
- Nel, J, G, A J Theron, C Durandt, G R Tintinger, R Pool, T J Mitchell, C Feldman, and R Anderson. 2016. "Pneumolysin Activates Neutrophil Extracellular Trap Formation." *Clin Exp Immunol* 184 (3): 358–67. <https://doi.org/10.1111/cei.12766>.
- Niederman, M. S. 2009. "Community-Acquired Pneumonia: The U.S. Perspective." *Semin Respir Crit Care Med.* 30: 179–88. <https://doi.org/10.1055/s-0029-1202937>.
- O'Brien, Katherine L, Lara J Wolfson, James P Watt, Emily Henkle, Maria Deloria-Knoll, Natalie McCall, Ellen Lee, Kim Mulholland, Orin S Levine, and Thomas Cherian. 2009. "Burden of Disease Caused by Streptococcus Pneumoniae in Children Younger than 5 Years: Global Estimates." *The Lancet* 374 (9693): 893–902. [https://doi.org/10.1016/S0140-6736\(09\)61204-6](https://doi.org/10.1016/S0140-6736(09)61204-6).
- Opitz, Bastian, Anja Püschel, Bernd Schmeck, Andreas C. Hocke, Simone Rosseau, Sven Hammerschmidt, Ralf R. Schumann, Norbert Suttorp, and Stefan Hippenstiel. 2004. "Nucleotide-Binding Oligomerization Domain Proteins Are Innate Immune Receptors for Internalized Streptococcus Pneumoniae." *Journal of Biological Chemistry* 279 (35): 36426–32. <https://doi.org/10.1074/jbc.M403861200>.

- Papayannopoulos, V, K D Metzler, A Hakkim, and A Zychlinsky. 2010. "Neutrophil Elastase and Myeloperoxidase Regulate the Formation of Neutrophil Extracellular Traps." *J Cell Biol* 191 (3): 677–91. <https://doi.org/10.1083/jcb.201006052>.
- Papayannopoulos, Venizelos. 2017. "Neutrophil Extracellular Traps in Immunity and Disease." *Nature Reviews Immunology* 18 (2): 134–47. <https://doi.org/10.1038/nri.2017.105>.
- Papayannopoulos, Venizelos, and Arturo Zychlinsky. 2009. "NETs: A New Strategy for Using Old Weapons." *Trends in Immunology* 30 (11): 513–21. <https://doi.org/10.1016/j.it.2009.07.011>.
- Parker, H, A M Albrett, A J Kettle, and C C Winterbourn. 2012. "Myeloperoxidase Associated with Neutrophil Extracellular Traps Is Active and Mediates Bacterial Killing in the Presence of Hydrogen Peroxide." *J Leukoc Biol* 91 (3): 369–76. <https://doi.org/10.1189/jlb.0711387>.
- Parker, Heather, Amelia M. Albrett, Anthony J. Kettle, and Christine C. Winterbourn. 2011. "Myeloperoxidase Associated with Neutrophil Extracellular Traps Is Active and Mediates Bacterial Killing in the Presence of Hydrogen Peroxide." *Journal of Leukocyte Biology* 91 (3): 369–76. <https://doi.org/10.1189/jlb.0711387>.
- Parkin, Jacqueline, and Bryony Cohen. 2001. "An Overview of the Immune System." *The Lancet* 357 (9270): 1777–89. [https://doi.org/10.1016/S0140-6736\(00\)04904-7](https://doi.org/10.1016/S0140-6736(00)04904-7).
- Pietrosimone, Kathryn M. 2015. "Contributions of Neutrophils to the Adaptive Immune Response in Autoimmune Disease." *World Journal of Translational Medicine* 4 (3): 60. <https://doi.org/10.5528/wjtm.v4.i3.60>.
- Pillay, Janesh, I. den Braber, Nienke Vrisekoop, Lydia M. Kwast, R. J. de Boer, J. A. M. Borghans, Kiki Tesselaar, and Leo Koenderman. 2010. "In Vivo Labeling with $^2\text{H}_2\text{O}$ Reveals a Human Neutrophil Lifespan of 5.4 Days." *Blood* 116 (4): 625–27. <https://doi.org/10.1182/blood-2010-01-259028>.
- Pleguezuelos, Olga, Eleni Hagi-Pavli, George Crowther, and Supriya Kapas. 2004. "Adrenomedullin Signals through NF- κ B in Epithelial Cells." *FEBS Letters* 577 (1–2): 249–54. <https://doi.org/10.1016/j.febslet.2004.10.019>.
- Poll, Tom; M Opal, Steven van der. 2009. "Pathogenesis, Treatment, and Prevention of Pneumococcal Pneumonia." *The Lancet* 374: 1543–56.

- Poll, Tom van der, and Steven M. Opal. 2009. "Pathogenesis, Treatment, and Prevention of Pneumococcal Pneumonia." *The Lancet* 374 (9700): 1543–56. [https://doi.org/10.1016/S0140-6736\(09\)61114-4](https://doi.org/10.1016/S0140-6736(09)61114-4).
- Porto, Bárbara Nery, and Renato Tetelbom Stein. 2016. "Neutrophil Extracellular Traps in Pulmonary Diseases: Too Much of a Good Thing?" *Frontiers in Immunology* 7 (AUG): 1–13. <https://doi.org/10.3389/fimmu.2016.00311>.
- Remijsen, Q, T W Kuijpers, E Wirawan, S Lippens, P Vandenabeele, and T Vanden Berghe. 2011. "Dying for a Cause: NETosis, Mechanisms behind an Antimicrobial Cell Death Modality." *Cell Death Differ* 18 (4): 581–88. <https://doi.org/10.1038/cdd.2011.1>.
- Rittirsch, Daniel, Michael A. Flierl, and Peter A. Ward. 2008. "Harmful Molecular Mechanisms in Sepsis." *Nature Reviews Immunology* 8 (10): 776–87. <https://doi.org/10.1038/nri2402>.
- Röhm, Marc, Melissa J. Grimm, Anthony C. D'Auria, Nikolaos G. Almyroudis, Brahm H. Segal, and Constantin F. Urban. 2014. "NADPH Oxidase Promotes Neutrophil Extracellular Trap Formation in Pulmonary Aspergillosis." Edited by G. S. Deepe. *Infection and Immunity* 82 (5): 1766–77. <https://doi.org/10.1128/IAI.00096-14>.
- Saffarzadeh, M, C Juenemann, M A Queisser, G Lochnit, G Barreto, S P Galuska, J Lohmeyer, and K T Preissner. 2012. "Neutrophil Extracellular Traps Directly Induce Epithelial and Endothelial Cell Death: A Predominant Role of Histones." *PLoS One* 7 (2): e32366. <https://doi.org/10.1371/journal.pone.0032366>.
- Saffarzadeh, M, and K T Preissner. 2013. "Fighting against the Dark Side of Neutrophil Extracellular Traps in Disease: Manoeuvres for Host Protection." *Curr Opin Hematol* 20 (1): 3–9. <https://doi.org/10.1097/MOH.0b013e32835a0025>.
- Saffarzadeh, Mona, Christiane Juenemann, Markus A. Queisser, Guenter Lochnit, Guillermo Barreto, Sebastian P. Galuska, Juergen Lohmeyer, and Klaus T. Preissner. 2012. "Neutrophil Extracellular Traps Directly Induce Epithelial and Endothelial Cell Death: A Predominant Role of Histones." Edited by Dominik Hartl. *PLoS ONE* 7 (2): e32366. <https://doi.org/10.1371/journal.pone.0032366>.
- Sayah, D M, B Mallavia, F Liu, G Ortiz-Munoz, A Caudrillier, A DerHovanessian, D J Ross, et al. 2015. "Neutrophil Extracellular Traps Are Pathogenic in Primary Graft Dysfunction after Lung Transplantation." *Am J Respir Crit Care Med* 191 (4): 455–63.

<https://doi.org/10.1164/rccm.201406-1086OC>.

- Schönrich, Günther, and Martin J. Raftery. 2016. "Neutrophil Extracellular Traps Go Viral." *Frontiers in Immunology* 7 (SEP): 11–14. <https://doi.org/10.3389/fimmu.2016.00366>.
- Shahraz, Anahita, Jens Kopatz, Rene Mathy, Joachim Kappler, Dominic Winter, Shoba Kapoor, Vlad Schütza, Thomas Scheper, Volkmar Gieselmann, and Harald Neumann. 2015. "Anti-Inflammatory Activity of Low Molecular Weight Polysialic Acid on Human Macrophages." *Scientific Reports* 5 (1): 16800. <https://doi.org/10.1038/srep16800>.
- Shishikura, Kyosuke, Takahiro Horiuchi, Natsumi Sakata, Duc-Anh Trinh, Ryutaro Shirakawa, Tomohiro Kimura, Yujiro Asada, and Hisanori Horiuchi. 2016. "Prostaglandin E 2 Inhibits Neutrophil Extracellular Trap Formation through Production of Cyclic AMP." *British Journal of Pharmacology* 173 (2): 319–31. <https://doi.org/10.1111/bph.13373>.
- Song, Chao, Haitao Li, Yi Li, Minhui Dai, Lemeng Zhang, Shuai Liu, Hongyi Tan, et al. 2019. "NETs Promote ALI/ARDS Inflammation by Regulating Alveolar Macrophage Polarization." *Experimental Cell Research* 382 (2): 111486. <https://doi.org/10.1016/j.yexcr.2019.06.031>.
- Spronk, P E, H Bootsma, G Horst, M G Huitema, P C Limburg, J W Tervaert, and C G Kallenberg. 1996. "Antineutrophil Cytoplasmic Antibodies in Systemic Lupus Erythematosus." *British Journal of Rheumatology* 35 (7): 625–31. <http://www.ncbi.nlm.nih.gov/pubmed/8670594>.
- Stamatos, Nicholas M, Lei Zhang, Anne Jokilammi, Jukka Finne, Wilbur H Chen, Abderrahman El-Maarouf, Alan S Cross, and Kim G Hankey. 2014. "Changes in Polysialic Acid Expression on Myeloid Cells during Differentiation and Recruitment to Sites of Inflammation: Role in Phagocytosis." *Glycobiology* 24 (9): 864–79. <https://doi.org/10.1093/glycob/cwu050>.
- Stoiber, W, A Obermayer, P Steinbacher, and W D Krautgartner. 2015. "The Role of Reactive Oxygen Species (ROS) in the Formation of Extracellular Traps (ETs) in Humans." *Biomolecules* 5 (2): 702–23. <https://doi.org/10.3390/biom5020702>.
- Sur Chowdhury, C, S Giaglis, U A Walker, A Buser, S Hahn, and P Hasler. 2014. "Enhanced Neutrophil Extracellular Trap Generation in Rheumatoid Arthritis: Analysis of Underlying Signal Transduction Pathways and Potential Diagnostic Utility." *Arthritis Res Ther* 16 (3):

- R122. <https://doi.org/10.1186/ar4579>.
- Temmesfeld-Wollbruck, B, B Brell, C zu Dohna, M Dorenberg, A C Hocke, H Martens, J Klar, N Suttorp, and S Hippenstiel. 2009. “Adrenomedullin Reduces Intestinal Epithelial Permeability in Vivo and in Vitro.” *Am J Physiol Gastrointest Liver Physiol* 297 (1): G43-51. <https://doi.org/10.1152/ajpgi.90532.2008>.
- Temmesfeld-Wollbruck, B, A C Hocke, N Suttorp, and S Hippenstiel. 2007. “Adrenomedullin and Endothelial Barrier Function.” *Thromb Haemost* 98 (5): 944–51. <https://www.ncbi.nlm.nih.gov/pubmed/18000597>.
- Tsuchiya, Atsunori, Wei-Yu Lu, Birgit Weinhold, Luke Boulter, Benjamin M. Stutchfield, Michael J. Williams, Rachel V. Guest, et al. 2014. “Polysialic Acid/Neural Cell Adhesion Molecule Modulates the Formation of Ductular Reactions in Liver Injury.” *Hepatology* 60 (5): 1727–40. <https://doi.org/10.1002/hep.27099>.
- Ulm, Christina, Mona Saffarzadeh, Poornima Mahavadi, Sandra Müller, Gerlinde Prem, Farhan Saboor, Peter Simon, et al. 2013. “Soluble Polysialylated NCAM: A Novel Player of the Innate Immune System in the Lung.” *Cellular and Molecular Life Sciences* 70 (19): 3695–3708. <https://doi.org/10.1007/s00018-013-1342-0>.
- Urban, Constantin F., David Ermert, Monika Schmid, Ulrike Abu-Abed, Christian Goosmann, Wolfgang Nacken, Volker Brinkmann, Peter R. Jungblut, and Arturo Zychlinsky. 2009. “Neutrophil Extracellular Traps Contain Calprotectin, a Cytosolic Protein Complex Involved in Host Defense against *Candida Albicans*.” Edited by Stuart M. Levitz. *PLoS Pathogens* 5 (10): e1000639. <https://doi.org/10.1371/journal.ppat.1000639>.
- Wang, H., C. Wang, M.-H. Zhao, and M. Chen. 2015. “Neutrophil Extracellular Traps Can Activate Alternative Complement Pathways.” *Clinical & Experimental Immunology* 181 (3): 518–27. <https://doi.org/10.1111/cei.12654>.
- Weiser, Jeffrey N, Daniela M Ferreira, and James C Paton. 2018. “Streptococcus Pneumoniae: Transmission, Colonization and Invasion.” *Nature Reviews Microbiology* 16 (6): 355–67. <https://doi.org/10.1038/s41579-018-0001-8>.
- Wen, Zongmei, Yan Liu, Feng Li, Feng Ren, Dexi Chen, Xiuhui Li, and Tao Wen. 2013. “Circulating Histones Exacerbate Inflammation in Mice with Acute Liver Failure.” *Journal of Cellular Biochemistry* 114 (10): 2384–91. <https://doi.org/10.1002/jcb.24588>.

- Witzenrath, M., F. Pache, D. Lorenz, U. Koppe, B. Gutbier, C. Tabeling, K. Reppe, et al. 2011. “The NLRP3 Inflammasome Is Differentially Activated by Pneumolysin Variants and Contributes to Host Defense in Pneumococcal Pneumonia.” *The Journal of Immunology* 187 (1): 434–40. <https://doi.org/10.4049/jimmunol.1003143>.
- Wong, S L, and D D Wagner. 2018. “Peptidylarginine Deiminase 4: A Nuclear Button Triggering Neutrophil Extracellular Traps in Inflammatory Diseases and Aging.” *FASEB J*, fj201800691R. <https://doi.org/10.1096/fj.201800691R>.
- Wright, Adam K. A., Mathieu Bangert, Jenna F. Gritzfeld, Daniela M. Ferreira, Kondwani C. Jambo, Angela D. Wright, Andrea M. Collins, and Stephen B. Gordon. 2013. “Experimental Human Pneumococcal Carriage Augments IL-17A-Dependent T-Cell Defence of the Lung.” Edited by Carlos Javier Orihuela. *PLoS Pathogens* 9 (3): e1003274. <https://doi.org/10.1371/journal.ppat.1003274>.
- Xu, J, X Zhang, R Pelayo, M Monestier, C T Ammollo, F Semeraro, F B Taylor, N L Esmon, F Lupu, and C T Esmon. 2009. “Extracellular Histones Are Major Mediators of Death in Sepsis.” *Nat Med* 15 (11): 1318–21. <https://doi.org/10.1038/nm.2053>.
- Yahiaoui, Rachid Y, Casper DJ den Heijer, Evelien ME van Bijnen, W John Paget, Mike Pringle, Herman Goossens, Cathrien A Bruggeman, François G Schellevis, and Ellen E Stobberingh. 2016. “Prevalence and Antibiotic Resistance of Commensal *Streptococcus Pneumoniae* in Nine European Countries.” *Future Microbiology* 11 (6): 737–44. <https://doi.org/10.2217/fmb-2015-0011>.
- Yildiz, C, N Palaniyar, G Otulakowski, M A Khan, M Post, W M Kuebler, K Tanswell, et al. 2015. “Mechanical Ventilation Induces Neutrophil Extracellular Trap Formation.” *Anesthesiology* 122 (4): 864–75. <https://doi.org/10.1097/ALN.0000000000000605>.
- Yipp, Bryan G, Björn Petri, Davide Salina, Craig N Jenne, Brittney N V Scott, Lori D Zbytniuk, Keir Pittman, et al. 2012. “Infection-Induced NETosis Is a Dynamic Process Involving Neutrophil Multitasking in Vivo.” *Nature Medicine* 18 (9): 1386–93. <https://doi.org/10.1038/nm.2847>.
- Yousefi, S, C Mihalache, E Kozłowski, I Schmid, and H U Simon. 2009. “Viable Neutrophils Release Mitochondrial DNA to Form Neutrophil Extracellular Traps.” *Cell Death & Differentiation* 16 (11): 1438–44. <https://doi.org/10.1038/cdd.2009.96>.

- Yousefi, Shida, Jeffrey A Gold, Nicola Andina, James J Lee, Ann M Kelly, Evelyne Kozlowski, Inès Schmid, et al. 2008. “Catapult-like Release of Mitochondrial DNA by Eosinophils Contributes to Antibacterial Defense.” *Nature Medicine* 14 (9): 949–53. <https://doi.org/10.1038/nm.1855>.
- Yuen, J, F G Pluthero, D N Douda, M Riedl, A Cherry, M Ulanova, W H Kahr, N Palaniyar, and C Licht. 2016. “NETosing Neutrophils Activate Complement Both on Their Own NETs and Bacteria via Alternative and Non-Alternative Pathways.” *Front Immunol* 7: 137. <https://doi.org/10.3389/fimmu.2016.00137>.
- Zeerleder, Sacha, Gavin CKW Koh, Hanna K de Jong, Nick PJ Day, Femke Stephan, W Joost Wiersinga, Anne J van der Meer, et al. 2014. “Neutrophil Extracellular Traps in the Host Defense against Sepsis Induced by *Burkholderia Pseudomallei* (Meliodiosis).” *Intensive Care Medicine Experimental* 2 (1): 1–15. <https://doi.org/10.1186/s40635-014-0021-2>.
- Zhong, X.-Y., I. von Muhlenen, Y. Li, A. Kang, A. K. Gupta, A. Tyndall, W. Holzgreve, S. Hahn, and P. Hasler. 2007. “Increased Concentrations of Antibody-Bound Circulatory Cell-Free DNA in Rheumatoid Arthritis.” *Clinical Chemistry* 53 (9): 1609–14. <https://doi.org/10.1373/clinchem.2006.084509>.

7. Abbreviations

AAV:	ANCA-associated vasculitis
ACT:	Adenylate cyclase toxin
ADM:	Adrenomedullin
ALI:	Acute lung injury
ANCA:	Anti-neutrophil cytoplasmic antibodies
APC:	Allophycocyanin
APC:	Activated protein C
APCs:	Antigen-presenting cells
ARDS:	Acute respiratory distress syndrome
AST:	Aspartate transaminase
AUC:	Area under the curve
BALF:	Bronchoalveolar lavage fluid
BM:	Bone marrow
BPI:	Bactericidal/permeability-increasing protein
BrV:	Brilliant violet
BSA:	Bovine serum albumin
cAMP:	Cyclic AMP (adenosine 3',5'-cyclic monophosphate)
CAP:	Community-acquired pneumonia
CAPNETZ:	German competence network for CAP
CbpA/C:	Choline-binding cell-surface protein A/C
CD:	Cluster of differentiation
cDNA:	Complementary deoxyribonucleic acid
CF:	Cystic fibrosis
CFTR:	CF transmembrane conductance regulator
CFU:	Colony-forming unit
CGD:	Chronic granulomatous disease
CGRP:	Calcitonin gene-related peptide
CRB65:	Confusion, respiratory rate, blood pressure, age \geq 65 years
CRLR:	Calcitonin receptor-like receptor
CXCL1/CXCR1:	C-X-C chemokine ligand/receptor type 1
DAMPs:	Damage-associated molecular patterns
DAPI:	4',6'-diamidino-2-phenylindole

DCFH-DA:	2',7'-dichlorodihydrofluorescein diacetate
DCs:	Dendritic cells
DMEM:	Dulbecco's modified eagle medium
ECL:	Enhanced chemiluminescence
EDTA:	Ethylenediaminetetraacetic acid
ELISA:	Enzyme-linked immunosorbent assay
pERK:	Phosphorylated extracellular signal-regulated kinase
ETs:	Extracellular traps
FACS:	Fluorescence-activated cell sorting
FITC:	Fluorescein isothiocyanate
FSC:	Forward scatter
GO:	Glucose oxidase
GRO α :	Growth-regulated oncogene alpha
H:	Hours
H ₂ O ₂ :	Hydrogen peroxide
H ₂ SO ₄ :	Sulfuric acid
HAP:	Hospital-acquired pneumonia
HBSS:	Hank's balanced salt solution
HIV:	Human immunodeficiency virus
HMGB1:	High mobility group box 1
HOCl:	Hypochlorous acid
HRP:	Horseradish-peroxidase
HSA:	Human serum albumin
ICAM1:	Intercellular adhesion molecule 1
IFN γ :	Interferon gamma
Ig:	Immunoglobulin
IL:	Interleukin
IL-1R:	IL receptor 1
iNOS:	Cytokine-inducible nitric oxide synthase
i.p.:	Intra-peritoneal
KC:	Keratinocyte-derived chemokine
LAGeSo:	Regional office for health and social affairs Berlin
LFA-1:	Lymphocyte function-associated antigen 1
LIX:	Lipopolysaccharide-induced CXC chemokine

LPS:	Lipopolysaccharide
LTA:	Lipoteichoic acid
LTB4:	Leukotriene B4
LytA:	N-acetylmuramoyl-L-alanine amidase
Mac1:	Macrophage-1 antigen
MAPK:	Mitogen-activated protein kinase
MEK:	MAPK kinase
MFI:	Median fluorescence intensity
MHC-Class II:	Major histocompatibility complex - class II
MIP-2:	Macrophage inflammatory protein-2
MMP8:	Matrix metalloproteinase 8
MPO:	Myeloperoxidase
MSA:	Mouse serum albumin
MV:	Mechanical ventilation
MyD88:	Myeloid-differentiation primary response protein 88
NADPH:	Nicotinamide adenine dinucleotide phosphate
NCAM:	Neural cell adhesion molecule
NE:	Neutrophil elastase
NETs:	Neutrophil extracellular traps
NK:	Natural killer cells
NLR:	Nucleotide oligomerization domain (NOD)-like receptor
NLRP3:	NLR family pyrin domain-containing 3
NOX:	NADPH oxidase
OD:	Optical-density
ON:	Overnight
PAD4:	Peptidylarginine deiminase 4
PAD4i:	PAD4 inhibitor
PAMPs:	Pathogen-associated molecular patterns
PBS:	Phosphate-buffered saline
PCV:	Pneumococcal conjugated vaccine
PE-Cy7:	Phycoerythrin coupled to a cyanine dye Cy7
PerCP:	Peridinin chlorophyll protein
PFA:	Paraformaldehyde
p.i.:	Post-infection

PKC:	Protein kinase C
PLY:	Pneumolysin
PMA:	Phorbol 12-myristate 13-acetate
PMN:	Polymorphonuclear cells
PPSV:	Pneumococcal polysaccharide vaccine
PR3:	Proteinase 3
PRRs:	Pattern recognition receptors
PSA:	Polysialic acid
PsaA:	Pneumococcal surface adhesin A
PSGL-1:	P-selectin glycoprotein ligand-1
PspA/C:	Pneumococcal surface protein A/C
RA:	Rheumatoid arthritis
RAMP:	Receptor activity-modifying protein
RLR:	Retinoic acid-inducible gene-I-like receptors
RLU:	Relative light unit
r/mRNA:	Ribosomal/messenger ribonucleic acid
ROC curve:	Receiver operating characteristic curve
ROS:	Reactive oxygen species
RT:	Room temperature
RT-qPCR	Real-time quantitative polymerase chain reaction
SEM:	Standard error of mean
SLE:	Systemic lupus erythematosus
<i>S.pn.</i> :	<i>Streptococcus pneumoniae</i>
SSC:	Side scatter
ssRNA:	Single-stranded RNA
T _H :	T helper cells
THY:	Todd-Hewitt Broth medium supplemented with yeast extract
TLR:	Toll-like receptor
TMB:	3,3',5,5'-tetramethylbenzidine
TNF:	Tumor necrosis factor
T _{reg} :	Regulatory T-cells
VEGF:	Vascular endothelial growth factor
VILI:	Ventilator-induced lung injury
WT:	Wild type